University of Padua

School of Medicine and Surgery

Master's Degree Programme in Medical Biotechnologies

Department of Molecular Medicine

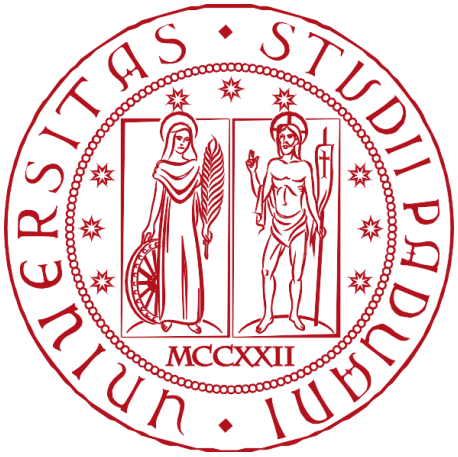

Targeting Neuronal Activity with Ampakine: A Therapeutic Approach for Rett Syndrome.

Supervisor: Prof.ssa Carla Mucignat

Co-Supervisor: Prof.ssa Nicoletta Landsberger

Student: Virginia Varotto

Academic year: 2025/2026

Index

1. Abstract 2

2. Introduction 3

2.1 Rett syndrome: clinical staging, phenotypic variants, and prognosis 3

2.2 MECP2 gene, structure and functions 4

2.3 Molecular knowledge of Rett syndrome 11

2.3.1 Mutations in RTT 11

2.3.2 Genotype-phenotype correlation in RTT 12

2.3.3 Rett syndrome is prevalently a girl-related disease 13

2.4 Pre-clinical research : *in vivo* models 14

2.5 Neurological Consequences of MeCP2 Deficiency 16

2.5.1 MeCP2 involvement in neuronal activity and synaptic plasticity 17

2.5.2 The role of MeCP2 in regulating neuronal activity in early neural development and mature neurons 18

2.6 The Glutamatergic System 19

2.6.1 Metabotropic receptors 20

2.6.2 Ionotropic receptors 20

2.7 Modulators of AMPARs: Ampakines 23

3. Materials and methods 24

3.1 Animals care 24

3.1.1 Genotyping 25

3.2 RNA purification, cDNA synthesis and quantitative RT–PCR 28

3.3 Pharmacological treatments 29

3.4 Behavioral assessment 29

3.4.1 Phenotypic scoring 29

3.4.2 Open Field test 30

3.4.3 Rotarod test 30

3.4.4 Pole test 30

3.4.5 Beam walking test 30

3.4.6 Novel Object Recognition Test (NOR) 31

3.5 Electrophysiology measurements: Patch clamp analysis 31

3.6 Primary cultures 31

3.6.1 Cortical neurons 31
3.6.2 Protein extraction 32
3.6.3 Western blots 32
3.6.4 Analysis of calcium transients 32
3.6.5 Cell immunofluorescence 33
3.6.6 Puncta Analysis 33
3.7 Statistical analysis 33
4. Preliminary Data 34
5. Aim 35
6. Results 35
6.1 Ampakine-mediated activation of AMPA receptor signalling rescues synaptic and functional deficits in Mecp2-null neuron 35
6.2 Early administration of Ampakine ameliorates behavioural phenotypes also in female heterozygous mouse models 39
6.3 Combination of early and alternate treatment is safe and elicits superior beneficial effects compared to the solely early intervention in *Mecp2*-null mice 42
6.4 Early intermittent treatment is effective also in HET female mice 44
6.5 Ampakine administration potentiates the spontaneous excitatory currents 46
6.6 Gene expression differences in WT and KO mice were rescued by the Ampakine treatment, supporting PFC as a valid target for transcriptomic profiling 48
7. Discussion 50
8. Conclusions 53
9. Abbreviations 54
10. Acknowledgments 56
11. References 57

1. Abstract

Rett syndrome (RTT) is a rare and severe neurodevelopmental disorder, primarily affecting females. Patients are characterized by an apparently normal early development followed by a regression phase between 6 and 18 months of age, which marks the onset of progressive motor and intellectual impairments. The majority of Rett cases are caused by mutations in the X-linked *MECP2* gene, which encodes for a master regulator of gene expression, ubiquitously expressed, but mainly present in the brain. In line with its role, *MeCP2*-null neurons show widespread transcriptional and functional deficits, including impaired maturation and reduced responsiveness to external stimuli. Although clinical symptoms emerge after the first year of life, increasing evidence indicates that MeCP2 deficiency disrupts brain development from early stages. In particular, *Mecp2*-null cortical neurons display early defects in transcription, neuronal activity, and morphology, which appear interconnected in a feed-forward mechanism where neuronal activity drives transcriptional and structural changes that further increase network maturity.

We thus investigated the therapeutic potential of a high-impact Ampakine, a positive modulator of AMPA receptors, to restore neuronal activity in *Mecp2*-deficient models.

Initially, we tested its efficacy *in vitro* using primary *Mecp2*-null mouse neurons. We were able to show a restoration of synaptic density in *Mecp2* KO treated neurons, as well as a rescue in neuronal functionality.

Then, we focused on two *in vivo* strategies. Since it was previously demonstrated that an early ampakine treatment (P3-P9) is able to improve RTT phenotype in male KO mouse model, we first evaluated the same therapy on female heterozygous mice, being the most clinically relevant model of Rett syndrome. Afterwards, we implemented a prolonged intermittent treatment (P3–P75) in both male null and female heterozygous mice, to assess whether a sustained modulation of neuronal activity could enhance and maintain long-term benefits.

As we proved that early intervention is crucial to obtain beneficial effects, we evaluated molecular and functional consequences of the early treatment by profiling gene expression in the prefrontal cortex at two developmental stages (P10 and P30), capturing both acute and late transcriptional effects. Additionally, *ex vivo* electrophysiological recordings were performed.

2. Introduction

2.1 Rett syndrome: clinical staging, phenotypic variants, and prognosis

Rett Syndrome (RTT) is a rare, complex, X-linked neurodevelopmental disorder mainly caused by mutations in the *MECP2* gene, although atypical forms may arise from mutations in different genes [1]. It affects brain function and development mainly in females with a prevalence of almost 1 out of 10000 born alive [2], [3]. It is considered a delayed onset disorder since patients seem to develop normally until 6-18 months of life, when first symptoms generally appear. From this point, the course of the disease can be divided into four main stages [4], [5], [6].

The first period is called the "early-onset stagnation period" and occurs between 6-18 months of age; it is marked by subtle but noticeable changes in an infant's social and developmental behaviour; indeed, the child may become less demanding of attention. Although postural development continues, it is delayed; sitting may be reached but crawling and standing are often absent. Language development is limited, with minimal babbling and few new words [7]. Furthermore, an abnormal deceleration in the rate of head circumference increase may be observed [8]. Despite these early atypical signs, the overall developmental progress may still seem broadly normal, which can lead primary healthcare providers to reassure parents and delay further evaluation [8], [9]. Unfortunately, a rapid "regression phase" occurs between 1 and 4 years of age in which RTT patients lose previously acquired developmental skills such as purposeful hand use, communication and motor skills [8]. In this phase the severe cognitive impairment that characterizes RTT becomes evident. After the end of the regression phase, patients with Rett syndrome enter a period of relative stability known as "pseudo-stationary stage", typically between 2 and 10 years of age. In this third stage the child may still be able to walk or to learn, the visual contact behaviour and eye pointing can re-emerge, although many other severe symptoms emerge such as epilepsy, breathing dysfunctions, growth failure, ataxia, anxiety, and gastrointestinal problems [10]. The final stage in the developmental course of Rett syndrome is marked by late motor deterioration, including gradual loss of motor skills, increased muscle rigidity and progressive scoliosis. While communication abilities may show some improvement, language is typically not restored. Most patients become wheelchair dependent. The definition of Rett syndrome symptomatology has a pivotal role since the diagnosis is still based on internationally clinically accepted criteria [6]. However, RTT is associated with a heterogeneous phenotype and, depending on the severity of clinical signs and on the onset of symptoms, it is classified into typical, atypical, and variant presentation [1].

The clinical criteria to diagnose typical RTT are the presence of all the main criteria which are the partial or progressive loss of purposeful hand movements, speech and language regression, gait abnormalities, and development of stereotyped hand motions. While the presence of supportive criteria is not mandatory for the diagnosis, patients usually present them [Table 1] [6], [8].

Milder forms of atypical RTT are (1) the *forme fruste,* characterized by a late onset – between 1 and 3 years old – and the maintenance of hand usage, and (2) the *preserved speech variant* that is addressed to patients capable of speaking few words. Most severe forms of atypical RTT include the (3) *early-onset seizures variant* and the (4) *congenital variant.* The former relates to patients that show seizures within the first five months of life, the latter, instead, is characterized by a grossly abnormal initial development and the lack of an intense eye gaze. Diagnosis for atypical phenotype

is based on the presence of regression followed by recovery or stabilization and at least two of the four main criteria, together with the presence of at least 5 of the so called "supportive features" that include sleep disturbances, bruxism, breathing abnormalities, autonomic dysfunction, seizures, intense eye gaze, weight loss and hypotonia **[Table.1]** [6], [11].

Historically, survival in Rett syndrome was limited, with median life expectancy reported to be less than 14 years. However, recent data indicate a substantial improvement in life expectancy, with median survival now exceeding 50 years in approximately 70% of patients [12]. The increase in longevity is attributed to earlier diagnosis and significant advances in clinical care, including better nutritional management, multidisciplinary healthcare teams, and focused physical and occupational therapies [8]. The only drug approved for the treatment of Rett syndrome is currently Trofinetide, a synthetic analogue of the N-terminal tripeptide of insulin-like growth factor 1 (IGF-1). The product received regulatory approval from the U.S. Food and Drug Administration (FDA) in March 2023 for use in the United States and subsequently in Canada (Vogel Ciernia et al., 2018; Neul et al., 2023). Clinical trials have demonstrated that Trofinetide can alleviate certain core symptoms of Rett syndrome and provide measurable clinical benefits. However, it is imperative to emphasize that this treatment is not a modifier of the disease trajectory. Rather, its primary objective is to improve symptom management, as no definitive cure for Rett syndrome currently exists and the majority of patients are treated with drugs meant to alleviate symptoms.

Table 1
Rett Syndrome (RTT) Clinical criteria

Typical or Classic RTT	Atypical or Variant RTT
Regression followed by recovery or stabilization	Regression followed by recovery or stabilization
All main criteria and all exclusion criteria	2 of 4 main criteria and all exclusion criteria
Main criteria: Partial or complete loss of purposeful hand skills; partial or complete loss of spoken language; dyspraxic or absent gait; stereotypic hand movements	
Supportive criteria not required; often present	5 of 11 supportive criteria required
Supportive criteria: Breathing disturbances when awake; bruxism when awake; impaired sleep pattern; abnormal muscle tone; peripheral vasomotor disturbances; scoliosis/kyphosis; growth retardation; small, cold hands and/or feet; inappropriate laughing/screaming spells; diminished response to pain; intense eye gaze – eye pointing	
Exclusion criteria: traumatic brain injury, neurometabolic disease, or severe infection; very abnormal development in first six months of life	

Neul et al. Ann Neurol 2010;68 : 944–950.

Table 1. International accepted clinical criteria and supportive criteria for the diagnosis of typical and atypical Rett syndrome [8].

2.2 MECP2 gene, structure and functions

Mutations in the *MECP2* gene account for the majority of Rett syndrome (RTT) cases, representing approximately 90% of patients. The gene was first characterized by Adrian Bird in 1992, but it was

not until 1998 that Dr. Huda Zoghbi and colleagues demonstrated its causative role in RTT [2], [15], [16].

The human *MECP2* gene is located on the reverse strand of the long arm of the X chromosome (Xq28) and spans approximately 76 kb. MeCP2 is the founding member of the methyl-CpG-binding domain (MBD) family of proteins, which are characterized by the presence of an MBD. While complete deletion of *Mecp2* in mice results in severe neurological symptoms and death around 10 to12 weeks of age, knockout of other MBD family members produces only minimal phenotypes [17], [18]. These findings suggest that MeCP2 plays the most critical role among MBD proteins in interpreting the DNA methylation landscape in the brain [19].

In both humans and mice, the gene consists of four exons and three introns. Currently, 21 transcripts of *MECP2* have been identified, of which two are protein-coding [20].

Alternative splicing of *MECP2* lead to production of two isoforms of the gene known as *MeCP2-e1* and *MeCP2-e2. MeCP2-E1* is encoded by exons 1, 3, and 4, whereas *MeCP2-e2 is* encoded by exons 2, 3, and 4. Both isoforms share the same protein domains but differ in their short N-terminal regions: MeCP2-e1 contains a unique 21-amino acid sequence, while MeCP2-e2 has a distinct 9-amino acid sequence [**Figure 1**] [21], [22], [23], [24].

The larger MeCP2-e1 isoform is the dominant protein in the brain with relatively consistent expression throughout different brain regions of the adult mice, and earlier appearance during brain development [24]. Several studies report that there is not overlapping in function of the two isoforms and the only one concurring for RTT phenotype is MeCP2-e1 [25]; [13]. Indeed, deficiency of the *Mecp2-e1* isoform in mice results in phenotypes similar to those observed in mice lacking the entire *Mecp2* gene. These include motor impairments, apraxia-like limb clasping, altered anxiety-related behaviours, and premature death in *Mecp2*-null mice [25]. Furthermore, *in vitro* studies using induced pluripotent stem cell (iPSC)-derived neurons from female *Mecp2308* heterozygous mice support the specific involvement of MeCP2-e1 in Rett syndrome. Neurons deficient in *Mecp2-e1* exhibit reduced soma size, decreased dendritic arborization, and defects in synapse formation and maturation—hallmarks commonly observed in neurons from Rett syndrome patients [26]. In contrast, mice deficient in *Mecp2-e2* do not display Rett-associated symptoms [27], suggesting that the E2 isoform may have limited or no direct relevance to the disorder [28], [29]**.** At subcellular level both MeCP2 isoforms localize into the nucleus and colocalize with methylated heterochromatic foci in mouse cells/neurons.

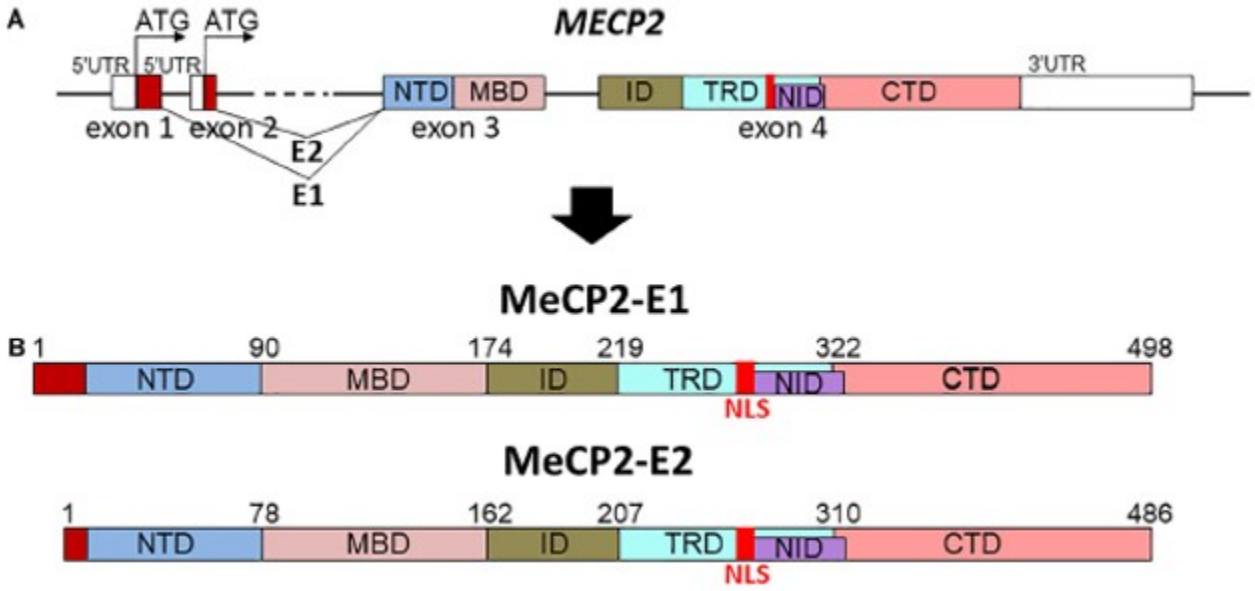

Figure 1: MeCP2 splicing and structure. Schematic representation of *MECP2* gene organization **(A)** and different protein domains of the MeCP2-E1 and MeCP2-E2 isoforms **(B)**. NTD, N-terminal; MBD, methyl binding; ID, intervening; TRD, transcription repression; NID, NCoR interaction; CTD, C-terminal domains; NLS, nuclear localization signal (modified from Good et al., 2021).

Although MeCP2 is expressed in various tissues, it is notably more abundant in the brain, particularly in mature post-migratory neurons [31], [32]. MeCP2 protein levels are low during embryogenesis but increase progressively throughout the postnatal period, coinciding with neuronal maturation [33], [34], [35], [36]. In detail, MeCP2 levels rise during embryonic and postnatal stages, reaching a plateau by approximately 10 years of age in humans and 5 weeks in mice [33]
In the cortex, this increase follows an inside-out pattern that parallels cortical development [34]. Similarly, in the olfactory epithelium, Mecp2 expression aligns with the maturation of olfactory receptor neurons (ORNs) and precedes synaptogenesis [34]. In this developmental pattern, its mutations do not appear to impair the proliferation or early differentiation of neuronal precursors [37]. To date, the mechanisms governing the complex spatial and temporal expression of *MECP2* remain unclear, but different studies have identified the core promoter region and several cis-regulatory elements as key regulatory sequences for its expression [38], [39].

The protein structure of MeCP2 is highly conserved, with the human and mouse amino acid sequences sharing 95% identity. Structurally, the human MeCP2 protein consists of 486 amino acids and contains five main functional domains: the N-terminal domain (NTD, residues 1–78), the methyl-CpG binding domain (MBD, 79–162), the intervening domain (ID, 163–206), the transcriptional repression domain (TRD, 207–310), and the C-terminal domain **[Figure. 2].**

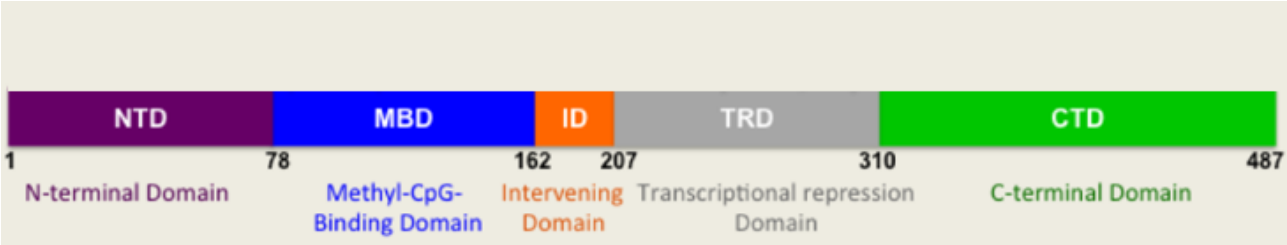

Figure 2: Schematic representation of MeCP2 domains (modified from Pejhan & Rastegar, 2021b)

MeCP2 is a pleiotropic multifunctional protein involved in diverse biological processes; however, gaps remain in understanding its full range of functions and interacting partners. It has been shown that the MBD and a short region of the TRD (residues 298e309), which is responsible for the interaction between MeCP2 and the NCoR1/2 corepressor complex, are the most biological relevant domains.

The MBD confers to MeCP2 the ability to bind DNA, in particular to methylated CpG dinucleotides with preference for CpG sequences with adjacent A/T-rich motifs [41]. MBD also binds to unmethylated four-way DNA junctions with a similar affinity [42], implicating a role for the MeCP2 MBD in higher-order chromatin interactions. Mutation in the MBD results in a decreased residence time at heterochromatic loci [43]. Interestingly, some evidence from chromatin immunoprecipitation assays reveals a preferential association of MeCP2 with methylated alleles of imprinted genes in mouse embryonic stem cells and in mouse brain [44], [45]. Moreover, recently MeCP2 was reported to interact also with CpA dinucleotide *in vitro* and *in viv*o in mouse brain (Deaton et al., 2011; Gabel et al., 2015).

The transcriptional repressor domain (TRD) of MeCP2 is a biologically significant region responsible for mediating its transcriptional repression function. Within this domain lies the NCOR-SMRT interaction domain (NID), which facilitates the recruitment of co-repressor complexes such as SIN3A, NCOR, and SMRT [46], [47]. Thus, MeCP2 specifically recognizes and binds to 5-methylcytosine (5MeCyt) residues in DNA, and upon binding, it attracts these co-repressor complexes [47]. Subsequently, the complex recruits histone deacetylases (HDACs), which catalyse the removal of acetyl groups from lysine residues on histone tails [48]. This deacetylation promotes chromatin condensation around methylated DNA, thereby increasing DNA compaction and physically inhibiting the binding of transcription factors [49], [50].

Although the C-terminal region of MeCP2 is not yet well characterized, it is clearly essential for protein function as evidenced by the numerous RTT-causing mutations that involve deletion of this domain [51]. Moreover, it has been demonstrated that a mouse model lacking the Mecp2 C-terminus reproduces many RTT phenotypes [52]. The C-terminus facilitates MeCP2 binding to naked DNA and to the nucleosome core, and it also contains evolutionarily conserved poly-proline runs that can bind to a domain typical of splicing factors (Buschdorf & Stratling, 2004).

MeCP2 was traditionally considered a transcriptional repressor, [54], [55], [56], [57], [58], [59]. To identify the possible targets of Mecp2, initial microarray analyses were performed on hippocampal, cortical, and whole forebrain tissues from *Mecp2*-null mice. These early studies revealed only modest

changes in gene expression [60], likely due to the use of heterogeneous brain regions, which may have masked region- and cellular-specific transcriptional effects. To overcome this limitation, a more targeted approach was adopted in a subsequent study [61], which focused specifically on the hypothalamus, a brain region closely associated with several key Rett syndrome phenotypes, including anxiety, growth deceleration, sleep-wake rhythm disturbances, and autonomic dysfunction [62]. In this analysis, gene expression profiles were compared across three groups of mice: *Mecp2*-null, wild-type (WT), and *Mecp2* transgenic (Tg) mice, the latter carrying an extra copy of the human *MECP2* gene, thereby mimicking the human *MECP2* duplication syndrome [61]. The use of this approach allowed the researchers to uncover more robust and biologically relevant transcriptional changes linked to *Mecp2* deficiency.

Indeed, the researchers proposed that true direct targets of Mecp2 should show opposite changes in expression in loss- and gain-of-function models. That is, genes that are downregulated in *Mecp2*-null mice should be upregulated in *Mecp2* transgenic (Tg) mice, and vice versa. Interestingly, the majority of genes were found to be upregulated in *Mecp2*-Tg mice and downregulated in *Mecp2*-null mice, indicating that MeCP2 primarily functions as a transcriptional activator rather than a repressor in the hypothalamus. This activator role was attributed to its ability to bind the cyclic AMP-responsive element binding protein (CREB1), which facilitates the recruitment and activation of RNA polymerase II at transcription start sites, thereby promoting the expression of target genes [61], [63]. Subsequent studies analysing the transcriptional profiles of *Mecp2*-mutant neurons across various brain regions, neurons and hESC derived RTT neuron confirmed that MeCP2 might also function as a transcriptional activator in the cerebellum, striatum, olfactory sensory neurons, and differentiated human embryonic stem cells [64], [65], [66], [67]. These findings expanded our understanding of MeCP2 functions beyond its traditional role as a transcriptional repressor, suggesting that its precise functions are context-dependent and influenced by the molecular environment. Over the following decade, research has further expanded MeCP2 roles, including its involvement in transcriptional regulation, chromatin organization, RNA splicing, microRNA processing, protein synthesis and microtubule and mitotic spindle regulator [68], [69], [70], [71], [72] [**Figure.3**].

Below a summary of the additional functions of this multifunctional protein.

1. MeCP2 can regulate protein synthesis through the AKT/mTOR-mediated pathway. The study revealed that this pathway is downregulated in *Mecp2* KO neurons along with ribosomal protein S6 (rpS6) phosphorylation [73]. It is important to note that the balance between protein synthesis and degradation is critical for tissue maturation and homeostasis, and alterations of these processes are often observed in ASD [68].
2. Some evidence indicates that MeCP2 may play a significant role not only in transcriptional regulation but also in RNA splicing. The first indication of its involvement in splicing emerged in 2005, when Young and colleagues reported splicing defects in *Mecp2*$^{308/y}$ male mice. These mice express a truncated form of the Mecp2 protein, and their phenotype revealed that loss of full-length *Mecp2* disrupts normal RNA splicing processes [74]. Subsequent *in vitro* studies further demonstrated that Mecp2 directly interacts with RNA and associates with Y-box binding protein 1 (YB-1), a known regulator of alternative splicing [75].They confirmed the interaction between Mecp2 and YB-1, and also identified additional associations with other RNA-binding and splicing regulators, including MATR3, SFPQ, and SFRS. Further support for this role was provided by Maunakea et al. (2013), who found that Mecp2 ablation was associated with increased exon

skipping events, indicative of disrupted alternative splicing[76] . Overall, these data suggest that Mecp2 modulates the recruitment of splicing factors to methylated DNA regions, and its absence leads to increased intron retention and altered splicing patterns, particularly in blood cells [77]. More recently it was reported that *Mecp2*-null neurons exhibited abnormal intron retention and exon skipping specifically in genes activated during neuronal stimulation [69]. These findings reinforce the emerging view that MeCP2 might play multifaceted roles in gene expression regulation both at the transcriptional and post-transcriptional levels, particularly in the context of neuronal function and plasticity [69].

3. Another role of Mecp2 at the post-transcriptional level is represented by the regulation of the biogenesis and function of microRNA (miRNA). One mechanism involves the direct binding to DiGeorge syndrome critical region 8 (DGCR8), a core component of the nuclear miRNA-processing complex [78]. This interaction interferes with the formation of the Drosha-DGCR8 complex, thereby inhibiting the processing of specific miRNAs. Several of these suppressed miRNAs target proteins vital for neural development, including CREB, LIMK1, and Pumilio2. Therefore, when MeCP2 is overexpressed, the resulting reduction in these miRNAs leads to abnormal levels of these proteins, which in turn disrupts the growth of dendrites and spines in neurons. This highlights the important role of MeCP2 in controlling neural development through miRNA regulation. [78]. In contrast to this inhibitory role, MeCP2 can also facilitate miRNA processing. Specifically, it promotes the maturation of miR-199a through its association with the Drosha complex. The MeCP2/miR-199a axis has been shown to regulate neural stem/precursor cell (NS/PC) differentiation, and deficiency of either MeCP2 or miR-199a leads to a shift in NS/PC fate from neuronal to astrocytic lineages, due to upregulation of Smad1 REF. Importantly, restoring miR-199a expression or inhibiting BMP signalling rescues normal differentiation patterns in Rett syndrome (RTT) patient-derived NS/PCs and brain organoids [70].
4. Recent investigations have uncovered a novel localization of MeCP2 at the centrosome in both proliferating and post-mitotic cells. Cellular and molecular studies indicated that this centrosomal association affects centrosome function, cell cycle progression, and neuronal maturation [71]. Subsequent studies further explored the connection between MeCP2 and centrosome-derived structures, particularly the primary cilium. Loss of MeCP2 was found to disrupt ciliogenesis in multiple cellular and organismal contexts, including cultured neurons, fibroblasts derived from RTT patients, and the mouse brain [72]. This impairment in cilium formation was associated with dysfunction of the Sonic Hedgehog (Shh) signalling pathway, a cilium-dependent cascade that is essential for proper neurodevelopment and brain function [72].

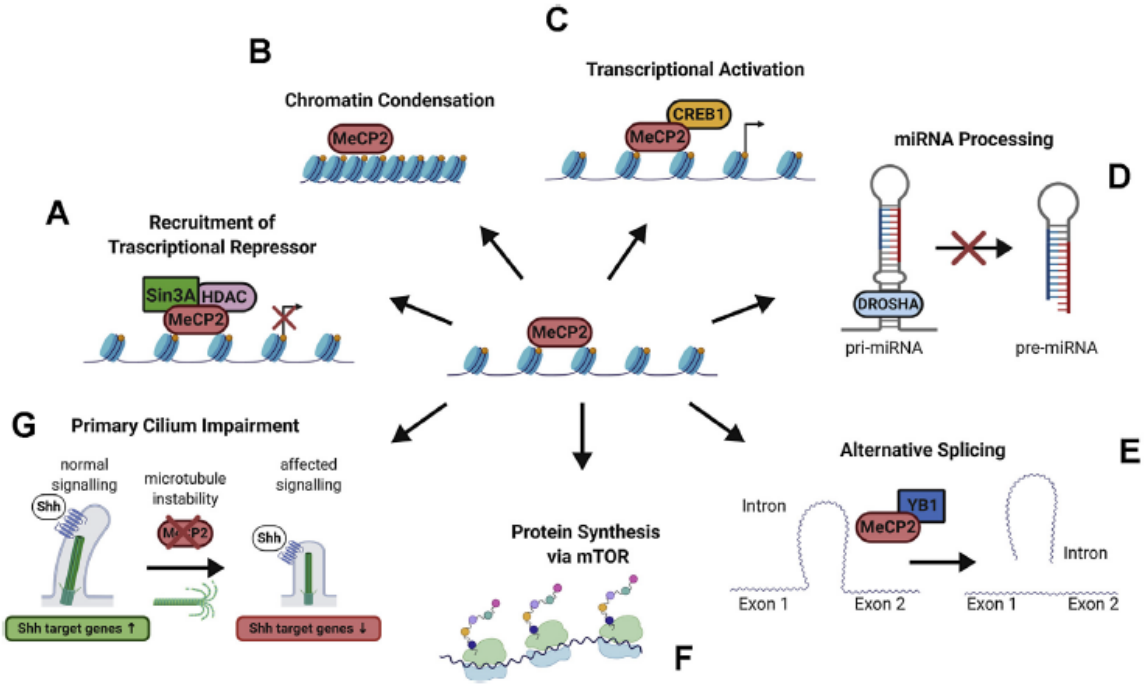

Figure 3: MeCP2 is a multifunctional protein associating with methylated DNA (central part; red dots indicate methyl-CpGs). The figure represents the proposed functions for MeCP2 [72].

2.3 Molecular knowledge of Rett syndrome

2.3.1 Mutations in RTT

De novo mutations in the *MECP2* gene account for approximately 95% of typical Rett syndrome cases and more than half of atypical RTT ones [79].

MECP2 mutations can be broadly categorized into three main groups. The first one comprises mutations affecting the N-terminal domain (NTD), deputed to the modulation of MeCP2 interaction with DNA, as well as to drive the turnover rate of the protein [80], [81], while the second group - particularly relevant for RTT - includes mutations in the methyl-CpG binding domain (MBD). Of note, missense mutations represent the most prevalent class of alterations affecting the MBD, accounting for over 70% of mutations in this region [82] and contributing to approximately 45% of RTT cases [83]. In general, MBD-associated missense mutations impact the stability of this domain and its affinity for DNA binding [84], [85].

The third group of mutations affect additional domains of MeCP2, such as the intervening domain (ID), the transcriptional repression domain (TRD) and the C-terminal domain (CTD) along with the nuclear localization domain (NID) and the RNA binding domain (RBD) [83]. A substantial number of nonsense mutations associated with Rett syndrome occur within these regions, with the exception for the TRD in which the most prevalent mutations are missense. Compared to the MBD, the structural and functional consequences of mutations in these domains have been investigated less thoroughly [82], [86], [87]; however structural studies from Alan Wolffe's laboratory provided some hints, demonstrating that MeCP2 C-terminal loss impairs its ability to bind nucleosomes, underscoring the possible role of the CTD in chromatin interaction [88]. Building on this, Nikitina et al. identified residues 295–486 as critical for chromatin binding and showed that the R294X mutation disrupts the MeCP2 capacity to cluster heterochromatin [89]. Importantly, the nonsense mutations R168X, R255X, R270X, and R294X, account for a substantial proportion (up to 60–70%) of nonsense mutations in *MECP2*, and around 20–30% of all pathogenic variants observed in RTT, have been shown to progressively impair MeCP2 ability to cluster heterochromatin [90].

Notably, eight recurrent mutations account for approximately 47% of all identified cases [28]. These include three mutations in the methyl-CpG-binding domain (R106W, R133C, and T158M), one in the intervening domain (R168X), and four within the transcriptional repression domain (R255X, R270X, R294X, and R306C) [80], [91] **[Figure 4].**

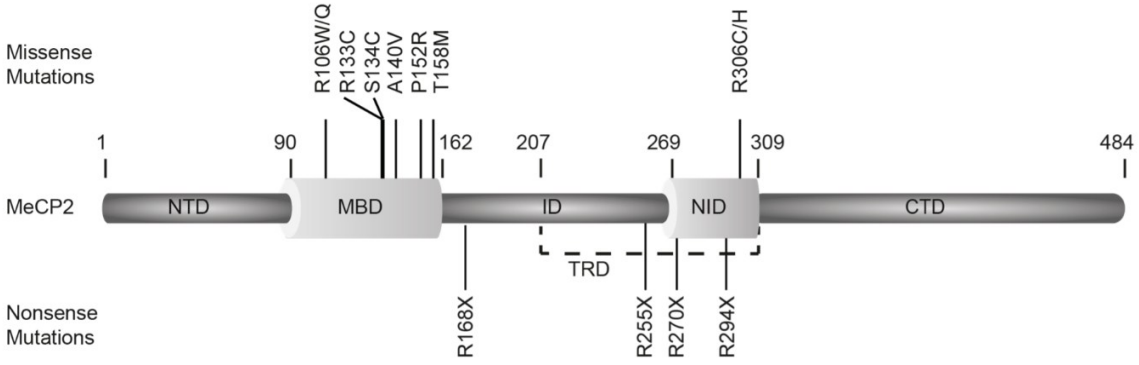

Figure 4: Domain-associated *MECP2* mutations. Most frequent *MECP2* mutations associated with RTT. Missense mutations are shown above and nonsense mutations below the scheme showing the structure of MeCP2. X indicates premature stop codons, thus generating a truncated protein [92].

2.3.2 Genotype-phenotype correlation in RTT

MECP2 genetic alterations are neither strictly necessary nor sufficient for a diagnosis of Rett syndrome. Indeed, approximately 3% of typical RTT patients and 30–40% of atypical RTT individuals do not carry detectable *MECP2* mutations. In fact, *MECP2* mutations can also be implicated in other neuropsychiatric disorders, such as autism spectrum disorder, intellectual disability, and early-onset psychosis [93], [94], [95], [96]. This complexity raises the question of whether *MECP2* mutations alone can explain the phenotypic variability observed in RTT.

To date, over 600 variants of the *MECP2* gene have been identified, with more than 70% of these being associated with RTT. Even though the pathogenic role of all identified *MECP2* mutations has not been fully elucidated yet, some genotype-phenotype correlation has been identified [79].

Indeed, certain mutations such as the missense mutation R133C and late truncating mutations are generally associated with milder clinical phenotypes. In contrast, missense mutations involving residues R306, T158, or R106, as well as early truncating mutations like R294X, tend to produce phenotypes of intermediate severity [97]. Early truncations and large deletions are usually linked to more severe RTT presentations. But what is the driver mechanism for the observed clinical variability?

The scientific community agrees that, beyond *MECP2* mutations, additional factors contribute to the clinical heterogeneity of RTT, among which the pattern of X-chromosome inactivation (XCI) plays a key role [1], [98]. XCI is a complex epigenetic process, initiated early in embryonic development, that ensures dosage compensation of X-linked genes between sexes by transcriptionally silencing one of the two X chromosomes in female mammals. This silencing is orchestrated by the X-inactive specific transcript (XIST) RNA, which coats the future inactive X chromosome *in cis*, recruiting chromatin-modifying complexes that induce repressive histone marks (e.g., H3K27me3), DNA methylation at promoter regions, and chromatin compaction [99], [100], [101]. In the context of RTT, skewing of XCI—favoring the silencing of the wild-type or mutant *MECP2* allele—has been implicated as a modulating factor in the phenotypic variability observed among female patients. Indeed, RTT girls are a mosaic of cells expressing either the wild-type or mutant allele; in general, in RTT girl patients XCI is balanced, with approximately half of the cells expressing the wild-type *MECP2* allele, while the other half express the mutant one [39]. Even though XCI is generally described as a random process, one X chromosome, as previously mentioned, can be preferentially inactivated over the other in a non-random manner (skewed). This can be due to selective advantages or disadvantages conferred by X-linked mutations to specific cell populations (C. Brown & Robinson, 2000; Plenge et al., 2002). When in cases of skewed XCI, the clinical phenotype can be markedly affected. Preferential inactivation of the X chromosome carrying the mutation can result in asymptomatic or very mild clinical manifestations, as observed in silent carriers. Conversely, preferential expression of the mutant allele can exacerbate disease severity, with the degree of clinical impact correlating with the extent of skewing [104] [Figure 5].

Another factor able to influence the severity of the diseases beside genotype-phenotype correlation concerns the presence of genetic modifiers of *MECP2*. Though the idea is well accepted, they have not been identified yet. Indeed, rare cases have been reported of females harbouring common *MECP2* mutations and exhibiting random XCI patterns who do not develop RTT symptoms, suggesting the presence of protective genetic factors elsewhere in the genome [105].

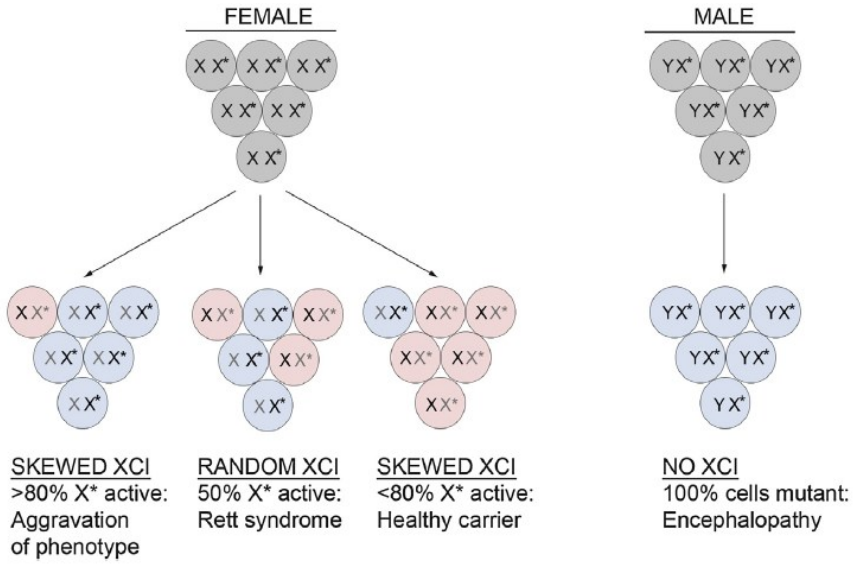

Figure 5. RTT phenotypic outcomes depend on X-chromosome inactivation pattern. Random X chromosome inactivation renders the tissue mosaic, with 50% of cells expressing the mutant allele (blue) and 50% expressing the wt one (pink). When X-inactivation is skewed toward the healthy allele, a majority of cells express the mutant gene, leading to a more severe phenotype **(left).** In healthy carriers favourably skewing of X-inactivation results in silencing of the mutant allele in most cells (right) (Modified from Frasca et al., 2023).

2.3.3 Rett syndrome is prevalently a girl-related disease

The predominance of RTT in females stems from the fact that *de novoMECP2* mutations primarily arise in male germline, and the paternal X chromosome is transmitted exclusively to daughters, as males inherit their single X chromosome from their mother [106]. Furthermore, the paternal bias is attributed to the elevated levels of DNA methylation in sperm and the numerous mitotic divisions that occur during spermatogenesis, both of which increase the likelihood of mutational events [52]. The underlying mechanism of C > T transitions likely involve oxidative deamination of methylated cytosines, a process more frequent in the male germline [30].

Of note these transitions, particularly at CpG dinucleotides, represent a well-known mechanism of spontaneous mutagenesis in the human genome [39], [106], [107], [108].

Although rare, *de novo MECP2* mutations can also be maternally transmitted or inherited from mothers who are asymptomatic or only mildly affected, often due to skewed X-chromosome inactivation favouring the expression of the wild-type allele and thus reducing clinical severity in carrier females [39]. Because these mothers carry the mutated X chromosome, they can pass it on to their sons, who, having only one X chromosome, may develop a range of clinical manifestations from developmental delay to severe early infantile epileptic encephalopathy with a reduced life span [109], [110], [111].

2.4 Pre-clinical research : *in vivo* models

Several mouse models carrying different *Mecp2* alterations were generated to improve the understanding of the functions of Mecp2 and of the pathogenesis of RTT. Soon after the identification of *MECP2* as the causative gene in RTT, two *Mecp2*-null male mouse models were generated, which are still the primary models used to study the disease. Exploiting the Cre-lox technology, Adrian Bird's laboratory generated the *Mecp2tm1.1Bird* model through the deletion of exons 3 and 4 of the gene in an inbred C57BL/6 background. The deleted region corresponds to the MBD, TRD and C-terminus domain of *Mecp2,* resulting in a complete lack of the protein [17]. Rudolph Jeanisch's laboratory, instead, removed only exon 3 -containing the MBD- and generated in a mixed genetic background (129, C57BL/6 and BALB/c) the *Mecp2tm1.1Jae* model, which expresses a small non-functional fragment of Mecp2 [18]. Both null models display a similar phenotype that recapitulates RTT features. Indeed, they appear phenotypically normal until 4 weeks of age when they begin to develop hind limb clasping, tremors, breathing irregularities, loss of muscle tone, and hypoactivity [17], [18]. These mice, which also display reduced brain volume and body weight, undergo rapid phenotypic regression and die between 6 and 12 weeks of age [17], [18].

Given that RTT predominantly affects females and considering that patients carry a heterozygous *MECP2* mutation, heterozygous female mice (het) represent the most appropriate genetic model for studying the disease pathogenesis. However, their use in experimental studies presents several limitations that must be taken into consideration. First, they require a longer period for symptoms to appear and show less consistency compared to null mice. In addition, they exhibit high phenotypic variability, likely caused by differential X-chromosome inactivation [112]. In particular, they appear normal up to 3-6 month of life, when they start manifesting RTT-like symptoms, such as inertia, ataxic gait, hind limb clasping and irregular breathing. In contrast to the null males, females usually do not have an abnormal life span compared to healthy controls, although they become overweight with ageing [113].

Even though the use of female mouse models is not so widespread, the scientific community is nowadays starting to consider sex as a relevant biological variable in diseases' onset and progression. Accordingly, heterozygous (het) *Mecp2*$^{-/+}$ mice are emerging as essential model to complement results coming from males. I believe that both animal models should be taken into account when studying RTT, since preclinical research relying exclusively on male *Mecp2*-null mice—which completely lack *Mecp2* expression—may fail to capture the influence of mutant alleles on neighbouring wild-type cells, the so-called "non-cell-autonomous effect," which can instead be consistently reproduced in heterozygous female mice [104], [114], [115].

However, maintaining the colony on the C57BL/6 background presents significant challenges. Specifically, C57BL/6 heterozygous females produce small litters, exhibit aggressive behaviour, and frequently engage in cannibalism, all of which negatively impact maternal care and, consequently, the phenotype of the offspring [116]. To address these limitations, our laboratory transferred the *Mecp2^tm1.1Bird^* mutation into the outbred CD1 (ICR) genetic background [116], observing a marked increase in litter size -nearly doubled compared to the C57BL/6 background- with a corresponding increased number of null and heterozygous animals obtained from a single litter.

Furthermore, CD1 females displayed significantly improved maternal behaviour, with a notable reduction in cannibalized litters [116]. Notably, an outbred strain allows to better recapitulate human genetic variability, although for the same principles it features greater phenotypic heterogenicity [117]. Importantly, when evaluated using a standardized scoring system for assessing the progression of typical Rett syndrome symptoms in mice [17], CD1 *Mecp2* null mice exhibited all the major phenotypic traits observed in C57BL/6 knock-out mice, even though delayed in time, **[Figure 6]** [116].

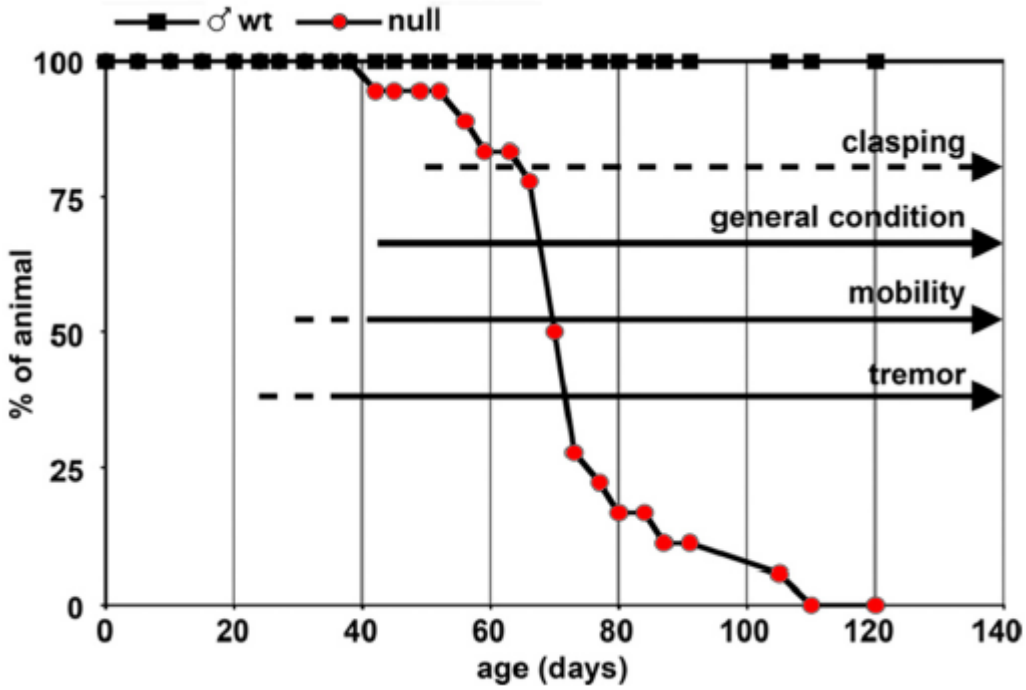

.

Figure 6: timeline of the onset of CD1 *Mecp2*-null phenotypic traits. Arrows represent the timing of appearance of the different symptoms of RTT mice. Dotted lines = 50–99% of animals have the given symptoms; continuous line = 100% of the animals have the symptoms [116].

In 2002, a third RTT male mouse model was generated to mimic a truncating mutation previously seen in RTT patients, the *Mecp2^308/y* mice [52]. Differently to null-mouse models, *Mecp2^308/y* mice was engineered to remove just the C-terminus, maintaining the MBD and the TRD [118]. In this case, obtained mice exhibited a milder phenotype characterized by tremors, hypoactivity, seizures, kyphosis, anxiety, forepaw stereotypies, and learning and memory defects starting from 6 weeks of age. Their lifespan is also extended up to one year [118].

Of the eight most common mutations in RTT patients, six have an established mouse model which recapitulates symptoms of the disease: for the nonsense mutations they generated *Mecp2* R168X, R255X mice and for the missense mutations *Mecp2* T158A, A140V, R133C, R306C, Y120D mice [118], [119], [120], [121].

All these animal models have been instrumental in understanding the functional consequences of RTT-causing mutations and their correlation to symptom severity [120], [122].

To elucidate the role of *Mecp2* in distinct tissues, brain regions, and cell types, conditional animal models were developed by introducing loxP sites flanking specific regions of the gene (Renieri et al., 2003; Tudor et al., 2002; Nuber et al., 2005). These floxed mice can be crossed with transgenic lines expressing Cre recombinase under tissue- or cell type-specific promoters, enabling spatially and temporally controlled deletion of *Mecp2* in targeted tissues or cell populations. Such models have significantly advanced our understanding of Mecp2 function both within the central nervous system (CNS) and peripheral tissues [18], [31], [125], [126], [127].

Of particular importance, a breakthrough in Rett syndrome research came from conditional mouse models that allowed reactivation of the endogenous *Mecp2* gene, demonstrating for the first time that RTT phenotypes are reversible. Indeed, Guy et al. (2007) generated a 'Floxed-Stop' mouse line carrying a transcriptional STOP cassette flanked by loxP sites inserted into the endogenous *Mecp2* gene, which globally silenced *Mecp2* expression [128]. These mice were crossed with a ubiquitously expressing tamoxifen-inducible Cre-ER line. Systemic tamoxifen treatment in severely affected RTT mice restored *Mecp2* expression to about 80% of wild-type levels. This led to a striking reversal of neurological deficits and normalization of survival, providing compelling evidence that *Mecp2* deficiency-induced neurological impairments are reversible—at least in the mouse model. This discovery opened new avenues for potential treatments of MeCP2-related disorders even at late stages of disease progression [128].

2.5 Neurological Consequences of MeCP2 Deficiency

Increasing evidence indicates that MeCP2 plays a critical role not only in postnatal brain function but also during prenatal development. Although Rett syndrome was initially considered a postnatal disorder primarily affecting synaptic function, mice studies suggested that its pathological mechanisms may begin much earlier. In agreement with this, Mecp2 is expressed from the earliest stages of embryogenesis and is found across multiple cell types, including neuronal progenitors, although its expression levels are higher in mature neurons [129]. Supporting this, both *Mecp2*-null mice and children with RTT exhibit subtle but consistent neurological abnormalities immediately after birth, suggesting that the disorder has prenatal origins [130].

Post-mortem analyses of RTT brains have revealed marked morphological abnormalities, including reduced dendritic arborization and smaller neuronal soma size all contributing to a decrease in overall brain volume [131], [132], [133], [134], [135], [136]. These alterations are especially pronounced in the prefrontal, posterior frontal, and anterior temporal regions (Duncan Armstrong & The Blue Bird, 2005). Notably, similar structural defects are observed in mouse models of RTT (Carli et al., 2023; Chao et al., 2007; Duncan Armstrong et al., 2003; Sampathkumar et al., 2016).

Unlike classical neurodegenerative disorders, RTT does not involve widespread neuronal death [141], [142], [143], supporting the view that it represents a neurodevelopmental disorder rather than a neurodegenerative condition [39].

In addition to these morphological and developmental abnormalities, RTT is also characterized by profound functional impairments at the synaptic level. Both Rett syndrome patients and *Mecp2*-deficient mouse models show significant dysregulation of genes involved in excitatory and inhibitory synaptic transmission, including alterations in AMPA (alpha-amino-3-hydroxy-5-methyl-4-

isoxazolepropionic acid), NMDA (N-methyl-D-aspartate), and GABA (gamma-aminobutyric acid) receptor expression and function [144], [145]. In line with these findings, long-term potentiation (LTP), a cellular mechanism underlying synaptic strengthening, is significantly impaired in various *Mecp2* mutant models in cortical and hippocampal slices (Asaka et al., 2006 ; Moretti et al., 2006). At the molecular level, these synaptic dysfunctions correlate with a strong reduction in VGlut1-PSD95 puncta, reflecting a loss of functional excitatory synapses [138].

Although most studies report global hypoactivity, region-specific differences have also been observed. Using *c-fos* expression as a marker for neuronal activation, Kron et al. (2012) showed that whole-brain activity in *Mecp2*-null mice is not homogeneous, with reduced activity in the forebrain and increased activity in the hindbrain [147]. Moreover, Calfa et al. (2015) demonstrated that hippocampal CA3 neurons exhibit hyperactivity, which is associated with decreased GABA-A receptor expression and increased levels of the GluA1 subunit. These findings indicate that MeCP2 deficiency does not affect all brain regions uniformly but instead leads to region-specific imbalances in excitatory and inhibitory signalling [147], [148]. Altogether these findings underscore the pivotal role of MeCP2 in maintaining synaptic plasticity, circuit homeostasis, and neuronal structure, and highlight the need for therapeutic strategies aimed at restoring excitatory–inhibitory balance across affected brain regions [149].

2.5.1 MeCP2 involvement in neuronal activity and synaptic plasticity

Neuronal activity is essential not only for preserving the functional integrity of mature neurons but also for proper brain development.
Neurons regulate their excitability by controlling the distribution of ions such as Na^+, K^+, and Cl^- across the plasma membrane. A key aspect of this regulation involves maintaining low intracellular concentrations of Ca^{2+}, as this ion serves as a potent activator of various intracellular signaling cascades (Leslie & Nedivi, 2011). At glutamatergic synapses, Ca^{2+} can enter the postsynaptic neuron through several mechanisms, including Ca^{2+}-permeable AMPA receptors, NMDA receptors, and voltage-gated Ca^{2+} channels. Each of these pathways initiates distinct cellular responses that ultimately converge in the nucleus to activate transcription factors, thereby influencing gene expression. Transcription factors such as CREB (cAMP response element binding), serum response factor, and myocyte enhancer factor 2 are key mediators of activity-dependent gene expression [150], [151]. Among them, CREB has been extensively studied for its role in promoting excitatory synapse formation. In hippocampal neurons, CREB activation via CaMKI or CaMKIV-mediated phosphorylation is necessary for dendritic arborization in response to membrane depolarization or NMDA receptor stimulation [152]. cAMP-dependent protein kinase (PKA)/CREB signalling pathway is also responsible for the activation of Immediate Early Genes (IEGs) [153] such as *c-fos*, *Arc/Arg3.1*, and *Egr1, Dusp1*, which play critical roles in key processes such as neuronal survival, dendritic morphogenesis, and synaptic plasticity [150]. They act as transcriptional hubs that link synaptic activity to downstream genetic programs. Their rapid and transient activation enables the nervous system to respond dynamically to environmental inputs [154].

MeCP2 is also classified as an activity-dependent transcriptional regulator. It is rapidly phosphorylated at Ser421 in response to synaptic activity in vivo, and similarly in vitro following NMDA receptor activation or membrane depolarization [56], suggesting that its function is

dynamically modulated by neuronal activity. As previously discussed, MeCP2 deficiency disrupts the balance between excitatory and inhibitory synapses [155], further implicating it in the regulation of synaptic development and plasticity. All these evidences suggest that RTT may be a disorder of impaired activity-dependent gene regulation [151]. Among the genes most consistently dysregulated in both RTT patients and *Mecp2*-null mice is Brain-Derived Neurotrophic Factor (BDNF). Given its role in neuronal development and plasticity, BDNF is the most extensively studied activity-regulated gene [150]. In line with its classification as a neurotrophin, BDNF contributes to the growth and branching of axons and dendrites during early neuronal development [156]. In addition to these structural effects, BDNF also modulates synaptic transmission at both excitatory and inhibitory synapses [157], [158] and plays a central role in the induction and maintenance of long-term potentiation (LTP), a key mechanism of synaptic plasticity [159]. Importantly, BDNF expression is consistently downregulated in both RTT patients and *Mecp2*-deficient mouse models [57], [160], likely because of impaired neuronal activity and plasticity caused by MeCP2 dysfunction. This downregulation may contribute to the synaptic immaturity observed in RTT neurons, reinforcing the idea that MeCP2 is essential for the regulation of genes critical for activity-dependent synaptic development and plasticity.

2.5.2 The role of MeCP2 in regulating neuronal activity in early neural development and mature neurons

During brain development, neurons begin to exhibit spontaneous activity even before forming mature and fully connected circuits. This early activity is mainly driven by intrinsic factors, such as high glutamate levels during early differentiation [161]. Early glutamatergic transmission is active and capable of stimulating both ionotropic (iGluRs) and metabotropic (mGluRs) glutamate receptors [162]. This spontaneous activity supports essential neurodevelopmental processes such as neuronal migration, maturation, identity specification, and survival [163]. Moreover, it has been observed in several brain regions, especially the cerebral cortex, that early calcium transients guide the assembly of neural circuits [164]. Thus, calcium signalling contributes to synaptic refinement by influencing activity-dependent processes that lead to the stabilization of some synaptic connections and the elimination of others, in parallel with dendritic and axonal growth and pruning (L. C. Katz & Shatz, 1996).

As development progresses, spontaneous activity is complemented by experience-driven plasticity, especially through sensory inputs. These inputs remodel neuronal circuits via calcium signalling mainly through NMDA receptors, which activate gene expression programs involved in learning, memory, and synaptic plasticity [150]. In mature neurons, the key neurotransmitters involved in triggering calcium influx are glutamate and GABA (gamma Aminobutyric acid). Glutamate promotes excitatory responses by depolarizing the membrane, while GABA generally has inhibitory effects through hyperpolarization [166].

Beyond transmitting signals, glutamate also support synaptic maturation. On one hand, NMDA receptor activation encourages cytoskeletal and scaffold protein accumulation within dendritic spines [167], [168]; on the other hand, AMPA receptor trafficking is essential for synapse stabilization and dendritic spine development [169], [170]. Indeed, when neurons are repeatedly activated together, the receiving neuron increases the number of AMPA receptors on its surface. This makes the connection

between them stronger and more efficient. This process is a key part of how the brain strengthens or weakens synapses over time, known also as LTP and LTD (long term-depression) [150].
Importantly, as mentioned before, neuronal activity is not just a consequence of maturation, it is also a driving force. This mutual relationship is described as a feed-forward cycle, where activity promotes the expression of genes that encodes for ion channels, receptors, and ligands. The secretion of the ligands drives electrical activity that generates transient elevation of calcium, which in turn regulates gene expression that enables further neuronal development and more complex activity patterns [171]. This cycle is essential for establishing mature and functional neural networks [163], [172], [173], acting as a checkpoint that fine-tunes genetic programs and guides neurons toward full maturity.

The transcriptional regulator MeCP2 plays a central role in this process. In *null*-neurons, both spontaneous activity and gene expression are altered, suggesting a breakdown in this activity-dependent maturation loop [87], [129]. Of note, these alterations appear early in development and persist into adulthood emphasizing the importance of early developmental phases [174], [175].
To further support this concept, a recent study from our laboratory demonstrated that stimulation of neuronal activity through early administration of the Ampakine CX546, partially restores gene expression and neuronal maturation in *Mecp2*-null neurons, as well as behavioural deficits in mouse models of RTT [176]. Notably, these improvements were long-lasting, suggesting that early intervention may help to re-initiate the feed-forward cycle and support more typical developmental trajectories.

2.6 The Glutamatergic System

Glutamate is the primary excitatory neurotransmitter in the central nervous system (CNS). Glutamate receptors play crucial roles in numerous cognitive and neurodevelopmental processes, including learning, memory formation, spine maturation, circuit development, and synaptic plasticity[177], [178], [179], [180], [181]. Dysregulation of glutamatergic signalling is a major contributor to neurodevelopmental disorders (NDDs), with glutamate emerging as a key molecule involved in the comorbidities observed among various neurological diseases [182].

Glutamate is present at high concentrations throughout almost all brain regions, and its receptors are widely expressed in both neuronal and non-neuronal cells. The concentration of glutamate in the synaptic cleft ranges in the low micromolar range (approximately 3–4 μM), while extracellular fluid and cerebrospinal fluid concentrations are around 10 μM [183]

Glutamate is primarily released from glutamatergic presynaptic terminals through synaptic vesicle fusion at the active zone. Once released into the synaptic cleft, glutamate binds to various classes of receptors located predominantly on the postsynaptic compartment, which is often represented by dendritic spines [184]. These spines extend from the dendrite via a narrow neck that expands opposite the presynaptic terminal.

Glutamatergic receptors (GluRs) are classified into two major categories: ionotropic glutamate receptors (iGluRs) and metabotropic glutamate receptors (mGluRs) [185]. The ionotropic receptors are named after their principal agonists and include N-methyl-D-aspartate receptors (NMDA receptors), α-amino-3-hydroxy-5-methyl-4-isoxazolepropionic acid receptors (AMPA receptors), and

kainate receptors [185]. The metabotropic receptor mGluR belong to the G protein-coupled receptor (GPCR) family [186], [187].

2.6.1 Metabotropic receptors

Metabotropic receptors or mGluR act in concert with G-proteins to induce second messenger pathways and trigger a cascade of biochemical reactions; they are widely expressed in the central and peripheral nervous system, and they mediate neuronal excitability and synaptic transmission [188]. These receptors produce slow responses and contribute to long-lasting changes in synaptic function [189]. Eight different mGluR subtypes have been identified so far based on sequence homology, second messenger coupling and on their pharmacological properties [190]. Their structure is composed by an extracellular N-termini domain, responsible for the binding of glutamate, a transmembrane domain and a cytoplasmatic C-terminal domain which interacts and activates G-proteins [191].

2.6.2 Ionotropic receptors

Ionotropic glutamate receptors (iGluRs) are transmembrane proteins which form glutamate-gated ion channels. They are responsible for rapid excitatory transmission capable of transmitting excitatory signals to postsynaptic neurons within milliseconds [189]. All iGluRs are nonselective channels that facilitate the entry of cations such as Na^+, K^+, and sometimes Ca^{2+}. The activation of NMDA, AMPA, and kainate receptors results in excitatory post-synaptic responses, with a minor role of the letter in synaptic plasticity [189].

Structurally, all iGluRs share a tetrameric assembly, with each subunit composed of distinct domains: an extracellular amino-terminal domain (ATD), the extracellular LBD, a transmembrane domain (TMD), and an intracellular carboxy-terminal domain (CTD) [192].

The activation mechanisms among iGluR subtypes are generally conserved and occur through a three-step process: initial binding of the agonist to the ligand-binding domain (LBD), a subsequent conformational change that stabilizes this binding (often described as 'clam shell' closure), and finally, structural rearrangements within the ion channel that permit ion flow [134], [193]. This ion movement generates an excitatory postsynaptic current, which can summate to trigger action potentials in the postsynaptic neuron. Termination of receptor activity can occur through either deactivation or desensitization [194], [195], [196]. Each subunit of the receptor has two extracellular domains that together form a V-shaped structure. Adjacent subunits interact through these V domains, forming two dimers within the tetrameric receptor complex [Figure 7b]. When a transmitter binds to one subunit, it induces a conformational change in which one domain moves toward its partner, closing the V and trapping the transmitter. This movement generates tension across the transmembrane region of the subunit, promoting channel opening [Figure 7b]. The channel returns to its closed state once the V reopens and the transmitter is released, a process referred as deactivation. Alternatively, the binding of the transmitter may destabilize the dimer interface, causing the V domains to remain closed while the channel closes, this ligand-bound but non-conducting state is known as desensitization [Figure 7b] [197].

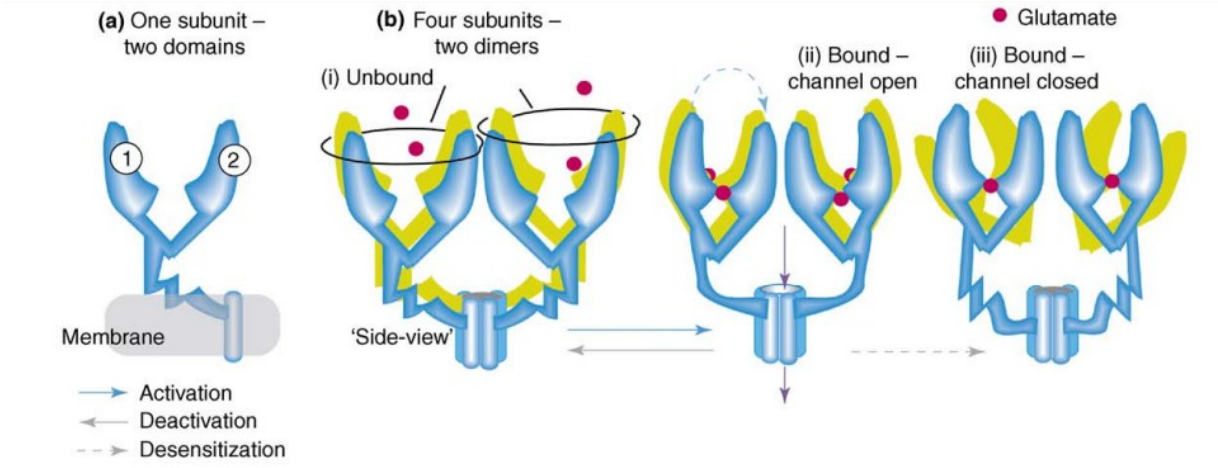

Figure 7: iGluR activation, deactivation, desensitization. (a) Schematic illustration of a single subunit of the tetrameric receptor. Included are two extracellular domains (1 and 2), a bridge segment and a transmembrane zone. Together four such zones form an ion channel. (b) (i) The unbound tetrameric receptor viewed perpendicular to a plane running through the two extracellular domains ('side-view'). The subunits in the complete receptor pair-up, forming two dimers. (ii) Binding sites for the transmitter glutamate (red dot) are located between the extracellular domains of each subunit. The binding event causes one domain to move towards the other, resulting in a conformational change in the subunit bridge region. This stresses the transmembrane zone and opens the receptor channel. Current is terminated when either of two events occurs: either the domains move apart, releasing the transmitter and removing the tension on the ion channel (deactivation; gray solid arrow), or the binding event disrupts the dimers, and thereby removes the tension on the channel (desensitization; gray broken arrow). Note that in this desensitized state (iii), the channel is closed although transmitter remains bound (*Modified from* Lynch & Gall, 2006).

2.6.2.1 NMDARs

NMDA receptors are heterotetrameric ion channels typically composed of two GluN1 subunits and two GluN2 (A–D) and/or GluN3 (A–B) subunits. The GluN1 subunit is essential for receptor function and is encoded by a single gene (GRIN1), while GluN2 and GluN3 subunits, encoded by the GRIN2 and GRIN3 gene families respectively, confer distinct biophysical and pharmacological properties to the receptor [198]. NMDARs are mainly involved in synaptic plasticity and, thus, in learning, memory and higher cognitive functions. Calcium influx, produced by the opening of NMDARs, induces a cascade of events crucial for these processes, resulting in synapse potentiation. This phenomenon occurs by increasing the size of the dendritic spine head and of the underlying PSD that allows more glutamate receptors to localize at the site, providing a stronger response to neurotransmitter release [198]. In the NMDA receptor, a Mg^{2+} binding site binds Mg^{2+} in the presence of hyperpolarized membrane potentials and eventually blocks the opening of the NMDA receptor channel, thus restricting the entry of Ca^{2+} ions [199]. However, when the synaptic membrane is depolarized, Mg^{2+} is removed, thereby allowing access to Ca^{2+} ions, a property that is the basis for synaptic plasticity. Activation of the NMDA receptor depends on the presence of two co-agonists: glutamate and glycine (or D-serine), which must bind to distinct but complementary sites on the receptor. Although both NMDA and AMPA receptors can allow entry for cations, weak stimulation causes the activation of only the AMPA receptors [199]

2.6.2.2 AMPARs

AMPA receptors are the earliest ionotropic glutamate receptors to appear during the embryonic development of the central nervous system, with functional receptors expressed as early as embryonic day 13 in rodent brains, particularly in the proliferative zones [200]. They serve as the principal mediators of fast excitatory synaptic transmission in the mammalian brain and are essential for synaptic plasticity, memory formation, and effective synaptic communication [201], [202]. Regarding their distribution across the brain, about 50% of all AMPARs in the adult rat brain are found in the cortex, while hippocampus and cerebellum together harbour another 40% [203]. A small percentage of AMPA receptors are also present in the peripheral nervous system, including sensory ganglia, cutaneous fibers, and immature Schwann cells, where they play a role in nociception and inflammatory pain [204], [205].

These receptors are assembled from four distinct subunits: GluA1, GluA2, GluA3, and GluA4 [185]. In the adult brain, AMPA receptors predominantly exist as heterotetramers composed of two dimers, mainly GluA1/GluA2 and GluA2/GluA3. The GluA4 subunit is highly expressed during early developmental stages but absent in mature neurons [203], [206]. Within the postsynaptic density, GluA1-2 receptors are relatively less abundant but are notably recruited to synapses during LTP [207]. Conversely, GluA2-3 receptors undergo constitutive cycling in and out of the PSD independently of synaptic activity [207].

The assembly of functional AMPA receptor tetramers occurs in the endoplasmic reticulum, after which they are trafficked via endosomes to the synaptic membrane, where they form ion channels [208], [209]. The specific combination of subunits influences channel kinetics, ion selectivity, and receptor trafficking patterns, thereby contributing to the functional diversity of AMPA receptors. Moreover, auxiliary proteins, such as transmembrane AMPA Receptor Regulatory Proteins (TARPs), modulate receptor trafficking, gating, channel conductance, and synaptic retention [209]. AMPA receptors are continuously trafficked to and from the synaptic surface on a timescale of seconds to minutes, a dynamic process critical for synaptic plasticity [210]. The insertion of AMPA receptors into the synaptic membrane is a key event underlying LTP, whereas their removal is associated with LTD [210], [211].

During strong excitatory stimulation, activation of AMPA receptors depolarizes the postsynaptic membrane sufficiently to remove the Mg^{2+} block from NMDA receptors, allowing the influx of cations, including Ca^{2+} [212]. The resulting rise in intracellular Ca^{2+} triggers signalling cascades, including the binding of Ca^{2+} to calmodulin (CaM). CaM subsequently activates Ca^{2+}/calmodulin-dependent protein kinase II (CaMKII), which phosphorylates AMPA receptors, enhancing their Na^{+} conductance [212]. Additionally, CaM promotes the trafficking of AMPA receptors from intracellular stores to the synaptic membrane, thereby increasing receptor density and strengthening synaptic responses. This process is fundamental to the mechanism of LTP [213], [214], [215].

In mature neurons, AMPA receptors are largely impermeable to calcium ions, a property regulated by the presence of the GluA2 subunit. This subunit undergoes RNA editing known as Q/R editing, where a glutamine (Q) residue in the second transmembrane domain is post-transcriptionally replaced by arginine (R). This modification blocks the passage of divalent cations such as Ca^{2+} and reduces channel conductance [216].

2.7 Modulators of AMPARs: Ampakines

Ampakines are positive allosteric modulators (PAMs) of AMPA receptors. They bind to an allosteric site distinct from the orthosteric glutamate-binding site, modulating receptor activity without acting as direct agonists or antagonists [217]. Upon glutamate binding, ampakines stabilize the receptor's open-channel state, thereby prolonging current flow and enhancing synaptic transmission [218]. These compounds efficiently cross the blood–brain barrier and exhibit sufficient potency to modulate AMPA receptor function *in vivo* [219].

Early efforts to modulate AMPA receptors focused on racetams, a class of non-selective compounds with proposed nootropic effects [220]. However, due to their inconsistent clinical efficacy, research gradually shifted toward the development of more selective AMPA receptor modulators, specifically, ampakines [213]. The majority of clinically investigated ampakines belong to the benzamide structural class. These molecules have been approved for clinical trials for various neuropsychiatric and neurodegenerative conditions, including Alzheimer's disease, attention-deficit/hyperactivity disorder (ADHD), mild cognitive impairment, and major depressive disorder [197], [221], [222], [223], [224], [225]. A summary of these compounds and their respective clinical applications is provided in **[Table 2]** [219]. All of them demonstrated cognitive-enhancing effects in preclinical studies (A. Arai & Kessler, 2007; Brogi et al., 2019;Kadriu et al., 2021).

At the neurobiological level, three principal mechanisms underlie these effects: (i) Ampakines enhance excitatory synaptic transmission, potentially correcting deficits in cortical signalling associated with cognitive dysfunction [226]; (ii) they increase brain-derived neurotrophic factor (BDNF) expression, promoting neurotrophic support [227]; and (iii) they promote LTP by lowering its induction threshold and increasing its magnitude, thereby explaining the observed improvements in learning [228].

Structural analyses using X-ray crystallography revealed that Ampakines bind near the dimer interface of the AMPA receptor's extracellular domain, a strategic position for both slowing deactivation (delaying channel closing after glutamate unbinding) and reducing desensitization by stabilizing the dimer configuration (Jin et al., 2005; A. Arai & Lynch, 1998). Based on their pharmacodynamic properties, Ampakines are classified into two major groups: high-impact and low-impact [230].

High-impact Ampakines destabilize the desensitized conformation of AMPA receptors, prolonging ion channel opening and increasing the duration of steady-state currents. They also enhance glutamate affinity under sub-saturating conditions, boosting peak currents. Although peak currents change little under saturating conditions, these compounds markedly reduce receptor desensitization [231], [232].

In contrast, low-impact ampakines modulate receptor function in an occupancy-dependent manner: at low occupancy, they accelerate channel opening; at high occupancy, they slow channel closing. This results in an increase in response amplitude rather than duration (Zivkovic et al., 2013; Lynch, 2006). Because they do not prolong receptor activation in a way that mimics excess glutamate exposure, a process associated with excitotoxicity, low-impact Ampakines are considered safer compared to high-impact ones (Arai et al., 2002; Krintel et al., 2013).

Nevertheless, high-impact Ampakines remain highly efficacious, and seizure risk typically appears only at doses slightly above the therapeutic range (Kunugi et al., 2019; Shaffer et al., 2013). To expand the therapeutic window of high-impact modulators, Takeda Pharmaceuticals developed a new generation of AMPAR-positive allosteric modulators (PAMs) specifically designed to act solely

through allosteric potentiation, without exhibiting intrinsic agonist activity (Suzuki et al., 2019; Taneka et al., 2019). This contrasts with earlier high impact compounds, which were initially believed to lack agonist activity but were later found to possess intrinsic agonism (Kunugi et al., 2019).

Ampakine	Class	Clinical endpoint
CX1739	Low-impact	Opiate-induced respiratory depression
CX717	Low-impact	ADHD
CX691, farampator	Low-impact	MDD, cognitive deficits in schizophrenia
S47445 ,CX1632 , turlampator	High-impact	AD, MDD
S18986	High-impact	MCI
BIIB-104	High-impact	Hearing loss, Ketamine-induced cognitive impairment, Cognitive impairment in schizophrenia
ORG-26576	High-impact	MDD, ADHD
CX546	High-impact	
GSK729327	High-impact	Schizophrenia
LY451395, mibampator	High-impact	Cognitive enhancer, ADHD
CX1942	Low-impact	
CX516,ampalex	Low-impact	Schizophrenia, Fragile X syndrome/autism, MCI, AD
CX1837	High-impact	
CX1846	High-impact	
TAK-653	High-impact	MDD

Table 2. AMPAkines with cognitive enhancing effects (Radin et al., 2025).

AD: Alzheimer's disease, ADHD: Attention Deficit Hyperactivity Disorder, MCI : Mild cognitive impairment, MDD: Major depressive disorder.

3. Materials and methods

3.1 Animals care

The *Mecp2* mouse strain was originally purchased from Jackson Laboratories (B6.129P2 (C)-*Mecp2*tm1.1Bird/J) and transferred on a CD1 genetic background. The phenotypes affecting these animals have been previously described [17], [116]. Time pregnant females were generated by crossing overnight wt CD1 males with *Mecp2* heterozygous females; the day of vaginal plug was considered E.0.5. Mice were housed in groups of five in Tecniplast cages, on a 12h light/dark cycle in a temperature-controlled environment (21+/-2°C) with food and water provided ad libitum.
All procedures were accomplished in accordance with European Community Council Directive 2010/63/UE for care and use of experimental animals with protocols approved by Italian Government and the San Raffaele Scientific Institutional Animal Care and Use Committee.

3.1.1 Genotyping

The genotype of mice and mouse embryos was assessed through Polymerase Chain Reaction (PCR) protocol. Genomic DNA was extracted from ear biopsies of P10 mice or from paws/tails of embryos and then subjected to PCR.

3.1.1.1 DNA extraction from mice biopsies.

Tail Lysis Buffer (Tris 100mM pH=8, EDTA 10mM pH=8, SDS 0.5%, NaCl 100mM) and Proteinase K (0.5 mg/mL, Genespin, #STS-OK500) were used to dissociate each sample and maintained O/N at 55° C. The day after, samples were centrifuged (13,000rpm, 10 minutes) to remove any debris left. Then, 1:1 of 100% isopropanol (SIGMA, #33539) was added to the supernatants to induce DNA precipitation (13,000rpm, 10 minutes, room temperature RT). Supernatants were removed and DNA pellets were washed with 500µL of 70% ethanol (EtOH) and centrifuged at 13,000rpm for 5 minutes. EtOH was eliminated, pellets were dried at RT and resuspended in 200µL of TE (Tris 10mM, EDAT 1mM, pH=8) for DNA quantification, performed with a spectrophotometer (Nanodrop 1000, ThermoFisher).

3.1.1.2 DNA extraction from embryonic paw biopsies.

Tissues were dissociated with "Phire animal tissue direct PCR kit" (Thermo Scientific F140WH) to rapidly extract DNA from samples used in primary cultures. In detail, each sample (mouse paw or tail) was incubated with a 20 µL mix (19.5µL Dilution Buffer + 0.5µL DNA Release Additive provided with the "Phire animal tissue direct PCR kit") for 3 minutes at RT. Then, the reaction was stopped at 98°C for 2 minutes and supernatant was diluted with 10µL of the Dilution buffer and directly used for DNA quantification. For embryonic samples, both genotyping and sex PCRs were conducted. The reaction mixes for one sample (Final volume=20µL) for PCR amplification are reported in Table 3.1 and 3.2.

***Mecp2* null protocol**			
Reagents	**Initial concentration**	**Final concentration**	**Final volume**
Xtra RTL GL Reaction Buffer (Genenspin, #XSTS-T5XRTL)	5X	1X	4µL
dNTPs (Promega, #U120A, U121A, U122A, U123A)	10mM	0,2mM	0,4µL

Common primer	10mM	0,25µM	0,5µL
Reverse primer (wt allele)	10mM	0,25µM	0,5µL
Reverse primer (ko allele)	10mM	0,25µM	0,5µL
XtraTaq Pol RTL (Genespin, #XSTS-T5XRTL)	5U/µL	0,125U/µL	0,5µL
H2O	-	-	12,6µL
gDNA	100ng	5ng/µL	1µL

Table 3.1 Reagents for determination of genotype.

Sex protocol			
Reagents	**Initial concentration**	**Final concentration**	**Final volume**
Xtra RTL GL Reaction Buffer (Genenspin, #XSTS-T5XRTL)	5X	1X	4µL
dNTPs (Promega, #U120A, U121A, U122A, U123A)	10mM	0,2mM	0,4µL
Forward primer	10mM	0,625µM	0,125µL
Reverse primer	10mM	0,625µM	0,125µL
XtraTaq Pol RTL (Genespin, #XSTS-T5XRTL)	5U/µL	0,125U/µL	0,5µL
H2O	-	-	13,85µL
gDNA	100ng	5ng/µL	1µL

Table 3.2 Reagents for determination of sex.

PCR products were resolved by electrophoresis run in 2% agarose gel (120V, 20 minutes run in TAE 1X buffer). Negative control (19 µL reaction mix + 1 µL H2O) and positive controls (19 µL reaction mix + 1 µL DNA of HET, WT, and KO mice) were always included.

Primers used for genotype:

Mecp2 FF: 5'-AAATTGGGTTACACCGCTGA-3',

Mecp2 RV: mut 5'-CCACCTAGCCTGCCTGTACT-3',

Mecp2 REV: wt 5'-CTGTATCCTTGGGTCAAGCTG-3'.

Primers used for sex determination:

FF: 5'-AAGTCTGCATTACATTCCTCGA-3',

REV: 5'-GTTTTCTGAAAGAGGGACAGTTT-3'.

Step	Mecp2 null	Sex
Heat lid	110°C	110°C
Denaturation	94°C (5min)	95°C (2min)
Start loop	35X	35X
Denaturation	94°C (30sec)	95°C (30sec)
Annealing	60°C (30sec)	59°C (30sec)
Extension	72°C (1min)	72°C (30sec)
Close loop	-	-
Final extension	72°C (5min)	72°C (5min)
Hold	4°C (∞)	4°C (∞)

Table 2: PCR cycles for genotyping and sex determination.

The resulting PCR products are:

- For *Mecp2* null strain: WT mice present a band of 465 bp, while *Mecp2* KO mice present a band of 240 bp. Heterozygous mice exhibit both bands, one for each allele.
- For sex determination: the amplification of *Jarid1* produces a fragment of 113bp only in males.

3.2 RNA purification, cDNA synthesis and quantitative RT–PCR

Mutant mice and WT littermates at the established post-natal day were sacrificed by dislocation and brains were rapidly removed. Selected tissues were dissected and immediately frozen on dry-ice and stored at -80°C until analysis. Tissues were lysed and total RNA was extracted using Purezol (Bio-Rad, #7326890) and a Potter-ELV glass grinder was used to mechanically triturate selected tissues. Samples were incubated for 5 minutes at RT and 100% chloroform (Sigma-Merk, #372978) was added 1:5 (200uL/1mL Purezol) and centrifugated (13,000g, 20 minutes, 4°C) to separate the aqueous and the organic phases. The aqueous solution containing the RNA was isolated and added with 100% isopropanol to induce RNA precipitation. Samples were stored at -20°C O/N. The following day, sample were centrifugated (13,000g, 20 minutes, 4°C) and washed with 70% EtOH. A step to remove genomic DNA was performed, DNase (Sigma AMPD1) was directly added to dried pellets (20 µL of a mix composed of: 17µL H2O RNAse-free + 2µL supplied DNAse buffer + 1µL DNase amplification grade) and incubated at 37°C for 15 minutes in a dry bath. RNA was further purified by adding 80µL Purezol/sample, following the exact protocol and proportions of the volumes mentioned above, until pellet precipitation in 100% isopropanol and wash in 70% EtOH the next day. At this step, RNA was completely dried at RT, resuspended in 30µL of H_2O RNAse-free for pre-frontal cortex, and stored at –80°C until analysis. RNA was quantified using a spectrophotometer (NanoDrop 1000) and RNA integrity was verified by agarose electrophoresis. Good quality RNA samples, exhibiting the 28S and 18S bands with a relative intensity of 2:1, were selected for the subsequent analysis. First strand cDNA was synthesized using the Maxima H minus cDNA Synthesis Master Mix with dsDNase (Thermoscientific , #3024226) following manufacturer instructions and used as a template for qPCR performed with SYBR Green Master Mix (Applied Biosystems, #4472908). The gene expression analysis was performed in triplicates for each sample and Ct values were normalized to the expression of the housekeeping genes:

-**CicloA** (forward primer 5'-GGCAAATGCTGGACCAAACACAA-3', reverse primer 5' GTAAAATGCCCGCAAGTCAAAAG-3');

-**Rpl13** (forward primer 5'-TGGCTGGCATCCACAAGAAA-3', reverse primer 5' TTCTTCAGCAGAACTGTCTC-3').

Excel (Microsoft) and Prism were used to analyse the transcriptional data. The relative changes in gene expression in KO compared to WT samples were calculated using the 2 (ΔΔCt) method.

Primers used for the analyses:

- **Cacna1g** (forward primer 5'-TGCTCGTCTACGGTCCCTTCGG-3', reverse primer 5'-GCCCACAATCTCCCACACGCTG-3');
- **Dlk1** (forward primer 5'-CTGCCCCTGGCTGTGTCAATGG-3', reverse primer 5'-TTGAGGTGCAAGCCCGAACGTC-3');
- **Efna5** (forward primer 5'-TGTAACCGGCCTCACTCCCCAA-3', reverse primer 5'-CCGTTGTCTGGGATTGCAGAGGAGA-3');
- **Gdf11** (forward primer 5'-GGAGCTGAGGGGCTGCATCCTT-3', reverse primer 5'-ATATCGGCAGCAGCGGGACTCA-3').

3.3 Pharmacological treatments

Ampakine (MedChemExpress, HY-109046-100mg) 3 mg/kg was administered daily via subcutaneous injection, for the P3-P9 treatment. A second treatment was delivered on an alternate schedule—one week of treatment followed by two weeks off—continuing until P75. The drug in this treatment was administered via intraperitoneal injection. The drug, according to manufacturing instructions, was solubilized in DMSO (100%), Tween-80 (5%), PEG400 (40%) and saline (45%) to obtain the working concentration. Control mice received only the vehicle.

3.4 Behavioral assessment

Animals were maintained on an inverted 12h light/darkness cycle at 22–24°C. A total of 20 WT male mice, 20 KO animals, 24 WT female mice and 26 HET mice were involved in the behavioural assessment, for each described experiment. To avoid any bias, the investigator blind to the genotypes and treatments of tested animals performed all the analyses.

3.4.1 Phenotypic scoring

Weight and phenotypic scoring assessments were evaluated twice a week starting from P20 or from P60, respectively for male or female mice. Severity score, typically used in RTT phenotypic assessments (Guy et al., 2001, Gigli et al., 2016) was used to generate punctual line graph where for each time point, a score (sum of all five criteria) was assigned depending on the severity. The assessment was performed by a blind operator at least for the treatment. Five parameters are considered:

• General conditions: coat condition, eye tidiness and presence of wounds were evaluated. 0: no differences between wt and ko, coat is bright and groomed, eyes are clean, no wounds are present. 0.5: with respect to the wt control coat is less shiny or tidy or eyes are less clean or small wounds on the mouse body or tail are present. 1: coat is ungroomed or dull or dirty or eyes are dull, or wounds are evident, or two of the 0.5-scored phenotypes are present together. 1.5: spot without fur evident and coat ungroomed/dull or two of the 1-scored phenotypes present together. 2: piloerection together with large alopecia or eyes crusted or extended and serious wounds.

• Mobility: the mouse is placed on the bench and let free to move, the spontaneity of the movements and the time spent not moving are evaluated. 0: as wt. 0.5: the mouse does not move immediately when let free but evidently requires more time than the control to start its movements or movements are less quick. 1: mouse movements are slow and/or interrupted by freezing periods. 1.5: mouse starts to move only in response to a prod or when encouraged with a food pellet placed nearby and spends long periods immobile. 2: no movements when placed on the bench (anyway mice may become active when in their cage).

• Hind limb clasping: the mouse is held for the tail and maintained suspended for 30 seconds. 0: legs are large and splayed outwards. 0.5: one leg is drawn to the body in a discontinuous manner. 1: one leg is firmly drawn into the body or both legs are drawn to the body towards each other, but discontinuously. 1.5: both legs are firmly drawn to the body, without touching each other. 2: both legs are tightly drawn to the body, touching each other.

• Tremor: mouse is placed on the palm of the hand. 0: no tremor. 0.5: slight basal tremor or long periods without tremor interspersed with sporadic events of mild tremor. 1: basal tremor or intermittent events of mild tremor. 1.5: prolonged events of tremor interspersed with moment in which a basal tremor is present. 2: continuous tremor or almost continuous violent tremor.

• Gait: 0: as wt. 1: hind legs are spread wider than wt when walking or running with reduced pelvic elevation, resulting in in a "waddling" gait. 2: more severe abnormalities, such as tremor when feet are lifted, walks backwards or "bunny hops" by lifting both rear feet at once.

To be noticed, mice scoring 2 for the general condition or tremor category, and mice that rapidly lost weight were euthanized for ethical reasons. The day of the sacrifice was considered as the endpoint of lifespan assessment.

3.4.2 Open Field test

Exploratory behaviour and general locomotor activity were assessed through Open Field test. Each animal was removed from its home cage and individually placed into the center of an open field. Test lasted 10 minutes, during which mice were free to move and explore. Total distance travelled (cm) was measured with the EthoVision 14 (Noldus) software, and it was used as a measure of locomotor activity.

3.4.3 Rotarod test

Mice were assessed on an accelerating rotarod (Ugo-Basile, Stoelting Co.). The test was carried out in 3 days, 2 days of training and 1 day of test. Each session consisted of three trials and each trial lasted 5 min. Revolutions per minute (rpm) were set at an initial value of 4 with a progressive increase to a maximum of 40 rpm. Each trial ended when the mouse fell down or after 5 min. Latency to fall was measured by the rotarod timer.

3.4.4 Pole test

The pole test is a widely used test to assess motor dysfunctions in mice. The procedure evaluates the ability of a mouse to grasp on a pole to descend to its home cage. Mice are trained to complete the pole test over three training trials. Mice are placed on the top of the pole with their head oriented upward. The animals will often naturally orient themselves downward and descend the length of the pole to return to their home cage. The time required for the animals to descend to the base of the pole (total time) is recorded for three trials.

3.4.5 Beam walking test

This test is used for the assessment of motor coordination, particularly of the hindlimb. Firstly, animals are placed in one corner of the narrow beam and allowed to walk across the narrow beam from one end to the other for at least three times. The narrow beam measures 1-3 cm wide and is elevated between a pole and their home cage (to attract the mouse to the finish point). Healthy animals can cross the beam without difficulty and in a short time, while animals with reduced functionality of the front or hind limbs take longer and often slip from the beam. The number of foot slips encountered, and time taken to cross the beam in each trial are recorded.

3.4.6 Novel Object Recognition Test (NOR)

The Novel Object Recognition test investigates learning and memory. Trial is divided into 2 steps. For the training session each animal was placed into the arena with two identical objects for 10 minutes. After 30 minutes, during the test session, one of the training objects was replaced with a novel one. Since the mice have an innate preference for novelty, they should spend most of the time at the novel object rather than at the familial one. Time spent exploring each object was scored by a blind operator and subsequently the discrimination index (DI) was calculated as follows: (time exploring the novel object – time exploring the familiar object)/ total object exploration time. Object exploration was defined as the mouse positioning its nose within 1 cm of the object for at least 2 seconds. This criterion was used to avoid counting instances where the animal simply passed by the object without showing active interest. The arena and object specifications were as follows: the arena measured 40 x 40 x 40 cm, and the objects were made of plastic. Specifically, we used a 50 mL Falcon tube filled with Ponceau stain and a star-shaped plastic item with concave parts.

3.5 Electrophysiology measurements: Patch clamp analysis

Patch-clamp recordings were performed in coronal brain slices containing the prefrontal cortex of the mouse. Mice (30-35 days old) were anesthetized via intraperitoneal injection of avertin (250 mg/kg) and perfused transcardially with ice-cold artificial cerebrospinal fluid (ACSF) containing (in mM): 125 NaCl, 3.5 KCl, 1.25 NaH_2PO_4, 2 $CaCl_2$, 25 $NaHCO_3$, 1 $MgCl_2$, and 11 D-glucose, saturated with 95% O_2 / 5% CO_2 (pH 7.3). After decapitation, brains were removed and 250 μm-thick coronal slices containing the prefrontal cortex were cut in ACSF at 4 °C using a VT1000S vibratome (Leica Microsystems, Wetzlar, Germany). Slices were incubated in ACSF at 31.5 °C for 15 min, then gradually cooled and maintained at 26.5 °C. Individual slices were transferred to a recording chamber on an upright BX51WI microscope (Olympus, Japan) equipped with DIC optics. Slices were continuously perfused with ACSF at 2–3 ml/min at 32 °C.

Whole-cell patch-clamp recordings were performed in the coronal prefrontal cortex (~2–3 mm from the pial surface, 1.5 mm interaural, and 0–1 mm from bregma) using pipettes filled with an internal solution containing (in mM): 30 KH_2PO_4, 100 KCl, 2 $MgCl_2$, 10 NaCl, 10 HEPES, 0.5 EGTA, 2 Na_2-ATP, and 0.02 Na-GTP (pH 7.2 adjusted with KOH; tip resistance: 6–8 MΩ). Glutamatergic neurons were identified by their morphology and their characteristic firing pattern. All recordings were obtained using a MultiClamp 700B amplifier connected via a Digidata 1440A digitizer (Molecular Devices, Sunnyvale, CA, USA).

3.6 Primary cultures

3.6.1 Cortical neurons

Time pregnant females were generated by crossing overnight WT CD1 males with *Mecp2*$^{-/+}$ heterozygous CD1 females; the day of vaginal plug was considered E0.5. Timed-gestation female mice were sacrificed by dislocation and E15.5 mouse embryos were collected for primary cultures. Embryos were individually dissected under a microscope and immersed in ice-cold Hank's Buffered Salt Solution (HBSS, Sigma-Merk, #H6648). Meninges were removed, and cerebral cortex was rapidly dissected and maintained in cold HBSS until tissue dissociation. Once embryos were dissected and neocortex isolated, tissues were washed in HBSS, incubated with 0.25% trypsin/EDTA (Sigma-Merk, #25200-056) for 10 min at 37°C and the digestion was blocked with HBSS. Then, cortices

were accurately washed and mechanically dissociated in DMEM containing 10% FBS, 1% L-glutamine (#G7513, Sigma-Aldrich), 1% P/S. Cell count was performed with an automated cell counter by using Trypan blue (Automated Cell Counter, Biorad). Depending on experimental needs, neurons were seeded in neuron culture medium (Neurobasal Plus medium (Thermo Fisher scientific #A3582901), Penicillin/Streptomicin 1% (Sigma-Merk #P0781), B27-Plus 50X 2% (Thermo Fisher scientific #A3582801)) on poly-D-lysine (0.1 mg/mL) (Sigma-Merk #P7886) -coated plates or poly-D-lysine-coated glass coverslips (Neuvitro #GG-12-PDL). Ampakine (5 μM) or equivalent volumes of neuron culture medium (vehicle) were added directly to the culture at DIV14 for Western Blot experiments. For calcium imaging experiments and for immunofluorescence assays, Ampakine was administered at DIV12 at a concentration of 0.75 μM or 1 μM respectively.

3.6.2 Protein extraction

After a rapid wash in D-PBS (Sigma, #D8537) to remove any cell debris, total protein content was extracted from primary cultures (DIV14) using ice-cold RIPA buffer (containing: 100mM Tris HCI pH=7.5, 300mM NaC1, 10mM EDTA, 2% NP-40. 0.2% SDS, 1% sodium deoxycholate, Protease Inhibitor Cocktail 1X (Thermo Fischer scientific #78444) and PhosSTOP 1X (Sigma Merck #4906845001). Samples were centrifuged at 13,000g for 20min at 4°C. Supernatants were then collected and stored at -80°C until analysis. Protein concentrations were calculated using bicinchoninic acid (BCA) assay kit (Thermo Scientific, #23228) following manufacturer's procedure.

3.6.3 Western blots

Equal amounts of protein lysates, 20μg, were separated on TGX Stain-Free gel (Criterion 12/18 wells 4–15%; Bio-Rad, #5678084).
Before transfer, a stain-free gel image was acquired by ChemiDoc Touch Imaging System (Bio-Rad) (5 minutes of activation). Proteins were blotted on a nitrocellulose membrane (Trans-blot Turbo Nitrocellulose Transfer Packs; Bio-Rad, midi #1704159) using the Trans-blot SD semidry apparatus (Bio-Rad); after the blot an image of the membrane was acquired by ChemiDoc and then used for data normalization. Membranes were incubated 1h at RT in blocking solution (Tris buffered saline containing: 0.1% Tween-20 (TBS-T) and either 5% non-fat milk or 5% BSA (Sigma, #A30659) and then incubated overnight (4°C) with the primary antibody diluted in blocking solution. The following primary antibodies were used: anti-AKT (Cell Signalling #4685; 1:1000); anti-phospho-AKT(Ser473) (Cell Signalling #4060; 1:1000); anti-GluA1 (Cell Signalling #13185; 1:1000); anti-phospho-GluA1(Ser845) (Abcam #76321; 1:1000). After 3 washes in TBS-T 1X, blots were incubated with the appropriate HRP-conjugated secondary antibody (Peroxidase-conjugated AffiniPure Goat anti-rabbit #111-035-144 or anti-mouse #115-035-003 IgG (H+L), Jackson ImmunoResearch) for 1h at room temperature. Immunocomplexes were visualized using the ECL substrates kit from Cyanagen (WESTAR SUN #XLS0630250) or Bio-Rad (Clarity Western ECL Substrate #1705061) and the Bio-Rad ChemiDocTM System. Quantification of bands was performed using the Image Lab 5.2.1 Software (Bio-Rad).

3.6.4 Analysis of calcium transients

Primary cortical neurons were loaded with 2 μM Fluo-4 (Invitrogen) in KRH (Krebs'–Ringer's–HEPES containing (in mM): 125 NaCl; 5 KCl; 1.2 $MgSO_4$; 1.2 KH_2PO_4; 25 HEPES; 6 glucose; 2 $CaCl_2$; pH 7.4) for 30 min at 37°C and then washed once with the same solution. Stimulation was

performed automatically by using the liquid handling system of the ArrayScan XTI HCA Reader (Thermo Fisher Scientific). To stimulate, one dose of NMDA (100µM at the rate of 50µl/ s) was added while images were digitally acquired with a high-resolution camera (Photometrics) through a 20× objective (Zeiss; Plan NEOFLUAR 0.4 NA). Hoechst fluorescence was imaged as well. 40 frames were acquired at 1 Hz with 40 ms exposure time for Fluo-4 and 25ms exposure time for Hoechst. At least 9 baseline images were acquired before stimulation. The analysis was done with HCS Studio software using Spot Detector bio application (Thermo Fisher Scientific). Hoechst-positive nuclei were identified and counted, and the mean intensity of the Fluo-4 signal was measured in the cell body area of each cell; background intensity was measured and subtracted from the mean intensity. Only cells with neuronal morphology were included in the analysis. Calcium responses were measured as ΔF/F0. Single cell analysis was performed using Excel.

3.6.5 Cell immunofluorescence

For immunofluorescence on cultured cells, (neurons DIV14) seeded on glass coverslips were fixed for 8 min with 4%PFA dissolved in PBS with 10% sucrose, then washed 3 times with PBS and stored in 0.1% NaN_3 in PBS at 4 °C. Cells were permeabilized in 0.2% Triton X-100 in PBS for 3 min on ice. Cells were washed in 0.2% BSA in PBS, then incubated in blocking solution (4%BSA in PBS) for 15 min and finally incubated with primary antibodies overnight at 4 °C. Primary antibodies were diluted in 0.2% BSA in PBS as follow: anti-Map2 (clone D5G1, 1:1000; #8707, Cell Signalling), anti-Synapsin1/2 (1:500; #106006, Synaptic System), anti-Shank2 (1:300; #162211, Synaptic System). After washing in BSA 0.2% in PBS, cells were incubated with the specific Alexa Fluor secondary antibody: (Goat anti-Chicken IgG (H+L) Alexa Fluor 488, Donkey anti-Rabbit IgG (H+L) Alexa Fluor 568, Donkey anti-Mouse IgG (H+L) Alexa Fluor 647), (1:500 in BSA 0.2% in PBS) for 1h at RT. After 5 washes in PBS, nuclei were stained with DAPI and cells were washed in PBS. Glass coverslips were mounted on microscope slides with Fluoromount mounting medium and stored at 4°C until image acquisition.

3.6.6 Puncta Analysis

To analyze synaptic puncta density and colocalization, we processed DIV14 neurons. Z-stacks images ($185\times185\mu m^2$,1024 × 1024-pixel resolution, 8-bit greyscale depth) were acquired at Nikon Ti2 Microscope equipped with an A1+ laser scanning confocal system and a SR Apo TIRF 100X oil-immersion objective, using a step size of 0.3µm. For each dataset, images were acquired in four channels and parameters were maintained constant within the experiment (offset back-ground, digital gain, laser intensity, pinhole size, scanning speed, scan direction, line average mode). Puncta density was calculated by counting synaptic puncta within a manually selected ROI (length 20µm on 3 primary branches/neuron) by using ImageJ software. Only puncta with a minimum size of $0.16\mu m^2$ were counted using Analyze Particles (ImageJ). To assess puncta colocalization of pre- and post-synaptic markers, the plugin Colocalization highlighter was run on each Z-stack image. Colocalized puncta were quantified in manually selected ROIs of the binary mask created from the maximum intensity projection. Only puncta with a minimum size of $0.1\mu m^2$ were counted.

3.7 Statistical analysis

Statistical analysis and plotting of data were performed with GraphPad Prism 10 (GraphPad Software Inc., La Jolla, CA). Student's t-test and Mann Whitney test were used for the statistical analysis when

wt were compared to wt treated samples. Two-way or One-way ANOVA was used to statistically compare the effects of Ampakines administrations on *Mecp2* null or het and wt mice. When there was a significant effect of treatment or genotype, or a significant interaction between the variables, appropriate post hoc test was applied (Tukey's post-hoc test). A P-value of 0.05 was considered significant. Possible outliers within an experimental group were identified with ROUT test and discarded from the final analysis. Each culture wells from *in vitro* analysis and mice from *in vivo* experiments were randomly assigned to treatments, and for all the experiments reported the investigators were blinded to the treatments and genotypes during data acquisition and analyses.

4. Preliminary Data

Ampakine CX546, previously used in our laboratory, produced remarkable long-lasting benefits *in vivo* in *Mecp2*-null treated mice including behavioural improvements and increased survival (Scaramuzza et al., 2021). However, safety concerns related to the epileptogenic profile of that compound limited its translational potential. To overcome this limitation, we tested a new generation high impact Ampakine, already proved safe in clinical trials for Alzheimer's Disease, Major Depressive Disorder and mild cognitive impairments (Bernard et al., 2019; Servier-47445_Synopsis, 2018; RespiRx/Servier, 2020).

To test the value of restoring the feedforward cycle in an early developmental time window characterized by high synaptic plasticity, the compound was subcutaneously injected daily from P3 to P9 (3 mg/kg).
Phenotypic severity scoring was significantly improved in treated *Mecp2*-null mice, along with significantly extended lifespan compared to untreated controls. Behavioural testing was carried out from P45 to P65, a period when symptoms are pronounced, but the mice are still physically capable of performing the tasks. Substantial improvements in motor functions (tested through Rotarod and Pole tests) were observed in Ampakine-treated *Mecp2*-null mice versus the vehicle treated littermates. Efficacy was particularly evident at P45, 36 days after the last injection of the drug.
Concerning the cognitive functions, the Novel Object Recognition (NOR) test conducted at P45 demonstrated the ability of the drug to normalize memory defects typically affecting the *Mecp2*-null mice. In fact, the defect initially observed between wild-type and *Mecp2*-null mice was no longer evident in the treated group.

Following these encouraging results, our laboratory chose to administer the drug in a later and more translational time window, corresponding to a stage in which symptoms begin to appear in humans, and the pathology can be diagnosed. Specifically, the Ampakine was administered for one week, from P28 to P34. However, no behavioural improvements were observed. Similarly, no beneficial effects were observed in survival or phenotypic score. A possible explanation for these results might be that the treatment, administered outside a time window characterized by high synaptic plasticity, might have not been long enough.

Based on these considerations, a third and more extended regimen of administration was tested. Considering that some regions of the *Mecp2*-deficient brain feature hyper-excitability [148], to minimize the risk of excitotoxicity, a chronic intermittent protocol, rather than a continuous administration, was selected. Specifically, the treatment started at P20 and was characterized by a daily administration for seven days followed by one-week pause. This new regimen led to observable

benefits in survival, as well as mild improvements in motor coordination. As already described, cognitive function, evaluated through the X maze test, was normalized in P45 *Mecp2*-null mice.

5. Aim

Ampakine treatment in *Mecp2*-null mouse models proved to be effective in modulating RTT phenotype; therefore, the first objective was to explore its molecular effects *in vitro*, in *Mecp2*-null mouse primary neurons. Further, we assessed whether the drug was effective on the typical defects in synaptic maturation and electric activity that affect human and mouse *MECP2*-deficient neurons.
Considering that female *Mecp2*-heterozygous mice represent the most clinically relevant model for Rett syndrome, the second aim was to extend the validation of Ampakine efficacy *in vivo* to females.
The third goal was to identify a strategy to maintain and enhance long-term benefits in both genders. For this purpose, we tested a prolonged intermittent regimen in KO and HET mice, initiated at P3 and maintained until P75 with one week of treatment alternating with two weeks off.
In parallel, we investigated the molecular mechanisms driving the observed therapeutic effects *ex vivo*. To this end, we analysed gene expression regulation in the prefrontal cortex of *Mecp2*-null mice at two developmental stages (P10 and P30) following early *in vivo* treatment, to capture both acute and long-term transcriptional effects. Finally, to assess the functional impact at the synaptic level, we performed electrophysiological recordings on brain slices from the prefrontal cortex of *Mecp2*-null mice. This approach enabled us to evaluate whether Ampakine treatment modulates synaptic function, thereby providing functional evidence in support of enhanced synaptic transmission as a potential mechanism of action.

6. Results

6.1 Ampakine-mediated activation of AMPA receptor signalling rescues synaptic and functional deficits in Mecp2-null neuron

Given the limited data available on the novel Ampakine and the encouraging results obtained *in vivo* before my stage, I initiated my training investigating molecular and cellular effects of the drug *in vitro*. To do so, we measured the phosphorylation of downstream effectors typically involved in AMPAR stimulation. We used primary cortical neurons obtained from E15 male mouse embryos (see Materials and Methods). Based on literature and on viability assays performed by us (data not shown), the compound was administered at a concentration of 5 μM at DIV14 (days in vitro) (Fig. 1A). Initially, we measured the phosphorylation of downstream effectors typically involved in AMPA receptors (AMPAR) stimulation. Considering the short half-life of the drug *in vivo* (approximately 30–60 minutes) and our interest in post-translational modifications that occur immediately after the receptor activation, neurons were collected for protein extraction one hour after the treatment. Protein abundance was assessed through Western Blot and normalized through TGX technology (BioRad). Receptor activation was assessed by measuring the ratio of the phosphorylated to the non-phosphorylated isoform of the GluA1 subunit (Fig. 1B, D). A significant upregulation of the phosphorylated S845 isoform was observed (Fig. 1C), together with an increased ratio between phospho-GluA1 and total GluA1 levels (Fig. 1D) (Student's T-test; *$P < 0.05$, ****$P < 0.0001$). We then assessed whether the treatment activated Akt, a kinase whose phosphorylation generally follows AMPAR stimulation [234]. A significant upregulation of phosphorylated Akt S473 was observed,

thereby confirming the activation of the AMPA signalling pathways (Fig. 1E, F; Student's T-test; *P < 0.05).

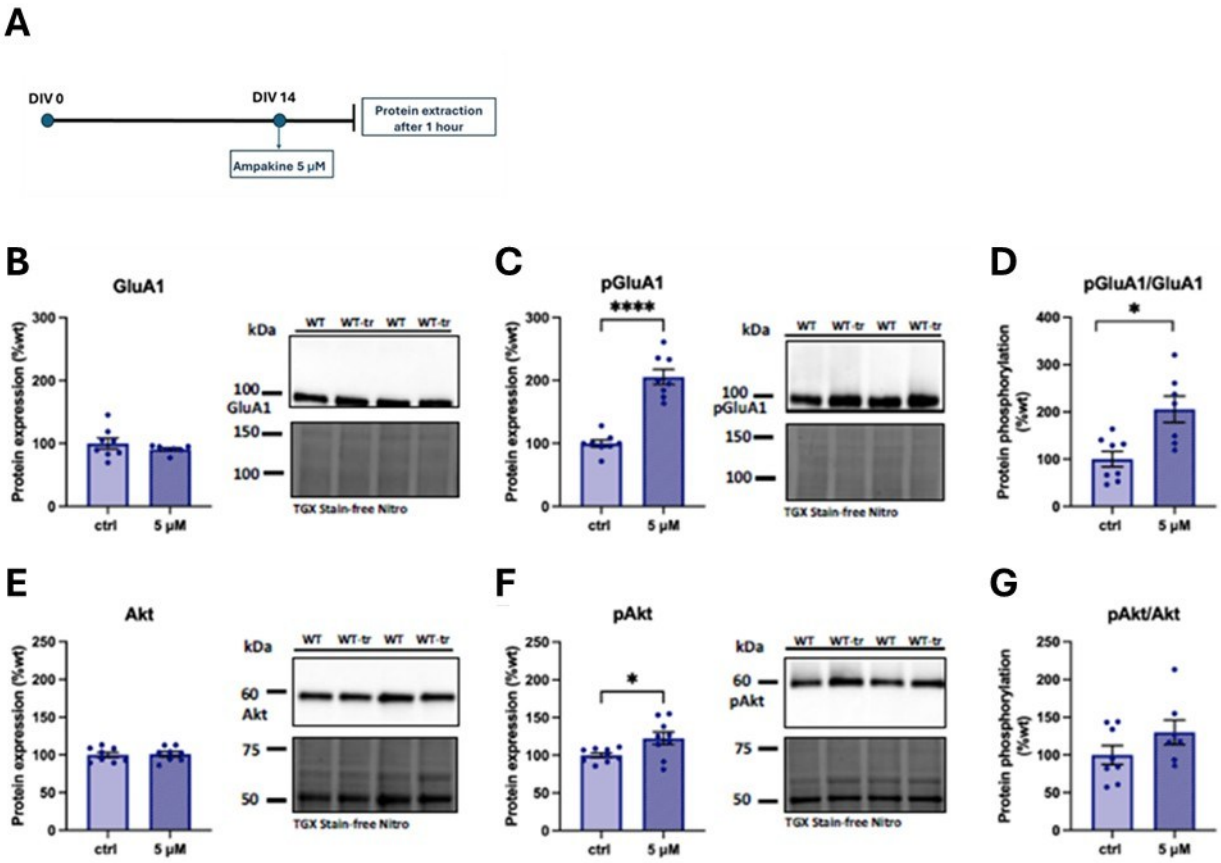

Figure 1: Acute Ampakine administration *in vitro* activates the AMPAR signalling pathways. (A): Schematic representation of the *in vitro* Ampakine administration protocol. **(B, C, D)**: The bar graphs show normalized expression levels of GluA1 (B), pGluA1 (C), and their ratio (D) in WT untreated and Ampakine-treated cortical mouse neurons. Right panels display representative western blots of GluA1 and pGluA1. **(F, G, H)**: The bar graphs show normalized expression levels of Akt (F), pAkt (G), and their ratio (H) in WT untreated and Ampakine-treated cortical mouse neurons. Right panels display representative western blots of total Akt and pAkt. Total protein content, visualized by TGX Stain-Free technology (Bio-Rad), was used for data normalization. Each dot represents a single embryo deriving from three independent preparations. Statistical significance was assessed by Mann-Whitney test (F) and Student's T-test (*: p-value<0.05, ****: p-value<0.0001). Values are represented as mean ± SEM.

Once demonstrated the capacity of the Ampakine to activate the AMPAR signalling pathway, we investigated if the treatment was effective on synaptic and electrical defects typically affecting *Mecp2*-null neurons.

An immunofluorescence for Synapsin1/2, a pre-synaptic marker protein [235], and Shank2, a post-synaptic one (Naisbitt et al., 1999), was performed in DIV14 WT and *Mecp2*-null cortical neurons treated with Ampakine from DIV12 (Fig. 2A). Based on previous dose-optimization studies and literature evidence, we selected a lower dose (1 µM) for a two day treatment, instead of the acute regimen used before.

The analysis of synaptic puncta density confirmed the expected significant reduction of both Synapsin1/2 and Shank2 puncta in *Mecp2*-null neurons. Importantly, the Ampakine completely

rescued these defects at both pre- and post-synaptic level (*$P < 0,05$; **P < 0,01; ***P < 0,001; ****$P < 0,0001$, two-way ANOVA, Fig. 2B, D).

As a measure of functional synapses, we also analysed the co-localization of Synapsin1/2 with Shank2 puncta. As expected, our data highlighted a defective co-localization in *Mecp2*-null neurons compared to WT cells, which was rescued by the treatment (**$P < 0,01$; ****$P < 0,0001$, two-way ANOVA, Fig. 2E).

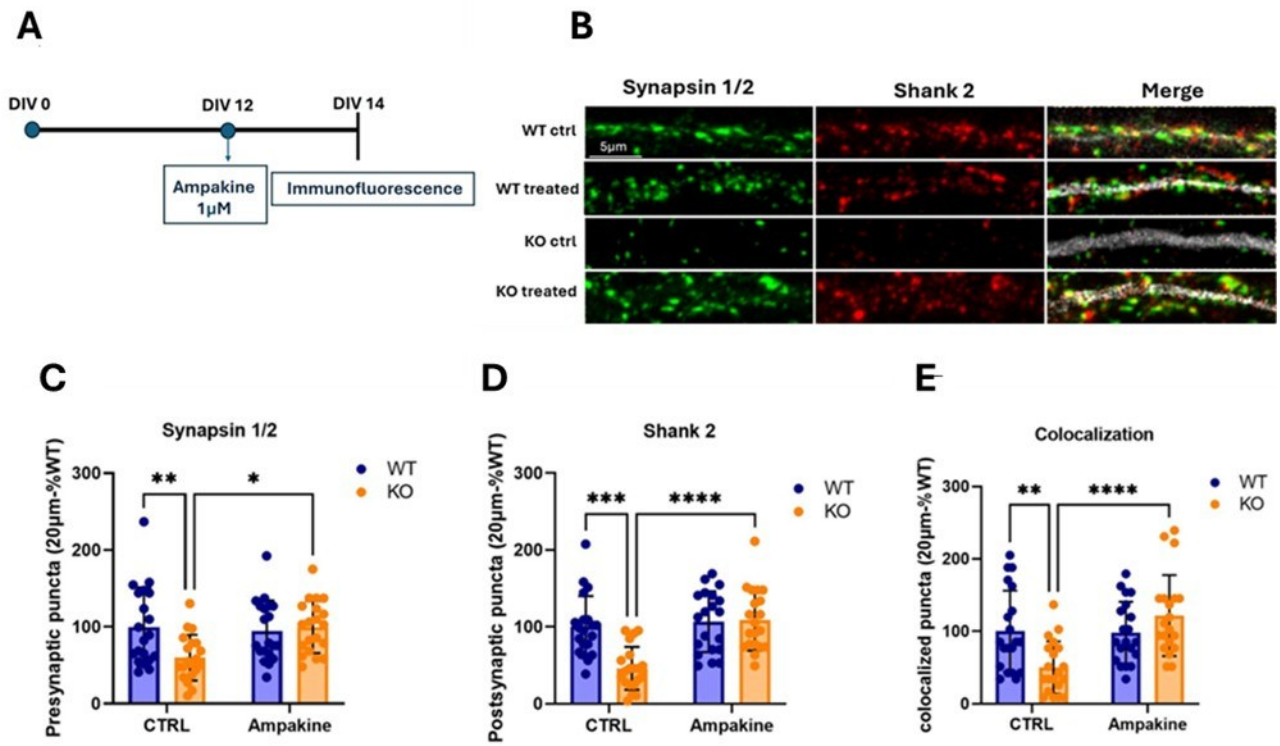

Figure 2. ***In vitro,*** **the Ampakine treatment rescues synaptic alterations. (A):** Schematic representation of the experimental workflow. **(B):** Representative images of the immunofluorescence for Synapsin1/2 (green), Shank2 (red) and their merge with Map2 of WT and KO untreated (CTRL), and WT and KO treated primary neurons at DIV14. Scale bar = 5 µm. **(C, D, E):** Histograms indicate the number of Synapsin1/2 and Shank2 puncta on 20 µm-long dendrite (C, D) and of colocalized puncta (E) of WT CTRL, KO CTRL, WT treated and KO treated neurons. Data were analysed by two-way ANOVA followed by Tukey post-hoc multiple comparison test.**p-value < 0.05;* ***p-value* < 0.01; ****p-value < 0.001*; *****p-value < 0.0001*. Each dot represents a single cell. n = 20 cells WT CTRL, n = 20 cells KO CTRL, n = 20 cells WT treated, n = 20 cells KO treated. Cells derived from at least two embryos E15.5. Values are presented as mean ± SEM.

To assess whether the compound could also rescue the functional activity of *Mecp2*-null neurons, we performed calcium imaging experiments. As previously mentioned, calcium influx serves as a marker of neuronal responsiveness to stimuli [236]. *Mecp2*-null neurons were treated with the Ampakine 0,75µM at DIV12, and calcium imaging was performed at DIV14 (Fig. 3A). In this case, we used a lower concentration compared to that used in the immunofluorescence experiments due to the specific experimental conditions. Since calcium imaging requires particularly stringent culture conditions and cells can be easily stressed, we avoided applying additional stress to the cells. Based on the vitality assay, we observed good cell viability at 0.75 µM, whereas at 1 µM the WT treated cells did not respond well, making it difficult to perform the readout analysis. Neurons were initially incubated with Fluo-4 AM (2µM) and Hoechst; the first is able to turn the fluorescence on when bound to Ca^{2+};

while the second is a non-toxic nuclear dye commonly used in live cell imaging. Cells were then stimulated with NMDA (100µM). Remarkably, to eliminate network-driven activity and isolate receptor-specific calcium responses, tetrodotoxin (TTX 1µM) was added. This ensured that the calcium signals measured were due to direct NMDAR activation, rather than synaptically propagated activity or spontaneous firing.

Calcium response was quantified by calculating the difference in fluorescence intensity before and after NMDA stimulation (Fig. 3B), directly proportional to the amount of Ca^{2+} entry, providing a readout of neuronal activation in response to the treatment.
As expected, the responsiveness of *Mecp2*-null neurons to chemical stimulation is significantly decreased compared to WT neurons, and the Ampakine totally rescued the defect (**P* <0,05; *****P* <0,0001, two-way ANOVA, Fig. 3C).

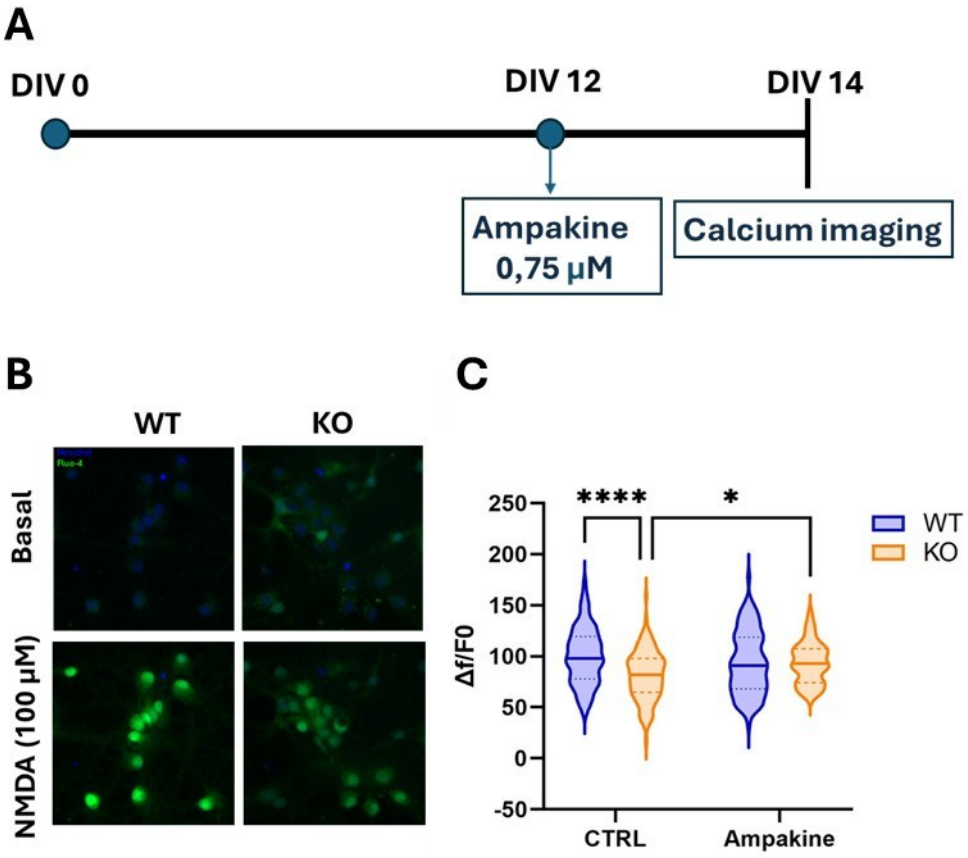

Figure 3. Ampakine treatment rescues neuronal activity of KO neurons (A): Schematic representation of the experimental workflow. **(B):** Representative fluorescence images of primary cortical neurons loaded with Fluo-4 AM (green) and Hoechst (blue) before and after NMDA stimulation. The images show the fluorescence signal intensity corresponding to intracellular calcium levels. Prior to NMDA application (Baseline), neurons exhibit low baseline fluorescence. Following NMDA stimulation, a clear increase in Fluo-4 fluorescence is observed, indicating a rise in intracellular calcium concentration due to NMDA receptor activation. **(C):** calcium transients ($\Delta F/F_0$) were measured in WT and KO primary cortical neurons, under control (CTRL) conditions and after treatment with the Ampakine. The violin plot presents the total of cells for each experimental group. n = 141 cells WT CTRL, n = 120 KO CTRL, n = 101 cells WT treated, n = 74 KO treated. Every cell derived from at least two embryos E15.5. Data were analysed by two way-ANOVA followed by Tukey post-hoc multiple comparison test *(*: p-value*<0.05, ***: p-value*<0.01, ****: p-value<0.*001, *****: p-value*<0.0001). Values are represented as mean ± SEM.

6.2 Early administration of Ampakine ameliorates behavioural phenotypes also in female heterozygous mouse models

As reported in the preliminary data, the most effective treatment window in *Mecp2*-null mouse models was the administration of Ampakine at a dose of 3 mg/kg from P3 to P9. Based on these results, we applied the same treatment regimen to female *Mecp2* heterozygous mice (HET), which, as previously discussed, represent the most appropriate genetic model. Mice were daily injected subcutaneously (SC) with either 3 mg/kg of Ampakine or vehicle from P3 to P9 (Fig. 4A).

Survival analysis was not performed in heterozygous mice, as the *Mecp2* heterozygous condition does not affect life expectancy. Evaluation of phenotypic severity and behavioural tests in heterozygous mice began at P70 and P90 respectively. This later stage with respect to *Mecp2*-null male mice was selected considering that HET females feature delayed onset and slower progression of symptoms [116]. As shown in Fig. 4B, a tendency to amelioration of the phenotype is visible at all time points, in particular at P90 ($P=0,059, Fig. 4B).

Motor coordination was assessed through the Beam walking and the Rotarod tests, memory was measured with the Novel Object Recognition (NOR) test.

Beam Walking Test, assessing both motor coordination (specifically related to hind limbs) and balance, was performed at P90 and P100. At P90, the test was carried out over three consecutive days: the first two days were used for habituation, allowing the mice to familiarize with the apparatus, the third day instead was considered the actual test session. Each day mice performed three trials, with a ten-minute interval between each trial to minimize fatigue and learning effects. At P100, since mice were already familiar with the task, the test was conducted in a single session.

At P90, the treatment normalized the defect present in vehicle treated mice in comparison to WT mice, thereby demonstrating a positive effect of the drug (Fig. 4C). Regarding the time required to cross the beam, no significant differences were detected among the different experimental groups (Fig. 4c'). At P100, a clear defect between WT and untreated heterozygous mice was observed for both the crossing time and the number of errors (Fig. 4D, d'). Importantly, the drug was able to fully rescue the observed defects (**P<0,01; $P = 0.053 two-way ANOVA, Fig. 4D, d').

To further evaluate motor coordination, we performed the Rotarod test at P100. The test was conducted over three consecutive days, with the final day designated as the test session. Each day consisted of three trials conducted using an accelerating paradigm (5–40 rpm), with each trial lasting 5 minutes. Importantly, since we aimed to evaluate also the learning capacity, all trials from the three days were plotted. The latency to fall reflects motor coordination.

A clear motor deficit was observed between WT and untreated HET mice. Ampakine treatment resulted in a statistically significant improvement in the treated heterozygous group compared to untreated controls (**P<0,01, ****P<0,0001; two-way ANOVA, Fig. 4E), although treatment did not fully restore motor performance.

Concerning motor learning, a progressive significant improvement in motor coordination, between CTRL and Ampakine treated HET mice was already evident starting from Day 2 (**P<0,01, two-way ANOVA, Fig. 4e'). Cognitive functions were examined through the NOR test, assessing short-term memory. NOR was performed at P90 using a two-phase test designed to evaluate the innate exploratory behaviour of mice. In the first phase (training), each mouse was placed in an arena containing two identical objects, and the time spent interacting with each object was recorded. Thirty minutes later, during the testing phase, one of the familiar objects was replaced with a novel one, and

the time spent exploring the novel versus the familiar object was measured using the discrimination index (DI). The DI is calculated as the ratio between the time spent from the mice in exploring the new object with respect to the time spent exploring the familiar one. Unlike motor behavioural tests, cognitive rescue could not be assessed at P90, as no significant deficit was observed between WT and HET control mice.

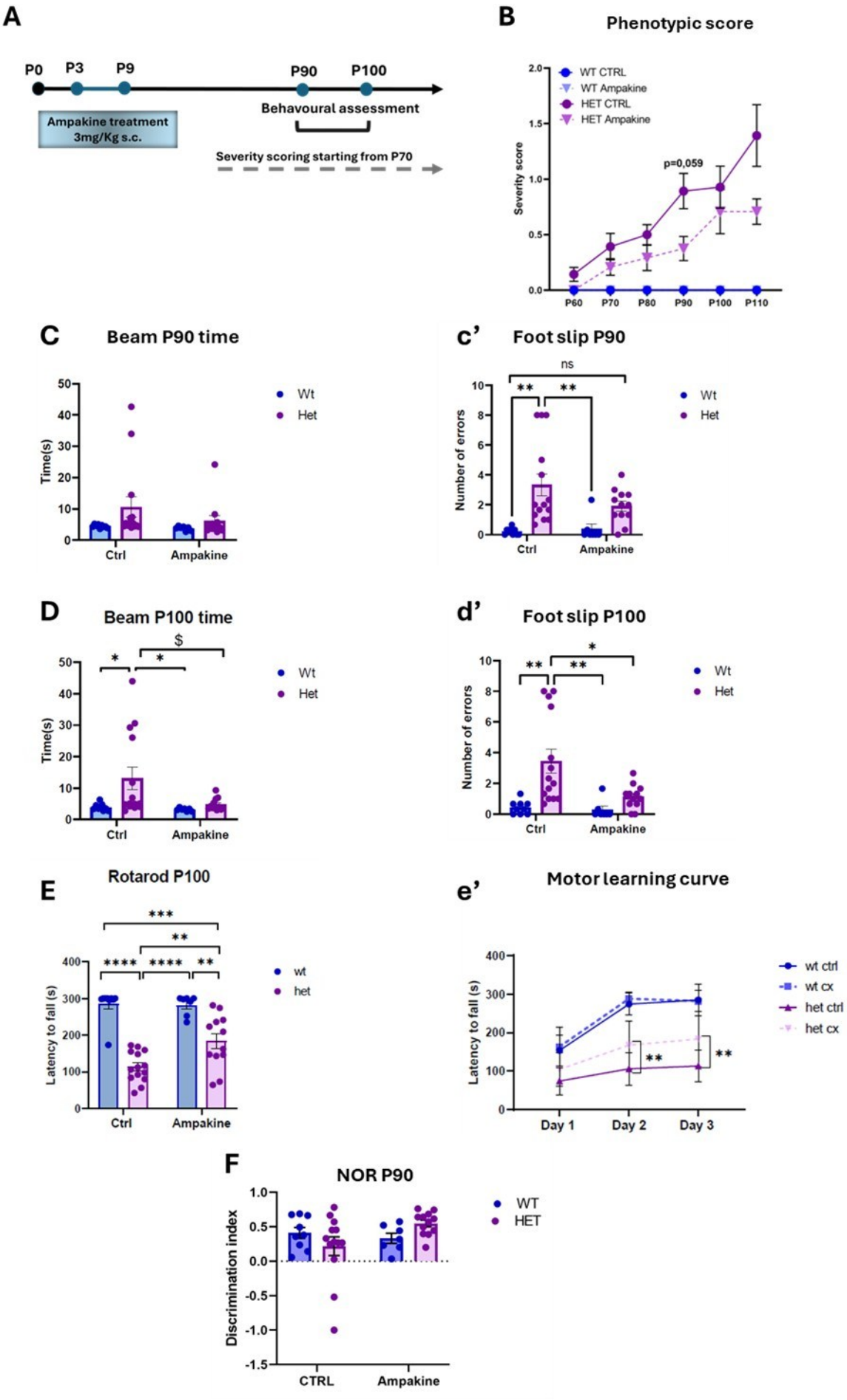
A
P0
P3
P9
P90
P100
Ampakine treatment
3mg/Kg s.c.
Behavioural assessment
Severity scoring starting from P70
B
Phenotypic score
WT CTRL
WT Ampakine
HET CTRL
HET Ampakine
Severity score
p=0,059
P60
P70
P80
P90
P100
P110
C
Beam P90 time
Time(s)
Wt
Het
Ctrl
Ampakine
c'
Foot slip P90
ns
Number of errors
D
Beam P100 time
d'
Foot slip P100
E
Rotarod P100
Latency to fall (s)
wt
het
e'
Motor learning curve
wt ctrl
wt cx
het ctrl
het cx
Day 1
Day 2
Day 3
F
NOR P90
Discrimination index
WT
HET
CTRL

Figure 4. Early administration of the Ampakine (P3-P9) ameliorates behavioural phenotypes in the HET mouse model. (A): Schematic representation of the Ampakine regimen of administration. Mice were daily injected from P3 to P9, (3mg/Kg). The severity score was weekly assessed from P70. Behavioural tests were performed at P90 and P100**. (B):** The line graph illustrates the punctual severity scores evaluated considering the general conditions, mobility, hind clasping, gait and tremor of mice. **(C, c'):** The graph shows the total time (in seconds) spent for crossing the beam and the number of foot slip events while the mice cross the beam in the beam walking test at P90. **(D, d'):** The graph shows the beam walking test, at P100, including total time and foot slip errors. **(E, e'):** The graphs show the latency to fall (in seconds) on the accelerating rotarod in the last trial at P100 (E) in the rotarod test. In (e') it is shown the improvement of performance over the three days of the trial between treated and untreated HET mice. **(F**): The graphs represent the discrimination index (DI) between two different objects during NOR test at 90. Each dot represents a single animal. Sample size: WT=9, WT treated with Ampakine=7, HET=14, HET treated with Ampakine=12. Statistical significance was assessed by Two-way ANOVA followed by Tukey's post-hoc multiple comparison test *($: p* =0,053, **: p-value*<0.05, ***: p-value*<0.01, ****: p-value*<0.001, *****: p-value*<0.0001). Values are represented as mean ± SEM.

6.3 Combination of early and alternate treatment is safe and elicits superior beneficial effects compared to the solely early intervention in *Mecp2*-null mice

Although early treatment showed promising results both in male and female RTT mice, our aim was to enhance and prolong its beneficial effects. We thus decided to combine the early treatment with the intermittent regimen. Specifically, the early treatment remained unchanged while the intermittent was extended until P75, alternating with two weeks off. From P3 to P9 we treated subcutaneously pups with 3mg/kg of Ampakine; starting from the second week of treatment the drug was administered through intraperitoneal injection. Initially we tested the treatment in *Mecp2*-null mice because the KO model displays lower phenotypic variability and faster experimental timings, as explained above.

Importantly, the early intermittent Ampakine treatment significantly prolonged the survival of *Mecp2*-null mice compared to untreated controls (Fig. 5B). Consistently, treated mice showed a significant amelioration of symptoms starting from P60 (Fig. 5C).

Motor performance was evaluated using the Pole and the Rotarod tests at P45 and P60; the NOR test was performed at P65. Pole test, which measures the ability of the mouse to descend from the top of a vertical pole to its home cage, specifically assesses motor coordination involving hind limb functions. Deficits in performance were observed at P45 and P60 in *Mecp2*-null mice (Fig. 5D, E). Although treated null mice still displayed impairment, a significant improvement in motor coordination was evident at P60 following Ampakine administration (***P<0,001, Fig. 5E). A significant beneficial effect of the treatment on motor coordination was demonstrated in the Rotarod test at P45 and P60 (*P<0,05; two-way ANOVA, Fig. 5F, G).
Concerning short term memory, the typical defect observed in *Mecp2*-null mice was normalized by the drug (Fig. 5H).
Comparing all results obtained in male mice we observed that the early intermittent treatment proved to be the most effective, achieving phenotypic rescue with long-lasting benefits.

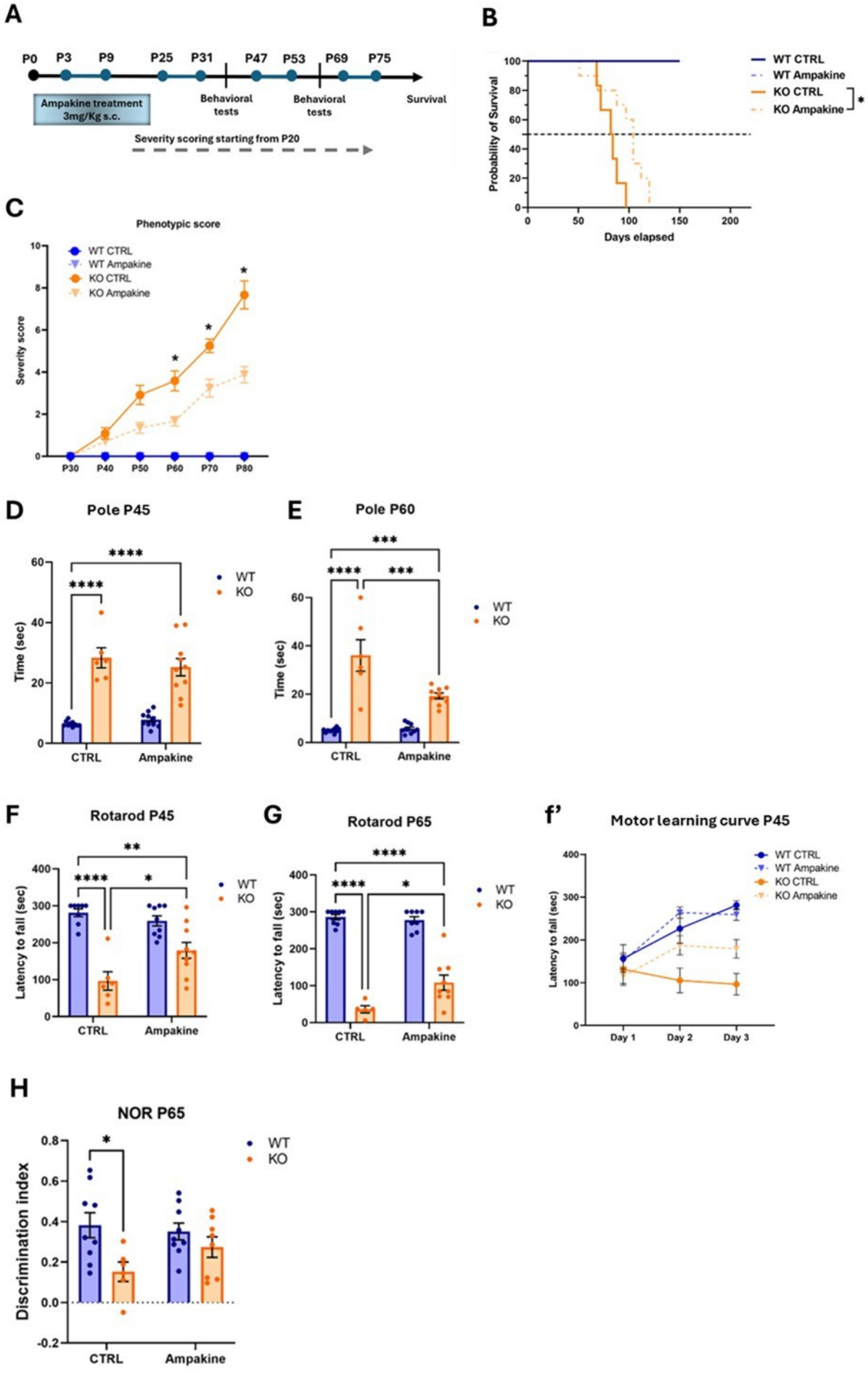
A
P0
P3
P9
P25
P31
P47
P53
P69
P75
Ampakine treatment 3mg/Kg s.c.
Behavioral tests
Behavioral tests
Survival
Severity scoring starting from P20
B
Probability of Survival
Days elapsed
WT CTRL
WT Ampakine
KO CTRL
KO Ampakine
*
C
Phenotypic score
Severity score
WT CTRL
WT Ampakine
KO CTRL
KO Ampakine
P30
P40
P50
P60
P70
P80
D
Pole P45
Time (sec)
WT
KO
CTRL
Ampakine
E
Pole P60
Time (sec)
WT
KO
CTRL
Ampakine
F
Rotarod P45
Latency to fall (sec)
WT
KO
CTRL
Ampakine
G
Rotarod P65
Latency to fall (sec)
WT
KO
CTRL
Ampakine
f'
Motor learning curve P45
Latency to fall (sec)
WT CTRL
WT Ampakine
KO CTRL
KO Ampakine
Day 1
Day 2
Day 3
H
NOR P65
Discrimination index
WT
KO
CTRL
Ampakine

Fig. 5: Early intermittent treatment with Ampakine has long-lasting efficacy in KO male mice. (A): Schematic representation of the *in vivo* Ampakine administration protocol: mice were injected starting from P3 to P75 every week followed by a two-week pause. Severity score was assessed from P20, twice a week. Behavioural tests were performed from P45 to P60**. (B):** Kaplan-Meier curve reveals a significant improvement in the lifespan of *Mecp2*-null treated mice compared to ko control mice. **(C):** The line graph illustrates the punctual severity score based on general conditions of the mice, mobility, gait abnormalities, clasping and tremor. **(D, E):** The graphs represent the total time spent in performing the pole test at P45 (D) and at P60 (E). **(F, G, f'):** The first two graphs show the latency to fall (in seconds) during the rotarod test at P45 and P65. The last graph shows the learning curve over the three days of trial at P45. **(H):** The graphs represent the discrimination index (DI) between two different objects during the NOR test at P65. Each dot represents a single animal. Sample size: WT CTRL=10, WT treated with Ampakine= 10, KO CTRL=6, KO treated with Ampakine =10. Statistical significance was assessed by Two-way ANOVA followed by Tukey's post-hoc multiple comparison test and Log-Rank (Mantel-Cox) test (*: *p-value*<0.05, **: *p-value*<0.01, ***: *p-value*<0.001, ****: *p-value*<0.0001). Values are represented as mean ± SEM.

6.4 Early intermittent treatment is effective also in HET female mice

Based on its efficacy in the male *Mecp2*-null model, we decided to apply the same early intermittent regimen to HET female mice. Severity score and behavioural tests were assessed at the same time of the early treatment (Fig. 6A). As expected, treated HET mice showed a milder phenotype than untreated mutant littermates, although the difference did not reach statistical significance (Fig. 6B). In the Beam Walking test, performed at P90 and P100, no deficits in the time required to cross the beam were observed among the four experimental groups (Fig. 6C, D). However, untreated HET mice exhibited a significantly higher number of foot slip events compared to WT controls at both time points (**P<0,01, Fig. 6c', d'). Notably, treatment normalized this phenotype only at P90 (Fig. 6c').

In the Rotarod test performed at P100, treated HET mice showed normalization of the motor performance since the difference between treated HET and WT mice was no longer present (Fig. 6E). Although a statistically significant difference between untreated and treated HET mice was not observed in the learning curve, a tendency to amelioration was observed from Day 2 (Fig. 6e').
Cognitive functions were assessed at P90 using the NOR test. Notably, control HET mice exhibited a significant defect that was normalized by the treatment (Fig. 6F).

Altogether these results suggest the efficacy and the safety of the drug in both genders, of relevance for translational purposes.

Of note, in all *in vivo* experiments, none of the WT-treated mice were affected by the drug, confirming its safety.

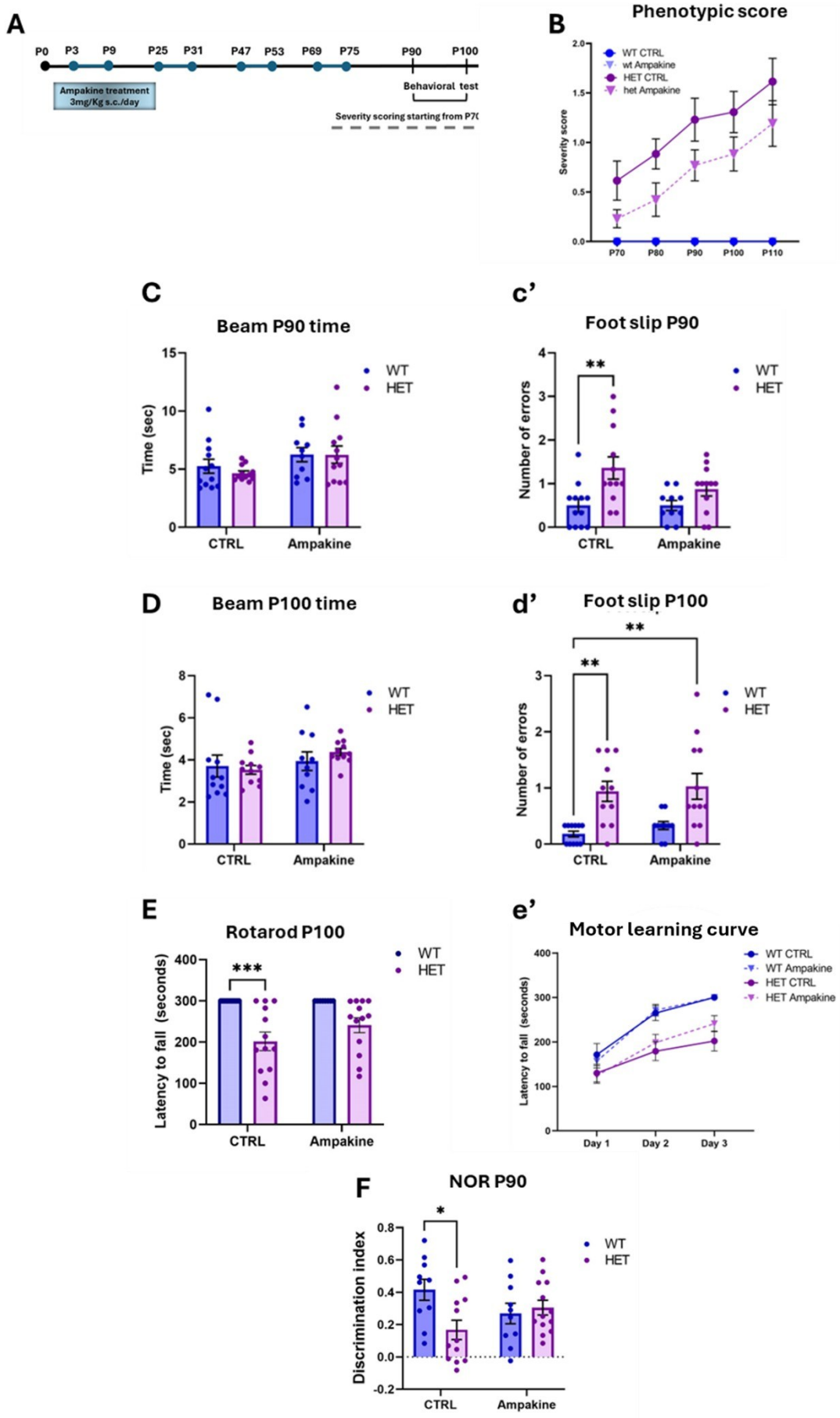
A
P0
P3
P9
P25
P31
P47
P53
P69
P75
P90
P100
Ampakine treatment
3mg/Kg s.c./day
Behavioral test
Severity scoring starting from P7
B
Phenotypic score
WT CTRL
wt Ampakine
HET CTRL
het Ampakine
Severity score
P70
P80
P90
P100
P110
C
Beam P90 time
WT
HET
Time (sec)
CTRL
Ampakine
c'
Foot slip P90
**
Number of errors
D
Beam P100 time
d'
Foot slip P100
E
Rotarod P100
***
Latency to fall (seconds)
e'
Motor learning curve
Day 1
Day 2
Day 3
F
NOR P90
*
Discrimination index

Fig. 6: The early intermittent treatment rescues cognitive and motor defects in heterozygous mice. (A): Schematic representation of the *in vivo* Ampakine administration protocol: mice were injected starting from P3 to P75 every week followed by a two-week pause. Severity score was assessed from P70, twice a week. Behavioural tests were performed from P90 to P100**. (B):** The line graph illustrates the punctual severity score considering general conditions, mobility, hind limb clasping, tremor and gait abnormalities of mice. **(C, c'):** The graph shows the total time (in seconds) spent to cross the beam and the number of foot slip events in the beam walking test at P90. **(D, d'):** The graph shows the total time (in seconds) spent to cross the beam and the number of foot slips events in the beam walking test at P100. **(E, e')**: The graph shows the latency to fall (in seconds) on the accelerating rotarod test at P100 (E). The last graph of the row shows the learning curve over the three days rotarod test trial. **(F):** The graphs represent the discrimination index (DI) between two different objects during NOR test at P100. Each dot represents a single animal. Sample size: WT CTRL=9, WT treated with Ampakine= 10, HET CTRL= 13, HET treated with Ampakine = 13. Statistical significance was assessed by Two-way ANOVA followed by Tukey's post-hoc multiple comparison test and Log-Rank (Mantel-Cox) test (*: *p-value*<0.05, **: *p-value*<0.01, ***: *p-value*<0.001, ****: *p-value*<0.0001). Values are represented as mean ± SEM.

6.5 Ampakine administration potentiates the spontaneous excitatory currents

After observing the beneficial effects of Ampakine *in vivo*, we investigated whether the early treatment was sufficient to induce long lasting and stable modifications in synaptic transmission. To this end, WT and KO mice that received the early treatment regimen (from P3 to P9) were sacrificed at P30. Whole-cell patch clamp recordings were then performed on excitatory neurons derived from the prefrontal cortex. The prefrontal cortex was selected because, although it plays a critical role in the pathophysiology of the disorder [237], it still remains largely uncharacterized. Patch clamp was performed by maintaining the membrane potential at a constant value of -70mV in voltage-clamp mode. This approach allowed us to isolate and record spontaneous excitatory postsynaptic currents (sEPSCs).

So far, we evaluated four parameters: i) the amplitude, that reflects the intensity of the inward current through receptors and is directly related to the amount of ions entering through the channels thus, higher the amplitude stronger the postsynaptic responses; ii) the decay time, that provides an indirect measure of how rapidly channels close, calculated as the time the current takes to return to baseline after reaching its peak; iii) the rise time, defined as the time required for the current to increase from 10% to 90% of its maximum amplitude, reflects the speed at which channels open in response to glutamate; and iv) the frequency, expressed in Hertz (Hz), that indicates the number of spontaneous synaptic events occurring per second, giving insight into presynaptic release activity and the overall excitatory synaptic input received by the neuron [238].
As reported in the graph (Fig. 7B), a significant amplitude defect was observed in untreated KO mice that however was normalized by the treatment. Consistent with this finding, an almost significant defect was observed in the rise time, that was normalized by the drug (Fig. 7C). No significant differences were found between KO and WT CTRL mice in the decay (Fig. 7D) and frequency (Fig. 7E). Altogether, these electrophysiological results confirmed a therapeutic effect of the drug on excitatory transmission in the KO prefrontal cortex. Moreover, since no differences were observed in the frequency, we can hypothesize that KO mice are not affected at the presynaptic level and in the release of neurotransmitters.

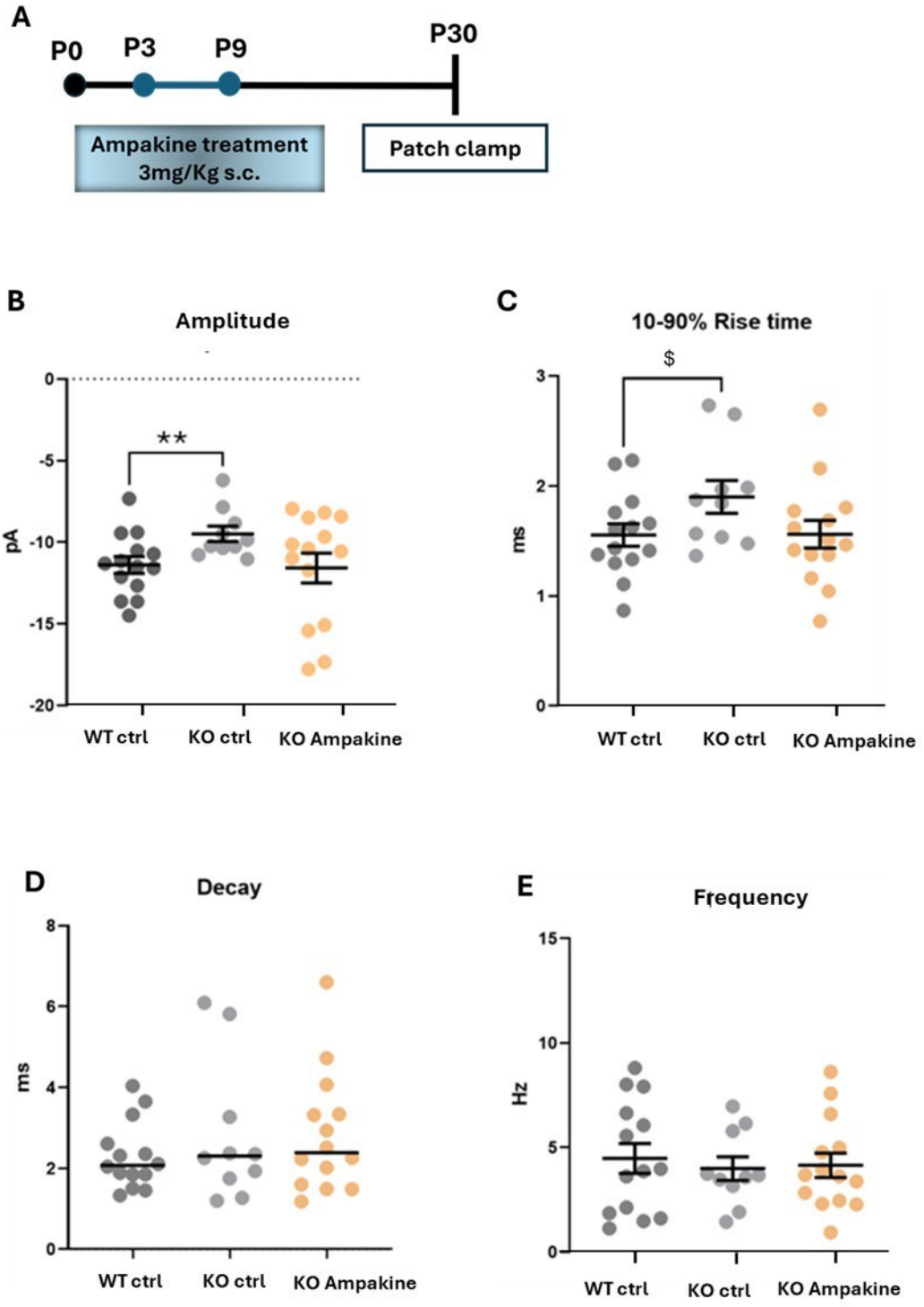

Fig. 7: Ampakine treatment increases EPSCs in PFC of KO mice. (A): Schematic representation of the Ampakine administration protocol. **(B):** The graph represents the amplitude measured in pA (picoAmperes). (**C**): It is shown the rise time of the current to pass from 10% to 90%, measured in milliseconds. (**D**): It represents the decay, calculated as the time required by excitatory receptors to close the ion channels. It is measured in milli seconds. (**E**): It is represented the frequency (Freq) of synaptic events, measured in Hertz. Every dot represents a single cell of excitatory neurons. The total number of cells were erived from three different mice per experimental group. Data were analysed by one-way ANOVA *($p*=0,0723, ***p-value* < 0.01).

6.6 Gene expression differences in WT and KO mice were rescued by the Ampakine treatment, supporting PFC as a valid target for transcriptomic profiling

The next step in our research will be to perform bulk RNA-seq, on WT and KO control, WT treated, and KO treated mice, to finally verify our hypothesis on the feedforward circle between gene expression and neuronal activity described in the introduction [171] and/or identify the mechanism of action (MOA) of the drug. Indeed, the positive effect of Ampakine could be due to an increase in neuronal activity, which in turn affects gene expression, contributing to the restoration of physiological E/I balance.
Considering all the results described above, we analyzed the PFC of mice at P10 (Fig. 8A, B, C, D) and P30 (Fig. 8A', B', C', D') after early treatment (P3-P9) in order to compare the acute and long-lasting effects of the Ampakine on gene expression.
Before sending the samples to the facility for bulk RNA sequencing, we verified RNA integrity and performed RT-qPCR on genes (*Efna5, Dlk1, Cacna1g,* and *Gdf11)* previously reported to be deregulated in *Mecp2*-deficient mice (Li et al., 2025; Pozzer et al., 2025). This step allowed us to obtain a first indication of the healing effects of the drug.

In detail, *Efna5 (Ephrin A5)* encodes for GPI-anchored ligand of Eph receptors, playing a key role in axon guidance, synapse formation, and activity-dependent synaptic plasticity. From bulk-RNA seq, it has been found upregulated both at P28 and P45 in the hippocampus [239] and at P60 in the cortex (Pozzer et al., 2025) of *Mecp2*-null mice. On the same line, *Dlk-1* (Delta-like homolog 1), that encodes for a non-canonical ligand of NOTCH signalling pathway, was found upregulated in *Mecp2*-null mice (Li et al., 2025; Pozzer et al., 2025). On the contrary, *Cacn1g* (calcium voltage-gated channel subunit alpha1 G), that encodes for T-type, low-voltage activated calcium channel, was found downregulated in *Mecp2*-null mice (Li et al., 2025; Pozzer et al., 2025). Similarly, *Gdf11 (*Growth differentiation factor 11) encodes for TGF-β family cytokine that is highly expressed in excitatory neurons in adult mouse cortex and hippocampus. In *Mecp2*-null mouse models, *Gdf11* is significantly downregulated in these two brain regions according to bulk RNA-seq, leading to neuronal hyperexcitability, dendritic pruning, impaired synaptic input and cognitive deficits (Bajikar et al., 2023; Li et al., 2025; Pozzer et al., 2025).

In line with previous studies, both *Efna5* and *Dlk1* were upregulated in our *Mecp2*-null samples, with *Efna5* reaching statistical significance at P30 and *Dlk1* at P10 (Fig. 8A', B). Notably, Ampakine treatment fully rescued *Efna5* expression at P30 and *Dlk1* at P10 (Fig. 8A, B'). However, for genes previously reported to be downregulated in *Mecp2*-null mice, namely *Cacna1g* and *Gdf11*, we did not observe a similar trend in our dataset (Fig. 8C, C', D, D'), possibly due to the different technique used to analyze their expression.-Further, we find it relevant to observe that these data were obtained by testing only six mice per experimental group, a useful number for the transcriptomics experiment but limited in the case of RT-qPCR validation. Additionally, we analysed gene expression in a different brain region compared to the hippocampus and the whole cortex.

Considering these results, we are confident that the upcoming bulk RNA-seq analysis will be useful to identify the beneficial molecular mechanisms set in motion by the drug and to reveal its MOA.

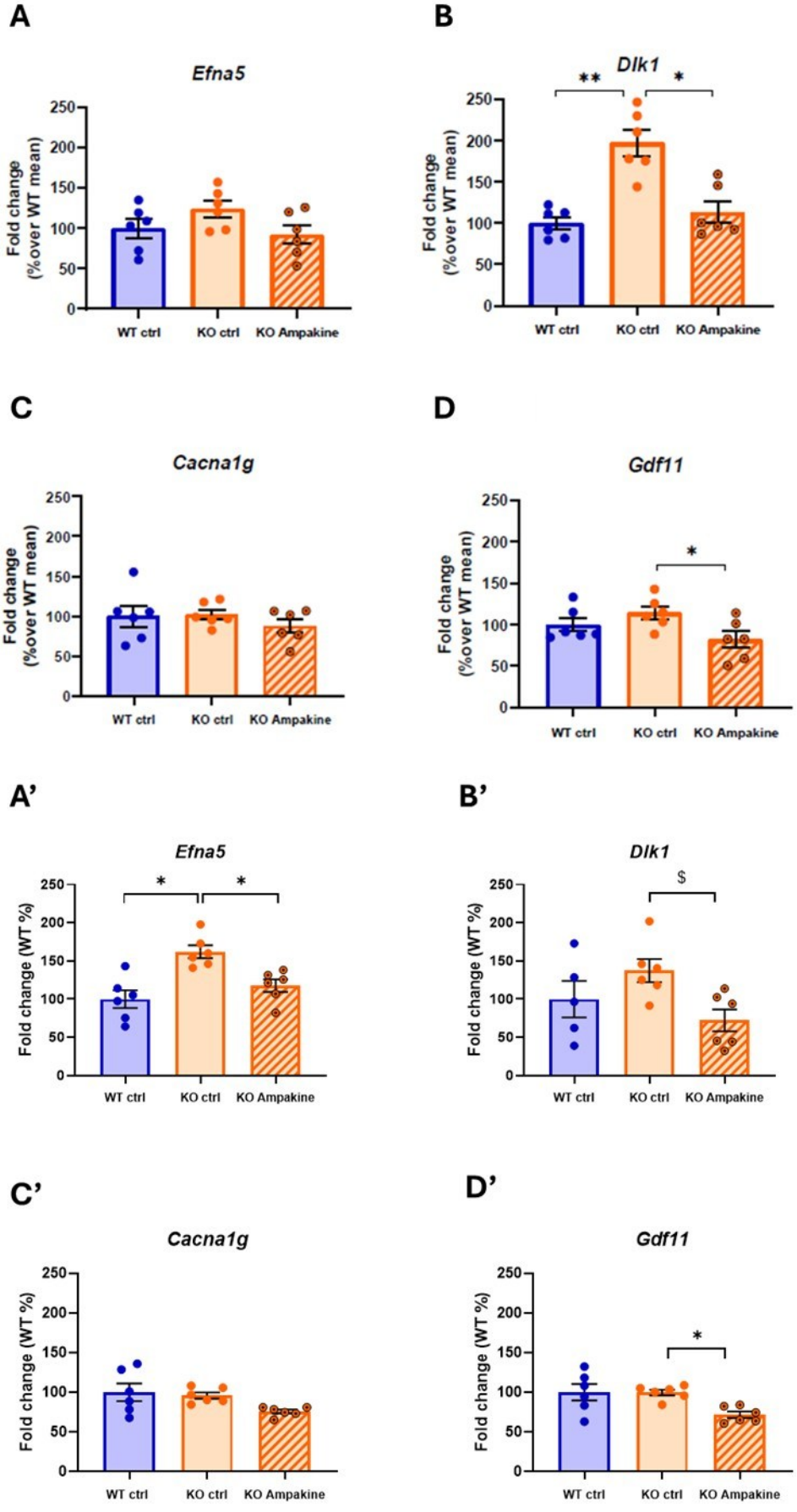
A
Efna5
Fold change (%over WT mean)
250
200
150
100
50
0
WT ctrl
KO ctrl
KO Ampakine
B
Dlk1
**
*
Fold change (%over WT mean)
C
Cacna1g
Fold change (%over WT mean)
D
Gdf11
*
Fold change (%over WT mean)
A'
Efna5
* *
Fold change (WT %)
B'
Dlk1
$
Fold change (WT %)
C'
Cacna1g
Fold change (WT %)
D'
Gdf11
*
Fold change (WT %)

Fig. 8: Gene expression differences in WT and KO mice are rescued by the treatment in the PFC of KO mice. At P10 (**A, B, C, D**) and at P30 (**A', B', C', D'**) the graphs represent the fold change over WT ctrl expressed as a percentage of the following genes: *Efna5, Dlk-1, Cacna1g, Gdf11* in the PFC of P10 mice. Every dot corresponds to different biological replicates. Data were analysed by one-way ANOVA ($p =0,057, **p-value < 0.05, ***p-value < 0.01).*

7. Discussion

Rett syndrome is a complex neurodevelopmental disorder, largely due to a wide range of mutations that affect the *MECP2* gene and its numerous, pleiotropic functions [1]. To date no cure is available for RTT. However, the recent FDA approval [242] of a treatment based on insulin-like growth factor 1 (IGF-1) and associated with behavioural improvements in a subset of patients represents an important step forward [14].

Many efforts have been made along the last 25 years to find new potential treatments. Two major therapeutic strategies have been explored. The first that aims to correct the underlying genetic defect, include gene therapy, gene editing, RNA editing, and tRNA read-through strategies as well as the reactivation of the inactive X-chromosome. However, these technologies are still associated with significant risks, such as off-target effects and insertional mutagenesis linked to vector-based delivery systems [243].

The second strategy focuses on targeting the downstream molecular pathways regulated directly or indirectly by MeCP2. These pathways become dysregulated in the absence of a perfectly functional MeCP2. While such approaches cannot be considered curative, they may offer effective treatments to alleviate the cognitive and motor impairments characteristic of the disorder [8]. In this context, ampakines represent a promising class of compounds, that by increasing neuronal excitability, may restore the feed-forward circle that connects neuronal activity, gene expression and neuronal maturation thereby partially compensating for MeCP2 loss. To test this hypothesis, we selected a high-impact Ampakine that has already been demonstrated safe in clinical trials for Alzheimer's disease, major depressive disorder, and mild cognitive impairment. Despite the already approved trials, poor information is present in literature on its action; therefore, we initially assessed its activity *in vitro*, on primary cortical neurons. In particular, we demonstrated that the drug activates GluA1, increasing its phosphorylation [244], [245]. The activation of the target receptor was confirmed by the increased phosphorylation of Akt, a downstream molecular signal that stimulates molecular processes regulating neuronal development, growth, and maintenance of maturation [246].

We also observed that Ampakine fully rescues key synaptic markers such as Synapsin and Shank2 suggesting enhanced glutamatergic transmission. Complementary calcium imaging experiments showed a full rescue of calcium influx in treated *Mecp2*-deficient neurons, indicating an improved responsiveness to excitatory inputs. Although these findings are already statistically significant, we will reinforce them because they are based on a limited number of biological replicates.

Given the promising *in vitro* results, we proceeded to test Ampakine *in vivo*, using mouse models of RTT. Before the starting of my internship, several data had already been collected demonstrating that a short and early treatment of KO male mice with the Ampakine exerts sustained beneficial effects. However, in a later time window benefits were observed only using a prolonged intermittent treatment suggesting the importance of intervening with ampakines either before the onset of evident symptoms and/or in a time window characterized by high neuroplasticity. Neuroplasticity indeed persists along life but appears particularly important during the time-sensitive periods of pre- and post-natal brain development, establishing the formation of a responsive neuronal network, able to adapt to stimuli [247]. During my stage, I confirmed in HET females, which more closely mimic the RTT genotype, the potency that this short and early pre-symptomatic intervention owns in inducing long-lasting beneficial effects. Of interest, the duration of therapeutic benefit differed between genders: while improvements in KO males, that are characterized by a fast-progressing disease, lasted around 35

days, persistent benefits remained detectable in HET females up to 90 days. This sex difference may arise from the mosaic expression of *Mecp2* in HET females, which results in a delayed and less severely compromised condition compared to the male counterpart. This interpretation also aligns with the inefficacy of one-week treatment administration during a later translational time window, which, however, did not correspond to the critical period of synaptic plasticity in KO males. By that stage, neuronal dysfunction and structural deficits may have progressed beyond the point at which a short stimulation of activity-dependent mechanisms can effectively trigger repair.
Testing the same late-onset regimen also in HET females will be crucial to determine whether efficacy primarily depends on the timing of treatment during a critical period of plasticity or instead on the overall degree of neuronal damage. A positive outcome in HET females would underscore the importance of preserving a sufficient degree of network integrity for Ampakine efficacy, while a negative outcome would strengthen the notion that a highly plastic brain is indispensable.

Building on the success of the early treatment, we then tested a combined regimen of early and intermittent treatment to further prolong the benefits and delay the onset of symptoms. This paradigm of administration protocol proved to be effective in recovering motor and cognitive defects as well as an overall amelioration of Rett phenotypes in both mouse models; survival was significantly prolonged in *Mecp2* null male mice.
These findings suggest that while a one-week treatment during the critical plasticity window can initiate a self-sustaining cycle of improvement, repeated dosing helps in maintaining and extending these benefits. However, to capture the full duration of the beneficial effects induced by early intermittent treatment, future experiments in HET females should include behavioural assessments beyond P90–P100, that is the time point by which we assessed behavioural phenotypes within the early treatment. Moreover, since only intermittent regimens were employed to minimize the risk of overstimulation or undue stress in mice, assessing the impact of a chronic, continuous treatment initiated at a later stage that aligns with clinical diagnosis, could provide valuable translational insight.
One important observation in our study was the phenotypic variability observed among HET mice under both treatment regimens. This variability reflects the biological complexity of the outbred CD1 background and the mosaic *Mecp2* expression pattern, and it parallels the heterogeneity seen in RTT patients. Rather than limiting our conclusions, this variability underscores the translational relevance of our findings, as Ampakine efficacy was evident despite biological diversity. An additional source of variability may be related to the estrous cycle. While previous studies have shown minimal differences in motor and cognitive performance across different cycle phases [248], [249], [250], [251], pharmacological responses may still be influenced by hormonal fluctuations. For instance, Picard et al. (2019) reported cycle-dependent effects of ketamine, and Galvin and Ninan (2014) described estrous modulation of AMPA receptor signalling[252], [253]. To minimize hormonal variability, the literature often recommends vaginal cytology and estrous cycle synchronization in female rodents. However, these procedures were deemed too invasive in our female cohorts in the context of this study. This is particularly relevant for CD1 mice; excessive handling could unintentionally accelerate recovery. In fact, even gentle tactile stimulation has been shown to mimic the effects of ampakines on behavioural phenotypes. This aligns with the concept that social or sensory inputs can directly modulate motor outputs via central neural pathways [171].

The next step of this study was to elucidate the molecular mechanisms underlying the long-lasting *in vivo* benefits after the early and short Ampakine treatment (from P3 to P9). We thus performed electrophysiological recordings on prefrontal cortex (PFC) excitatory neurons of KO mice. Although behavioural improvements were observed at P45, we chose to perform the patch clamp at P30 hypothesizing that it might be close to the peak time for sustained synaptic changes induced by the treatment and before any potential decline in efficacy. Since AMPA receptors are expressed post-synaptically and Ampakine modulate their activity, we expected a post-synaptic drug mechanism of action. The normalization of both the reduced amplitude of spontaneous excitatory postsynaptic

currents (sEPSCs) and the slower channel opening kinetics observed in KO mice confirmed our hypothesis. Notably, decay kinetics remained unchanged in treated KO, consistent with the pharmacological profile of the second generation of high-impact ampakines that enhance channel opening speed without prolonging receptor activation, thus minimizing excitotoxicity risk. Given that *Mecp2* deficiency leads to a widespread imbalance in excitation and inhibition (E/I) across the brain, it remains to be explored whether Ampakines can also modulate inhibitory circuits in regions exhibiting hyperactivity, such as the hippocampus. Indeed, Philips et al. (2019) proposed that hippocampal hyperactivity in *Mecp2*-null mice contributes to prefrontal cortex hypoactivity[254]. This may occur through excessive excitatory inputs that over activates PV+ GABAergic interneurons in the PFC, leading to increased inhibition of excitatory neurons. Assessing inhibitory function in this region could therefore help determine whether the drug supports a more global restoration of network dynamics. At the transcriptional level, RT-qPCR analysis provided additional support for the re-establishing of the aforementioned virtuous feed-forward circuit. Consistent with previous transcriptomic studies, *Mecp2*-null PFC displayed upregulation of *Efna5 and Dlk1*, both of which were normalized by Ampakine treatment. Given their roles in axon guidance and neurodevelopmental signalling, this finding suggests that Ampakine influence not only synaptic activity but also transcriptional programs critical for neuronal maturation. Building on this, bulk RNA sequencing of PFC tissue at P10 and P30 is planned. Analysis at P10 will capture early transcriptional changes immediately following treatment, while P30 will reveal long-lasting adaptations underlying the sustained behavioural benefits. Bulk RNA-seq might be particularly appropriate as RTT-related transcriptional alterations are subtle and distributed. Once broad patterns are established, more refined single-cell approaches may help delineate cell-type-specific responses.

The relevance of our findings extends beyond Rett syndrome, as the intervention does not target a specific mutation but rather acts on a broader mechanism namely the restoration of activity-dependent transcription through normalization of neuronal responsiveness. This suggests that enhancing the positive feedforward loop between neuronal activity and gene expression could be a viable therapeutic strategy for a range of neurodevelopmental disorders characterized by impaired synaptic plasticity and dysregulated transcriptional programs. However open questions regarding the translational potential of this early intervention remain. To date, the most effective treatment started early from P3 to P9, corresponding approximately to late gestation through the first year of life in humans [255], [256]. Defining an equivalent critical period in humans is complex, as synaptogenesis begins prenatally and proceeds at different rates across brain regions [255]. Since RTT is diagnosed on the basis of established clinical criteria, patients are identified only after symptom onset. If Ampakine efficacy depends strictly on intervention within an early plasticity window, presymptomatic treatment would require improved strategies for timely genetic diagnosis. Of note, preliminary results indicate that also the intermittent treatment retains a significant degree of efficacy, even when initiated at later stages. This suggests that, in cases where an early diagnosis is not feasible, a late-onset treatment regimen may still offer meaningful therapeutic benefits for patients. In particular we aim to compare the efficacy of a chronic treatment in respect to an intermittent one in both KO and HET and determine whether therapeutic effects can be enhanced within a more translationally relevant time window. Moreover, careful optimization of dosing regimens tailored to human pharmacokinetic and pharmacodynamic profiles will be crucial to fully realize the clinical potential of this intervention. Notably, it is also conceivable that Ampakine treatment could exert additive or synergistic effects when combined with compounds acting on complementary pathways, such as Trofinetide [14] or modified NGF (nerve growth factor)[257]. These drugs, which support neuronal survival, synaptic maintenance, and anti-inflammatory responses, have shown efficacy even when administered at more advanced stages of disease progression, and may complement the activity-dependent transcriptional and plasticity-enhancing effects of Ampakine. A combined approach could therefore maximize therapeutic efficacy, especially when intervention occurs beyond the early developmental window.

8. Conclusions

All in all, this study provides converging evidence that pharmacological enhancement of excitatory synaptic transmission with Ampakines is a promising therapeutic strategy for RTT. Our experiments demonstrated synaptic recovery *in vitro,* behavioural improvements *in vivo* under both early and early intermittent regimens (with the latter producing more sustained effects), and postsynaptic rescue confirmed by *ex vivo* electrophysiology, together with normalization of dysregulated genes at the transcriptional level. These findings highlight not only the potential of Ampakines for treating RTT, but also the broader relevance of targeting critical windows of neuroplasticity, an approach that may extend to other neurodevelopmental disorders characterized by impaired activity-dependent maturation. Further investigations, including comprehensive transcriptomic and proteomic analyses, are necessary to fully uncover the molecular mechanisms behind these effects. Taken together, we believe that these preclinical data provide a strong rationale for advancing Ampakines toward clinical application.

9. Abbreviations

AMPA: a-amino-3-hydroxy-5-methyl-4-isoxazoleproprionic acid

AKT: AKT Serine/Threonine Kinase 1

ARC: Activity Regulated Cytoskeleton Associated Prot

ASD: Autism Spectrum Disorder

AAV: adeno-associated viral vector

BBB: Blood-brain barrier

BDNF: Brain-derived neurotrophic factor

BSA: Bovine Serum Albumin

CaMKII: Calmodulin-dependent protein kinase II

cFOS: Fos Proto-Oncogene, AP-1 Transcription Factor Subunit

CREB1: Cyclic AMP-responsive Element-Binding Protein 1

CNS: Central nervous system

CTD: C-terminal domain

CTZ: cyclothiazide

DIV: Day in vitro

DNMT1: DNA Methyl Transferase 1

E: Embryonic days

E/I: excitatory/inhibitory

EEG: electro-encephalogram

EPSP: excitatory postsynaptic potential

FC: Fold Change

FDA: Food and Drug Administration

FOXG1: Forkhead box protein G1

GABA: γ-aminobutyric acid

GLUA: Glutamate Ionotropic Receptor AMPA Type Subunit 1

HBSS: Hank's Buffered Salt Solution

HDAC: Histone deacetylase

HETT: Heterozygous

HPCAL4: Hippocalcin Like 4

ID: Intervening domain

IEG: immediate early gene

IGF-1: Insulin-like growth factor 1

iGluR: Ionotropic Glutamate Receptros

I.P.: intraperitoneal injection

KI: knock-in

KO: knock-out

LTD: Long-Term Depression

LTP: Long-Term Potentiation

MBD: Methyl-CpG-binding domain

MECP2: Methyl-cCpG-binding protein 2

mGluR: Metabotropic Glutamate Receptor

mTOR: Mechanistic Target Of Rapamycin Kinase

NCoR-SMRT: Nuclear receptor Co-Repressor and the Silencing Mediator of Retinoic acid and Thyroid hormone receptor

NCS: neuronal calcium sensor

NID: NCoR/SMRT Interaction Domain

NMDA: N-methyl-D-aspartate

NOR: Novel Object Recognition

NPCs: neural progenitor cells

NTD: N-terminal domain

P: Post-natal day

PAM: Positive allosteric modulator

PBS: Phosphate-Buffered Saline

PCR: Polymerase Chain Reaction

PIC: Protease inhibitor cocktail

PSD: Post synaptic density

qRT-PCR: quantitative reverse transcription polymerase chain reaction

RNASeq: RNA sequencing

RTT: Rett syndrome

S.C.: subcutaneous injection

SEM: Standard error mean

TBS-T: Tris-buffered saline containing 0.1% Tween-20

TRD: Transcriptional repressor domain

WB: Western blot

WT: wild type

XCI: X chromosome inactivation

10. Acknowledgments

I would like to express my profound gratitude to Professor Landsberger for warmly welcoming me into her laboratory and for her continuous availability for thoughtful and stimulating discussions. Her vast experience, scientific rigor, and deep commitment to research have been a constant source of inspiration. The meticulous review of my entire thesis, her ability to challenge my reasoning, and the exceptional attention she devoted to every aspect of my work were truly invaluable in enhancing both the quality of this research and my academic growth.

I am equally grateful to Professor Mucignat for her continuous support throughout my academic journey. Her guidance in selecting the internship and her thoughtful supervision of this thesis enriched the project with valuable insights.

A heartfelt thank you to Andrea, whose attentive mentorship and genuine dedication to my learning played a key role in this experience. His support extended beyond the academic realm, helping me cultivate a mindset of precision, organization, and curiosity, while also offering personal encouragement when most needed.

My warmest thanks go to Pepi, whose experience and unwavering support have been a true pillar of strength throughout this journey. She has been an exceptional role model and an encouraging presence during the most challenging moments.

I am also thankful to the entire laboratory team for their kindness, constant support, and for making me feel part of a collaborative and stimulating environment. They were a valuable point of reference during my time in Milan, both professionally and personally.

To my parents and my sister, thank you for standing by me through every decision, for believing in me even when I doubted myself, and for being my greatest source of strength. I truly hope to have made you proud.

I would also like to thank my uncle Stefano, aunt Laura, and Leo for making me feel at home and treating me like a daughter during this time. Your support and affection have meant a great deal to me.

A special thank you to my grandmother Fiamma, who has always been present and cheering me on from the front row in every important moment of my life.

Thank you, Dario, for everything. Your presence has brought light and strength to this journey. You have helped me face challenges with courage and shown me what true love really means. You are a constant source of inspiration.

To Francesca, thank you for being the kind of best friend everyone wishes they had: reliable, supportive, and always there.

Finally, to all my friends, thank you for your patience and affection. A special mention goes to Giada, Giulia, Anna, and Carlotta, whose presence has made a lasting difference.

11. References

[1] J. L. Neul, "The relationship of Rett syndrome and MECP2 disorders to autism.," *Dialogues Clin Neurosci*, vol. 14, no. 3, pp. 253–62, Sep. 2012, doi: 10.31887/DCNS.2012.14.3/jneul.

[2] R. E. Amir, I. B. Van den Veyver, M. Wan, C. Q. Tran, U. Francke, and H. Y. Zoghbi, "Rett syndrome is caused by mutations in X-linked MECP2, encoding methyl-CpG-binding protein 2.," *Nat Genet*, vol. 23, no. 2, pp. 185–8, Oct. 1999, doi: 10.1038/13810.

[3] C. L. Laurvick *et al.*, "Rett syndrome in Australia: a review of the epidemiology.," *J Pediatr*, vol. 148, no. 3, pp. 347–52, Mar. 2006, doi: 10.1016/j.jpeds.2005.10.037.

[4] B. Hagberg and I. Witt-Engerström, "Rett syndrome: Epidemiology and nosology — progress in knowledge 1986 — A conference communication," *Brain Dev*, vol. 9, no. 5, pp. 451–457, Jan. 1987, doi: 10.1016/S0387-7604(87)80062-1.

[5] B. Hagberg, "Clinical manifestations and stages of rett syndrome," *Ment Retard Dev Disabil Res Rev*, vol. 8, no. 2, pp. 61–65, Jan. 2002, doi: 10.1002/mrdd.10020.

[6] Jeffrey L. Neul *et al.*, "Rett syndrome: Revised diagnostic criteria and nomenclature," *Ann Neurol*, vol. 68, no. 6, pp. 944–950, Dec. 2010, doi: 10.1002/ana.22124.

[7] J. E. Allanson, R. C. M. Hennekam, U. Moog, and E. E. Smeets, "Rett syndrome: A study of the face," *Am J Med Genet A*, vol. 155, no. 7, pp. 1563–1567, Jul. 2011, doi: 10.1002/ajmg.a.34027.

[8] A. K. Percy, "Rett syndrome: A coming of age," *Transl Sci Rare Dis*, pp. 1–13, Aug. 2024, doi: 10.3233/trd-240069.

[9] Z. U. N. Mughal *et al.*, "Trofinetide receives FDA approval as first drug for Rett syndrome," *Annals of Medicine & Surgery*, vol. 86, no. 5, pp. 2382–2385, May 2024, doi: 10.1097/MS9.0000000000001896.

[10] E. E. Smeets, G. S. Townend, and L. M. G. Curfs, "Rett syndrome and developmental regression," *Neurosci Biobehav Rev*, vol. 104, pp. 100–101, Sep. 2019, doi: 10.1016/j.neubiorev.2019.06.038.

[11] A. S. Ivy and S. Standridge, "Rett Syndrome: A Timely Review From Recognition to Current Clinical Approaches and Clinical Study Updates," *Semin Pediatr Neurol*, vol. 37, p. 100881, Apr. 2021, doi: 10.1016/j.spen.2021.100881.

[12] D. C. Tarquinio *et al.*, "The Changing Face of Survival in Rett Syndrome and MECP2-Related Disorders," *Pediatr Neurol*, vol. 53, no. 5, pp. 402–411, Nov. 2015, doi: 10.1016/j.pediatrneurol.2015.06.003.

[13] A. Vogel Ciernia *et al.*, "MeCP2 isoform e1 mutant mice recapitulate motor and metabolic phenotypes of Rett syndrome," *Hum Mol Genet*, Sep. 2018, doi: 10.1093/hmg/ddy301.

[14] J. L. Neul *et al.*, "Trofinetide for the treatment of Rett syndrome: a randomized phase 3 study," *Nat Med*, vol. 29, no. 6, pp. 1468–1475, Jun. 2023, doi: 10.1038/s41591-023-02398-1.

[15] A. Rett, "[On a unusual brain atrophy syndrome in hyperammonemia in childhood].," *Wien Med Wochenschr*, vol. 116, no. 37, pp. 723–6, Sep. 1966.

[16] J. Guy, H. Cheval, J. Selfridge, and A. Bird, "The role of MeCP2 in the brain," *Annu Rev Cell Dev Biol*, vol. 27, pp. 631–652, 2011, doi: 10.1146/annurev-cellbio-092910-154121.

[17] J. Guy, B. Hendrich, M. Holmes, J. E. Martin, and A. Bird, "A mouse Mecp2-null mutation causes neurological symptoms that mimic Rett syndrome," 2001. [Online]. Available: http://genetics.nature.com

[18] R. Z. Chen, S. Akbarian, M. Tudor, and R. Jaenisch, "Deficiency of methyl-CpG binding protein-2 in CNS neurons results in a Rett-like phenotype in mice," *Nat Genet*, vol. 27, no. 3, pp. 327–331, Mar. 2001, doi: 10.1038/85906.

[19] R. Tillotson and A. Bird, "The Molecular Basis of MeCP2 Function in the Brain," Mar. 13, 2020, *Academic Press*. doi: 10.1016/j.jmb.2019.10.004.

[20] F. Ehrhart, S. L. M. Coort, E. Cirillo, E. Smeets, C. T. Evelo, and L. M. G. Curfs, "Rett syndrome - Biological pathways leading from MECP2 to disorder phenotypes," Nov. 25, 2016, *BioMed Central Ltd.* doi: 10.1186/s13023-016-0545-5.

[21] G. N. Mnatzakanian *et al.*, "A previously unidentified MECP2 open reading frame defines a new protein isoform relevant to Rett syndrome," *Nat Genet*, vol. 36, no. 4, pp. 339–341, Apr. 2004, doi: 10.1038/ng1327.

[22] S. Kriaucionis, "The major form of MeCP2 has a novel N-terminus generated by alternative splicing," *Nucleic Acids Res*, vol. 32, no. 5, pp. 1818–1823, Mar. 2004, doi: 10.1093/nar/gkh349.

[23] R. M. Zachariah and M. Rastegar, "Linking epigenetics to human disease and Rett syndrome: the emerging novel and challenging concepts in MeCP2 research.," *Neural Plast*, vol. 2012, p. 415825, 2012, doi: 10.1155/2012/415825.

[24] C. O. Olson, R. M. Zachariah, C. D. Ezeonwuka, V. R. B. Liyanage, and M. Rastegar, "Brain region-specific expression of MeCP2 isoforms correlates with DNA methylation within Mecp2 regulatory elements," *PLoS One*, vol. 9, no. 3, Mar. 2014, doi: 10.1371/journal.pone.0090645.

[25] D. H. Yasui *et al.*, "Mice with an isoform-ablating Mecp2 exon 1 mutation recapitulate the neurologic deficits of Rett syndrome," *Hum Mol Genet*, vol. 23, no. 9, pp. 2447–2458, May 2014, doi: 10.1093/hmg/ddt640.

[26] N. Farra, W. B. Zhang, P. Pasceri, J. H. Eubanks, M. W. Salter, and J. Ellis, "Rett syndrome induced pluripotent stem cell-derived neurons reveal novel neurophysiological alterations," *Mol Psychiatry*, vol. 17, no. 12, pp. 1261–1271, Dec. 2012, doi: 10.1038/mp.2011.180.

[27] M. Itoh *et al.*, "Methyl CpG-binding Protein Isoform MeCP2_e2 Is Dispensable for Rett Syndrome Phenotypes but Essential for Embryo Viability and Placenta Development," *Journal of Biological Chemistry*, vol. 287, no. 17, pp. 13859–13867, Apr. 2012, doi: 10.1074/jbc.M111.309864.

[28] S. Pejhan and M. Rastegar, “biomolecules Role of DNA Methyl-CpG-Binding Protein MeCP2 in Rett Syndrome Pathobiology and Mechanism of Disease,” 2021, doi: 10.3390/biom.

[29] B. E. Collins and J. L. Neul, “Rett Syndrome and MECP2 Duplication Syndrome: Disorders of MeCP2 Dosage,” 2022, *Dove Medical Press Ltd*. doi: 10.2147/NDT.S371483.

[30] K. V. Good, J. B. Vincent, and J. Ausió, “MeCP2: The Genetic Driver of Rett Syndrome Epigenetics,” Jan. 21, 2021, *Frontiers Media S.A.* doi: 10.3389/fgene.2021.620859.

[31] P. D. Ross *et al.*, “Exclusive expression of MeCP2 in the nervous system distinguishes between brain and peripheral Rett syndrome-like phenotypes,” *Hum Mol Genet*, vol. 25, no. 20, pp. 4389–4404, 2016, doi: 10.1093/hmg/ddw269.

[32] B. P. Jung, D. G. M. Jugloff, G. Zhang, R. Logan, S. Brown, and J. H. Eubanks, “The expression of methyl CpG binding factor MeCP2 correlates with cellular differentiation in the developing rat brain and in cultured cells,” *J Neurobiol*, vol. 55, no. 1, pp. 86–96, Apr. 2003, doi: 10.1002/neu.10201.

[33] M. D. Shahbazian, “Insight into Rett syndrome: MeCP2 levels display tissue- and cell-specific differences and correlate with neuronal maturation,” *Hum Mol Genet*, vol. 11, no. 2, pp. 115–124, Jan. 2002, doi: 10.1093/hmg/11.2.115.

[34] D. R. S. Cohen *et al.*, “Expression of MeCP2 in olfactory receptor neurons is developmentally regulated and occurs before synaptogenesis,” *Molecular and Cellular Neuroscience*, vol. 22, no. 4, pp. 417–429, Apr. 2003, doi: 10.1016/S1044-7431(03)00026-5.

[35] N. Kishi and J. D. Macklis, “MECP2 is progressively expressed in post-migratory neurons and is involved in neuronal maturation rather than cell fate decisions,” *Molecular and Cellular Neuroscience*, vol. 27, no. 3, pp. 306–321, Nov. 2004, doi: 10.1016/j.mcn.2004.07.006.

[36] B. C. Mullaney, M. V. Johnston, and M. E. Blue, “Developmental expression of methyl-CpG binding protein 2 is dynamically regulated in the rodent brain,” *Neuroscience*, vol. 123, no. 4, pp. 939–949, Jan. 2004, doi: 10.1016/j.neuroscience.2003.11.025.

[37] K. Miyake and K. Nagai, “Phosphorylation of methyl-CpG binding protein 2 (MeCP2) regulates the intracellular localization during neuronal cell differentiation,” *Neurochem Int*, vol. 50, no. 1, pp. 264–270, Jan. 2007, doi: 10.1016/j.neuint.2006.08.018.

[38] J. Liu and U. Francke, “Identification of cis-regulatory elements for MECP2 expression,” *Hum Mol Genet*, vol. 15, no. 11, pp. 1769–1782, Jun. 2006, doi: 10.1093/hmg/ddl099.

[39] M. Chahrour and H. Y. Zoghbi, “The Story of Rett Syndrome: From Clinic to Neurobiology,” Nov. 08, 2007. doi: 10.1016/j.neuron.2007.10.001.

[40] S. Pejhan and M. Rastegar, “biomolecules Role of DNA Methyl-CpG-Binding Protein MeCP2 in Rett Syndrome Pathobiology and Mechanism of Disease,” 2021, doi: 10.3390/biom.

[41] R. J. Klose, S. A. Sarraf, L. Schmiedeberg, S. M. McDermott, I. Stancheva, and A. P. Bird, “DNA Binding Selectivity of MeCP2 Due to a Requirement for A/T Sequences Adjacent to

Methyl-CpG," *Mol Cell*, vol. 19, no. 5, pp. 667–678, Sep. 2005, doi: 10.1016/j.molcel.2005.07.021.

[42] T. C. Galvao, "Structure-specific binding of MeCP2 to four-way junction DNA through its methyl CpG-binding domain," *Nucleic Acids Res*, vol. 33, no. 20, pp. 6603–6609, Nov. 2005, doi: 10.1093/nar/gki971.

[43] J. D. Lewis *et al.*, "Purification, sequence, and cellular localization of a novel chromosomal protein that binds to Methylated DNA," *Cell*, vol. 69, no. 6, pp. 905–914, Jun. 1992, doi: 10.1016/0092-8674(92)90610-O.

[44] A. M. Deaton *et al.*, "Cell type–specific DNA methylation at intragenic CpG islands in the immune system," *Genome Res*, vol. 21, no. 7, pp. 1074–1086, Jul. 2011, doi: 10.1101/gr.118703.110.

[45] H. W. Gabel *et al.*, "Disruption of DNA-methylation-dependent long gene repression in Rett syndrome," *Nature*, vol. 522, no. 7554, pp. 89–93, Jun. 2015, doi: 10.1038/nature14319.

[46] K. Kokura *et al.*, "The Ski Protein Family Is Required for MeCP2-mediated Transcriptional Repression," *Journal of Biological Chemistry*, vol. 276, no. 36, pp. 34115–34121, Sep. 2001, doi: 10.1074/jbc.M105747200.

[47] M. J. Lyst *et al.*, "Rett syndrome mutations abolish the interaction of MeCP2 with the NCoR/SMRT co-repressor," *Nat Neurosci*, vol. 16, no. 7, pp. 898–902, Jul. 2013, doi: 10.1038/nn.3434.

[48] X. Xu, A. P. Kozikowski, and L. Pozzo-Miller, "A selective histone deacetylase-6 inhibitor improves BDNF trafficking in hippocampal neurons from Mecp2 knockout mice: implications for Rett syndrome," *Front Cell Neurosci*, vol. 8, Mar. 2014, doi: 10.3389/fncel.2014.00068.

[49] F. Fuks, P. J. Hurd, D. Wolf, X. Nan, A. P. Bird, and T. Kouzarides, "The Methyl-CpG-binding Protein MeCP2 Links DNA Methylation to Histone Methylation," *Journal of Biological Chemistry*, vol. 278, no. 6, pp. 4035–4040, Feb. 2003, doi: 10.1074/jbc.M210256200.

[50] V. Kruusvee, M. J. Lyst, C. Taylor, Ž. Tarnauskaitė, A. P. Bird, and A. G. Cook, "Structure of the MeCP2–TBLR1 complex reveals a molecular basis for Rett syndrome and related disorders," *Proceedings of the National Academy of Sciences*, vol. 114, no. 16, Apr. 2017, doi: 10.1073/pnas.1700731114.

[51] A. Bebbington *et al.*, "Updating the profile of C-terminal MECP2 deletions in Rett syndrome," *J Med Genet*, vol. 47, no. 4, pp. 242–248, Apr. 2010, doi: 10.1136/jmg.2009.072553.

[52] M. D. Shahbazian and H. Y. Zoghbi, "REVIEW ARTICLE Rett Syndrome and MeCP2: Linking Epigenetics and Neuronal Function," 2002.

[53] J. P. Buschdorf and W. H. Str□tling, "A WW domain binding region in methyl-CpG-binding protein MeCP2: impact on Rett syndrome," *J Mol Med*, vol. 82, no. 2, pp. 135–143, Feb. 2004, doi: 10.1007/s00109-003-0497-9.

[54] R. Klose and A. Bird, “MeCP2 Repression Goes Nonglobal,” *Science (1979)*, vol. 302, no. 5646, pp. 793–795, Oct. 2003, doi: 10.1126/science.1091762.

[55] W. G. Chen *et al.*, “Derepression of BDNF Transcription Involves Calcium-Dependent Phosphorylation of MeCP2,” *Science (1979)*, vol. 302, no. 5646, pp. 885–889, Oct. 2003, doi: 10.1126/science.1086446.

[56] Z. Zhou *et al.*, “Brain-Specific Phosphorylation of MeCP2 Regulates Activity-Dependent Bdnf Transcription, Dendritic Growth, and Spine Maturation,” *Neuron*, vol. 52, no. 2, pp. 255–269, Oct. 2006, doi: 10.1016/j.neuron.2006.09.037.

[57] L. Abuhatzira, K. Makedonski, Y. Kaufman, A. Razin, and R. Shemer, “MeCP2 Deficiency in the Brain Decreases BDNF Levels by REST/CoREST-Mediated Repression and Increases TRKB Production,” *Epigenetics*, vol. 2, no. 4, pp. 214–222, Oct. 2007, doi: 10.4161/epi.2.4.5212.

[58] P. L. Jones *et al.*, “Methylated DNA and MeCP2 recruit histone deacetylase to repress transcription,” *Nat Genet*, vol. 19, no. 2, pp. 187–191, Jun. 1998, doi: 10.1038/561.

[59] X. Nan *et al.*, “Transcriptional repression by the methyl-CpG-binding protein MeCP2 involves a histone deacetylase complex,” *Nature*, vol. 393, no. 6683, pp. 386–389, May 1998, doi: 10.1038/30764.

[60] M. Tudor, S. Akbarian, R. Z. Chen, and R. Jaenisch, “Transcriptional profiling of a mouse model for Rett syndrome reveals subtle transcriptional changes in the brain,” *Proceedings of the National Academy of Sciences*, vol. 99, no. 24, pp. 15536–15541, Nov. 2002, doi: 10.1073/pnas.242566899.

[61] M. Chahrour *et al.*, “MeCP2, a key contributor to neurological disease, activates and represses transcription,” *Science (1979)*, vol. 320, no. 5880, pp. 1224–1229, May 2008, doi: 10.1126/science.1153252.

[62] F. B. Axelrod, G. G. Chelimsky, and D. E. Weese-Mayer, “Pediatric Autonomic Disorders,” *Pediatrics*, vol. 118, no. 1, pp. 309–321, Jul. 2006, doi: 10.1542/peds.2005-3032.

[63] P. M. Horvath and L. M. Monteggia, “MeCP2 as an Activator of Gene Expression,” *Trends Neurosci*, vol. 41, no. 2, pp. 72–74, Feb. 2018, doi: 10.1016/j.tins.2017.11.005.

[64] S. Ben-Shachar, M. Chahrour, C. Thaller, C. A. Shaw, and H. Y. Zoghbi, “Mouse models of MeCP2 disorders share gene expression changes in the cerebellum and hypothalamus,” *Hum Mol Genet*, vol. 18, no. 13, pp. 2431–2442, Jul. 2009, doi: 10.1093/hmg/ddp181.

[65] Y. Li *et al.*, “Global Transcriptional and Translational Repression in Human-Embryonic-Stem-Cell-Derived Rett Syndrome Neurons,” *Cell Stem Cell*, vol. 13, no. 4, pp. 446–458, Oct. 2013, doi: 10.1016/j.stem.2013.09.001.

[66] W. Lee *et al.*, “MeCP2 regulates activity-dependent transcriptional responses in olfactory sensory neurons,” *Hum Mol Genet*, vol. 23, no. 23, pp. 6366–6374, Dec. 2014, doi: 10.1093/hmg/ddu358.

[67] M. Mahgoub *et al.*, “MeCP2 and histone deacetylases 1 and 2 in dorsal striatum collectively suppress repetitive behaviors,” *Nat Neurosci*, vol. 19, no. 11, pp. 1506–1512, Nov. 2016, doi: 10.1038/nn.4395.

[68] R. J. Kelleher and M. F. Bear, “The Autistic Neuron: Troubled Translation?,” *Cell*, vol. 135, no. 3, pp. 401–406, Oct. 2008, doi: 10.1016/j.cell.2008.10.017.

[69] S. Osenberg *et al.*, “Activity-dependent aberrations in gene expression and alternative splicing in a mouse model of Rett syndrome,” *Proceedings of the National Academy of Sciences*, vol. 115, no. 23, Jun. 2018, doi: 10.1073/pnas.1722546115.

[70] H. Nakashima *et al.*, “MeCP2 controls neural stem cell fate specification through miR-199a-mediated inhibition of BMP-Smad signaling,” *Cell Rep*, vol. 35, no. 7, p. 109124, May 2021, doi: 10.1016/j.celrep.2021.109124.

[71] A. Bergo *et al.*, “Methyl-CpG Binding Protein 2 (MeCP2) Localizes at the Centrosome and Is Required for Proper Mitotic Spindle Organization,” *Journal of Biological Chemistry*, vol. 290, no. 6, pp. 3223–3237, Feb. 2015, doi: 10.1074/jbc.M114.608125.

[72] A. Frasca *et al.*, “*MECP2* mutations affect ciliogenesis: a novel perspective for Rett syndrome and related disorders,” *EMBO Mol Med*, vol. 12, no. 6, Jun. 2020, doi: 10.15252/emmm.201910270.

[73] S. Ricciardi *et al.*, “Reduced AKT/mTOR signaling and protein synthesis dysregulation in a Rett syndrome animal model,” *Hum Mol Genet*, vol. 20, no. 6, pp. 1182–1196, Mar. 2011, doi: 10.1093/hmg/ddq563.

[74] J. I. Young *et al.*, “Regulation of RNA splicing by the methylation-dependent transcriptional repressor methyl-CpG binding protein 2,” *Proceedings of the National Academy of Sciences*, vol. 102, no. 49, pp. 17551–17558, Dec. 2005, doi: 10.1073/pnas.0507856102.

[75] D. H. Yasui *et al.*, “Mice with an isoform-ablating Mecp2 exon 1 mutation recapitulate the neurologic deficits of Rett syndrome,” *Hum Mol Genet*, vol. 23, no. 9, pp. 2447–2458, May 2014, doi: 10.1093/hmg/ddt640.

[76] A. K. Maunakea, I. Chepelev, K. Cui, and K. Zhao, “Intragenic DNA methylation modulates alternative splicing by recruiting MeCP2 to promote exon recognition,” *Cell Res*, vol. 23, no. 11, pp. 1256–1269, Nov. 2013, doi: 10.1038/cr.2013.110.

[77] J. J.-L. Wong *et al.*, “Intron retention is regulated by altered MeCP2-mediated splicing factor recruitment,” *Nat Commun*, vol. 8, no. 1, p. 15134, May 2017, doi: 10.1038/ncomms15134.

[78] T.-L. Cheng *et al.*, “MeCP2 Suppresses Nuclear MicroRNA Processing and Dendritic Growth by Regulating the DGCR8/Drosha Complex,” *Dev Cell*, vol. 28, no. 5, pp. 547–560, Mar. 2014, doi: 10.1016/j.devcel.2014.01.032.

[79] J. L. Neul *et al.*, “Specific mutations in Methyl-CpG-Binding Protein 2 confer different severity in Rett syndrome,” *Neurology*, vol. 70, no. 16, pp. 1313–1321, 2008, doi: 10.1212/01.wnl.0000291011.54508.aa.

[80] T. I. Sheikh, A. M. de Paz, S. Akhtar, J. Ausió, and J. B. Vincent, “MeCP2_E1 N-terminal modifications affect its degradation rate and are disrupted by the Ala2Val Rett mutation,” *Hum Mol Genet*, vol. 26, no. 21, pp. 4132–4141, Nov. 2017, doi: 10.1093/hmg/ddx300.

[81] A. Martínez De Paz *et al.*, “MeCP2-E1 isoform is a dynamically expressed, weakly DNA-bound protein with different protein and DNA interactions compared to MeCP2-E2,” *Epigenetics Chromatin*, vol. 12, no. 1, Oct. 2019, doi: 10.1186/s13072-019-0298-1.

[82] O. Spiga *et al.*, “Structural investigation of Rett-inducing MeCP2 mutations,” *Genes Dis*, vol. 6, no. 1, pp. 31–34, Mar. 2019, doi: 10.1016/j.gendis.2018.09.005.

[83] R. P. Ghosh, R. A. Horowitz-Scherer, T. Nikitina, L. S. Shlyakhtenko, and C. L. Woodcock, “MeCP2 Binds Cooperatively to Its Substrate and Competes with Histone H1 for Chromatin Binding Sites,” *Mol Cell Biol*, vol. 30, no. 19, pp. 4656–4670, Oct. 2010, doi: 10.1128/mcb.00379-10.

[84] T. G. Kucukkal and E. Alexov, “Structural, dynamical, and energetical consequences of RETT syndrome mutation R133c in MeCP2,” *Comput Math Methods Med*, vol. 2015, 2015, doi: 10.1155/2015/746157.

[85] Y. Yang, T. G. Kucukkal, J. Li, E. Alexov, and W. Cao, “Binding Analysis of Methyl-CpG Binding Domain of MeCP2 and Rett Syndrome Mutations,” *ACS Chem Biol*, vol. 11, no. 10, pp. 2706–2715, Oct. 2016, doi: 10.1021/acschembio.6b00450.

[86] C. J. Saunders, B. E. Minassian, E. W. C. Chow, W. Zhao, and J. B. Vincent, “Novel exon 1 mutations in MECP2 implicate isoform MeCP2-e1 in classical rett syndrome,” *Am J Med Genet A*, vol. 149, no. 5, pp. 1019–1023, May 2009, doi: 10.1002/ajmg.a.32776.

[87] R. R. Shah and A. P. Bird, “MeCP2 mutations: Progress towards understanding and treating Rett syndrome,” Feb. 17, 2017, *BioMed Central Ltd.* doi: 10.1186/s13073-017-0411-7.

[88] T. M. Yusufzai, “Functional consequences of Rett syndrome mutations on human MeCP2,” *Nucleic Acids Res*, vol. 28, no. 21, pp. 4172–4179, Nov. 2000, doi: 10.1093/nar/28.21.4172.

[89] T. Nikitina, R. P. Ghosh, R. A. Horowitz-Scherer, J. C. Hansen, S. A. Grigoryev, and C. L. Woodcock, “MeCP2-Chromatin Interactions Include the Formation of Chromatosome-like Structures and Are Altered in Mutations Causing Rett Syndrome,” *Journal of Biological Chemistry*, vol. 282, no. 38, pp. 28237–28245, Sep. 2007, doi: 10.1074/jbc.M704304200.

[90] R. Krishnaraj, G. Ho, and J. Christodoulou, “RettBASE: Rett syndrome database update,” *Hum Mutat*, vol. 38, no. 8, pp. 922–931, Aug. 2017, doi: 10.1002/humu.23263.

[91] A. Schmidt, H. Zhang, and M. Cristina Cardoso, “MeCP2 and chromatin compartmentalization,” Apr. 01, 2020, *Multidisciplinary Digital Publishing Institute (MDPI)*. doi: 10.3390/cells9040878.

[92] A. Schmidt, H. Zhang, and M. C. Cardoso, “MeCP2 and Chromatin Compartmentalization,” *Cells*, vol. 9, no. 4, p. 878, Apr. 2020, doi: 10.3390/cells9040878.

[93] R. M. Carney *et al.*, “Identification of MeCP2 mutations in a series of females with autistic disorder,” *Pediatr Neurol*, vol. 28, no. 3, pp. 205–211, Mar. 2003, doi: 10.1016/S0887-8994(02)00624-0.

[94] P. Moretti *et al.*, “Learning and memory and synaptic plasticity are impaired in a mouse model of Rett syndrome,” *Journal of Neuroscience*, vol. 26, no. 1, pp. 319–327, Jan. 2006, doi: 10.1523/JNEUROSCI.2623-05.2006.

[95] P. Couvert, “MECP2 is highly mutated in X-linked mental retardation,” *Hum Mol Genet*, vol. 10, no. 9, pp. 941–946, Apr. 2001, doi: 10.1093/hmg/10.9.941.

[96] M. Chahrour and H. Y. Zoghbi, “The Story of Rett Syndrome: From Clinic to Neurobiology,” Nov. 08, 2007. doi: 10.1016/j.neuron.2007.10.001.

[97] E. Frullanti *et al.*, “Analysis of the Phenotypes in the Rett Networked Database,” *Int J Genomics*, vol. 2019, pp. 1–9, Mar. 2019, doi: 10.1155/2019/6956934.

[98] N. Takagi, “The role of X-chromosome inactivation in the manifestation of Rett syndrome,” *Brain Dev*, vol. 23, pp. S182–S185, Dec. 2001, doi: 10.1016/S0387-7604(01)00362-X.

[99] S. Augui, E. P. Nora, and E. Heard, “Regulation of X-chromosome inactivation by the X-inactivation centre,” *Nat Rev Genet*, vol. 12, no. 6, pp. 429–442, Jun. 2011, doi: 10.1038/nrg2987.

[100] C. G. Duncan *et al.*, “Dosage compensation and DNA methylation landscape of the X chromosome in mouse liver,” *Sci Rep*, vol. 8, no. 1, p. 10138, Jul. 2018, doi: 10.1038/s41598-018-28356-3.

[101] C. Patrat, J.-F. Ouimette, and C. Rougeulle, “X chromosome inactivation in human development,” *Development*, vol. 147, no. 1, Jan. 2020, doi: 10.1242/dev.183095.

[102] C. Brown and W. Robinson, “The causes and consequences of random and non-random X chromosome inactivation in humans,” *Clin Genet*, vol. 58, no. 5, pp. 353–363, Nov. 2000, doi: 10.1034/j.1399-0004.2000.580504.x.

[103] R. M. Plenge, R. A. Stevenson, H. A. Lubs, C. E. Schwartz, and H. F. Willard, “Skewed X-Chromosome Inactivation Is a Common Feature of X-Linked Mental Retardation Disorders,” *The American Journal of Human Genetics*, vol. 71, no. 1, pp. 168–173, Jul. 2002, doi: 10.1086/341123.

[104] J. I. Young and H. Y. Zoghbi, “X-Chromosome Inactivation Patterns Are Unbalanced and Affect the Phenotypic Outcome in a Mouse Model of Rett Syndrome,” *The American Journal of Human Genetics*, vol. 74, no. 3, pp. 511–520, Mar. 2004, doi: 10.1086/382228.

[105] S. Takahashi *et al.*, “Skewed X chromosome inactivation failed to explain the normal phenotype of a carrier female with *MECP2* mutation resulting in Rett syndrome,” *Clin Genet*, vol. 73, no. 3, pp. 257–261, Mar. 2008, doi: 10.1111/j.1399-0004.2007.00944.x.

[106] J. P. Cheadle, “Long-read sequence analysis of the MECP2 gene in Rett syndrome patients: correlation of disease severity with mutation type and location,” *Hum Mol Genet*, vol. 9, no. 7, pp. 1119–1129, Apr. 2000, doi: 10.1093/hmg/9.7.1119.

[107] M. Wan *et al.*, “Rett Syndrome and Beyond: Recurrent Spontaneous and Familial MECP2 Mutations at CpG Hotspots,” *The American Journal of Human Genetics*, vol. 65, no. 6, pp. 1520–1529, Dec. 1999, doi: 10.1086/302690.

[108] R. Trappe *et al.*, “MECP2 Mutations in Sporadic Cases of Rett Syndrome Are Almost Exclusively of Paternal Origin,” 2001.

[109] G. Chahil, A. Yelam, and P. C. Bollu, “Rett Syndrome in Males: A Case Report and Review of Literature,” *Cureus*, Oct. 2018, doi: 10.7759/cureus.3414.

[110] J. L. Neul *et al.*, “The array of clinical phenotypes of males with mutations in Methyl-CpG binding protein 2,” *American Journal of Medical Genetics, Part B: Neuropsychiatric Genetics*, vol. 180, no. 1, pp. 55–67, Jan. 2019, doi: 10.1002/ajmg.b.32707.

[111] B. Reichow, A. George-Puskar, T. Lutz, I. C. Smith, and F. R. Volkmar, “Brief Report: Systematic Review of Rett Syndrome in Males,” *J Autism Dev Disord*, vol. 45, no. 10, pp. 3377–3383, Oct. 2015, doi: 10.1007/s10803-015-2519-1.

[112] L. M. Lombardi, S. A. Baker, and H. Y. Zoghbi, “MECP2 disorders: From the clinic to mice and back,” Aug. 03, 2015, *American Society for Clinical Investigation*. doi: 10.1172/JCI78167.

[113] D. M. Katz *et al.*, “Preclinical research in Rett syndrome: Setting the foundation for translational success,” Nov. 2012. doi: 10.1242/dmm.011007.

[114] D. Braunschweig, T. Simcox, R. C. Samaco, and J. M. LaSalle, “X-chromosome inactivation ratios affect wild-type MeCP2 expression within mosaic Rett syndrome and Mecp2-/+ mouse brain,” *Hum Mol Genet*, vol. 13, no. 12, pp. 1275–1286, Jun. 2004, doi: 10.1093/hmg/ddh142.

[115] R. C. Samaco, C. M. Mcgraw, C. S. Ward, Y. Sun, J. L. Neul, and H. Y. Zoghbi, “Female Mecp2+/- mice display robust behavioral deficits on two different genetic backgrounds providing a framework for pre-clinical studies,” *Hum Mol Genet*, vol. 22, no. 1, pp. 96–109, Jan. 2013, doi: 10.1093/hmg/dds406.

[116] C. C. Gigli *et al.*, “MeCP2 related studies benefit from the use of CD1 as genetic background,” *PLoS One*, vol. 11, no. 4, Apr. 2016, doi: 10.1371/journal.pone.0153473.

[117] A. H. Tuttle, V. M. Philip, E. J. Chesler, and J. S. Mogil, “Comparing phenotypic variation between inbred and outbred mice,” Dec. 01, 2018, *Nature Publishing Group*. doi: 10.1038/s41592-018-0224-7.

[118] M. D. Shahbazian *et al.*, “Mice with Truncated MeCP2 Recapitulate Many Rett Syndrome Features and Display Hyperacetylation of Histone H3,” *Neuron*, vol. 35, no. 2, pp. 243–254, Jul. 2002, doi: 10.1016/S0896-6273(02)00768-7.

[119] C. Brendel *et al.*, “Readthrough of nonsense mutations in Rett syndrome: evaluation of novel aminoglycosides and generation of a new mouse model,” *J Mol Med*, vol. 89, no. 4, pp. 389–398, Apr. 2011, doi: 10.1007/s00109-010-0704-4.

[120] K. Brown *et al.*, “The molecular basis of variable phenotypic severity among common missense mutations causing Rett syndrome,” *Hum Mol Genet*, vol. 25, no. 3, pp. 558–570, Feb. 2016, doi: 10.1093/hmg/ddv496.

[121] A. Gandaglia *et al.*, “A Novel Mecp2Y120D Knock-in Model Displays Similar Behavioral Traits But Distinct Molecular Features Compared to the Mecp2-Null Mouse Implying Precision Medicine for the Treatment of Rett Syndrome,” *Mol Neurobiol*, vol. 56, no. 7, pp. 4838–4854, Jul. 2019, doi: 10.1007/s12035-018-1412-2.

[122] V. A. Cuddapah *et al.*, “*Methyl-CpG-binding protein 2* (*MECP2*) mutation type is associated with disease severity in Rett syndrome,” *J Med Genet*, vol. 51, no. 3, pp. 152–158, Mar. 2014, doi: 10.1136/jmedgenet-2013-102113.

[123] A. Renieri *et al.*, “Rett syndrome: The complex nature of a monogenic disease,” Jun. 01, 2003, *Springer Verlag*. doi: 10.1007/s00109-003-0444-9.

[124] U. A. Nuber *et al.*, “Up-regulation of glucocorticoid-regulated genes in a mouse model of Rett syndrome,” *Hum Mol Genet*, vol. 14, no. 15, pp. 2247–2256, Aug. 2005, doi: 10.1093/hmg/ddi229.

[125] S. L. Fyffe *et al.*, “Deletion of Mecp2 in Sim1-Expressing Neurons Reveals a Critical Role for MeCP2 in Feeding Behavior, Aggression, and the Response to Stress,” *Neuron*, vol. 59, no. 6, pp. 947–958, Sep. 2008, doi: 10.1016/j.neuron.2008.07.030.

[126] H. T. Chao *et al.*, “Dysfunction in GABA signalling mediates autism-like stereotypies and Rett syndrome phenotypes,” *Nature*, vol. 468, no. 7321, pp. 263–269, Nov. 2010, doi: 10.1038/nature09582.

[127] D. T. Lioy *et al.*, “A role for glia in the progression of Rett’s syndrome,” *Nature*, vol. 475, no. 7357, pp. 497–500, Jul. 2011, doi: 10.1038/nature10214.

[128] J. Guy, J. Gan, J. Selfridge, S. Cobb, and A. Bird, “Reversal of Neurological Defects in a Mouse Model of Rett Syndrome,” *Science (1979)*, vol. 315, no. 5815, pp. 1143–1147, Feb. 2007, doi: 10.1126/science.1138389.

[129] F. Bedogni *et al.*, “Defects during Mecp2 Null Embryonic Cortex Development Precede the Onset of Overt Neurological Symptoms,” *Cerebral Cortex*, vol. 26, no. 6, pp. 2517–2529, Jun. 2016, doi: 10.1093/cercor/bhv078.

[130] J. P. K. Ip, N. Mellios, and M. Sur, “Rett syndrome: Insights into genetic, molecular and circuit mechanisms,” *Nat Rev Neurosci*, vol. 19, no. 6, pp. 368–382, Jun. 2018, doi: 10.1038/s41583-018-0006-3.

[131] P. V. Belichenko *et al.*, “Widespread changes in dendritic and axonal morphology in Mecp2-mutant mouse models of Rett syndrome: Evidence for disruption of neuronal networks,”

Journal of Comparative Neurology, vol. 514, no. 3, pp. 240–258, May 2009, doi: 10.1002/cne.22009.

[132] B. Subramaniam, S. Naidu, and A. L. Reiss, "Neuroanatomy in Rett syndrome," *Neurology*, vol. 48, no. 2, pp. 399–407, Feb. 1997, doi: 10.1212/WNL.48.2.399.

[133] W. E. Kaufmann, "Dendritic Anomalies in Disorders Associated with Mental Retardation," *Cerebral Cortex*, vol. 10, no. 10, pp. 981–991, Oct. 2000, doi: 10.1093/cercor/10.10.981.

[134] D. D. Armstrong, "Rett syndrome neuropathology review 2000," *Brain Dev*, vol. 23, pp. S72–S76, Dec. 2001, doi: 10.1016/S0387-7604(01)00332-1.

[135] S. Akbarian, "Diseases of the Mind and Brain," *American Journal of Psychiatry*, vol. 159, no. 7, pp. 1103–1103, Jul. 2002, doi: 10.1176/appi.ajp.159.7.1103.

[136] V. Saywell, A. Viola, S. Confort-Gouny, Y. Le Fur, L. Villard, and P. J. Cozzone, "Brain magnetic resonance study of Mecp2 deletion effects on anatomy and metabolism," *Biochem Biophys Res Commun*, vol. 340, no. 3, pp. 776–783, Feb. 2006, doi: 10.1016/j.bbrc.2005.12.080.

[137] D. Duncan Armstrong and F. The Blue Bird, "Neuropathology of Rett Syndrome."

[138] H. T. Chao, H. Y. Zoghbi, and C. Rosenmund, "MeCP2 Controls Excitatory Synaptic Strength by Regulating Glutamatergic Synapse Number," *Neuron*, vol. 56, no. 1, pp. 58–65, Oct. 2007, doi: 10.1016/j.neuron.2007.08.018.

[139] D. Duncan Armstrong, K. Deguchi, B. Antallfy, and D. Armstrong, "Survey of MeCP2 in the Rett Syndrome and the Non-Rett Syndrome Brain From the Departments of Pathology (," 2003.

[140] C. Sampathkumar, Y. J. Wu, M. Vadhvani, T. Trimbuch, B. Eickholt, and C. Rosenmund, "Loss of MeCP2 disrupts cell autonomous and autocrine BDNF signaling in mouse glutamatergic neurons," *Elife*, vol. 5, no. OCTOBER2016, Oct. 2016, doi: 10.7554/eLife.19374.001.

[141] S. Carli *et al.*, "A comprehensive longitudinal study of magnetic resonance imaging identifies novel features of the Mecp2 deficient mouse brain," *Neurobiol Dis*, vol. 180, May 2023, doi: 10.1016/j.nbd.2023.106083.

[142] A. L. Reiss *et al.*, "Neuroanatomy of Rett syndrome: A volumetric imaging study," *Ann Neurol*, vol. 34, no. 2, pp. 227–234, Aug. 1993, doi: 10.1002/ana.410340220.

[143] K. Jellinger, D. Armstrong, H. Y. Zoghbi, and A. K. Percy, "Neuropathology of Rett syndrome," *Acta Neuropathol*, vol. 76, no. 2, pp. 142–158, 1988, doi: 10.1007/BF00688098.

[144] X. Meng *et al.*, "Manipulations of MeCP2 in glutamatergic neurons highlight their contributions to Rett and other neurological disorders," *Elife*, vol. 5, Jun. 2016, doi: 10.7554/eLife.14199.

[145] M. V. Johnston, M. E. Blue, and S. Naidu, "Rett Syndrome and Neuronal Development," *J Child Neurol*, vol. 20, no. 9, pp. 759–763, Sep. 2005, doi: 10.1177/08830738050200091101.

[146] Y. Asaka, D. G. M. Jugloff, L. Zhang, J. H. Eubanks, and R. M. Fitzsimonds, "Hippocampal synaptic plasticity is impaired in the Mecp2-null mouse model of Rett syndrome," *Neurobiol Dis*, vol. 21, no. 1, pp. 217–227, Jan. 2006, doi: 10.1016/j.nbd.2005.07.005.

[147] M. Kron *et al.*, "Brain activity mapping in Mecp2 mutant mice reveals functional deficits in forebrain circuits, including key nodes in the default mode network, that are reversed with ketamine treatment," *Journal of Neuroscience*, vol. 32, no. 40, pp. 13860–13872, Oct. 2012, doi: 10.1523/JNEUROSCI.2159-12.2012.

[148] G. Calfa, W. Li, J. M. Rutherford, and L. Pozzo-Miller, "Excitation/inhibition imbalance and impaired synaptic inhibition in hippocampal area CA3 of *Mecp2* knockout mice," *Hippocampus*, vol. 25, no. 2, pp. 159–168, Feb. 2015, doi: 10.1002/hipo.22360.

[149] D. M. Katz *et al.*, "Rett Syndrome: Crossing the Threshold to Clinical Translation," *Trends Neurosci*, vol. 39, no. 2, pp. 100–113, Feb. 2016, doi: 10.1016/j.tins.2015.12.008.

[150] J. H. Leslie and E. Nedivi, "Activity-regulated genes as mediators of neural circuit plasticity," Aug. 2011. doi: 10.1016/j.pneurobio.2011.05.002.

[151] P. L. Greer and M. E. Greenberg, "From Synapse to Nucleus: Calcium-Dependent Gene Transcription in the Control of Synapse Development and Function," *Neuron*, vol. 59, no. 6, pp. 846–860, Sep. 2008, doi: 10.1016/j.neuron.2008.09.002.

[152] G. A. Wayman *et al.*, "Activity-Dependent Dendritic Arborization Mediated by CaM-Kinase I Activation and Enhanced CREB-Dependent Transcription of Wnt-2," *Neuron*, vol. 50, no. 6, pp. 897–909, Jun. 2006, doi: 10.1016/j.neuron.2006.05.008.

[153] S. Didier, F. Sauvé, M. Domise, L. Buée, C. Marinangeli, and V. Vingtdeux, "AMP-activated Protein Kinase Controls Immediate Early Genes Expression Following Synaptic Activation Through the PKA/CREB Pathway," *Int J Mol Sci*, vol. 19, no. 12, p. 3716, Nov. 2018, doi: 10.3390/ijms19123716.

[154] S. Loebrich and E. Nedivi, "The Function of Activity-Regulated Genes in the Nervous System," *Physiol Rev*, vol. 89, no. 4, pp. 1079–1103, Oct. 2009, doi: 10.1152/physrev.00013.2009.

[155] V. S. Dani, Q. Chang, A. Maffei, G. G. Turrigiano, R. Jaenisch, and S. B. Nelson, "Reduced cortical activity due to a shift in the balance between excitation and inhibition in a mouse model of Rett Syndrome," 2005. [Online]. Available: www.pnas.orgcgidoi10.1073pnas.0506071102

[156] S. Cohen-Cory, A. H. Kidane, N. J. Shirkey, and S. Marshak, "Brain-derived neurotrophic factor and the development of structural neuronal connectivity," *Dev Neurobiol*, vol. 70, no. 5, pp. 271–288, Apr. 2010, doi: 10.1002/dneu.20774.

[157] L. C. Rutherford, A. DeWan, H. M. Lauer, and G. G. Turrigiano, "Brain-Derived Neurotrophic Factor Mediates the Activity-Dependent Regulation of Inhibition in Neocortical Cultures," *The Journal of Neuroscience*, vol. 17, no. 12, pp. 4527–4535, Jun. 1997, doi: 10.1523/JNEUROSCI.17-12-04527.1997.

[158] L. C. Rutherford, S. B. Nelson, and G. G. Turrigiano, “BDNF Has Opposite Effects on the Quantal Amplitude of Pyramidal Neuron and Interneuron Excitatory Synapses,” *Neuron*, vol. 21, no. 3, pp. 521–530, Sep. 1998, doi: 10.1016/S0896-6273(00)80563-2.

[159] W. Guo, Y. Ji, S. Wang, Y. Sun, and B. Lu, “Neuronal activity alters BDNF-TrkB signaling kinetics and downstream functions,” *J Cell Sci*, Jan. 2014, doi: 10.1242/jcs.139964.

[160] M. E. Klein, D. T. Lioy, L. Ma, S. Impey, G. Mandel, and R. H. Goodman, “Homeostatic regulation of MeCP2 expression by a CREB-induced microRNA,” *Nat Neurosci*, vol. 10, no. 12, pp. 1513–1514, Dec. 2007, doi: 10.1038/nn2010.

[161] J. W. Lischalk, C. R. Easton, and W. J. Moody, “Bilaterally propagating waves of spontaneous activity arising from discrete pacemakers in the neonatal mouse cerebral cortex,” *Dev Neurobiol*, vol. 69, no. 7, pp. 407–414, Jun. 2009, doi: 10.1002/dneu.20708.

[162] A. C. Flint, R. S. Dammerman, and A. R. Kriegstein, “Endogenous activation of metabotropic glutamate receptors in neocortical development causes neuronal calcium oscillations,” *Proceedings of the National Academy of Sciences*, vol. 96, no. 21, pp. 12144–12149, Oct. 1999, doi: 10.1073/pnas.96.21.12144.

[163] H. J. Luhmann *et al.*, “Spontaneous Neuronal Activity in Developing Neocortical Networks: From Single Cells to Large-Scale Interactions,” *Front Neural Circuits*, vol. 10, May 2016, doi: 10.3389/fncir.2016.00040.

[164] S. E. Webb and A. L. Miller, “Calcium signalling during embryonic development,” *Nat Rev Mol Cell Biol*, vol. 4, no. 7, pp. 539–551, Jul. 2003, doi: 10.1038/nrm1149.

[165] L. C. Katz and C. J. Shatz, “Synaptic Activity and the Construction of Cortical Circuits,” *Science (1979)*, vol. 274, no. 5290, pp. 1133–1138, Nov. 1996, doi: 10.1126/science.274.5290.1133.

[166] J. E. Crandall, D. M. McCarthy, K. Y. Araki, J. R. Sims, J.-Q. Ren, and P. G. Bhide, “Dopamine Receptor Activation Modulates GABA Neuron Migration from the Basal Forebrain to the Cerebral Cortex,” *The Journal of Neuroscience*, vol. 27, no. 14, pp. 3813–3822, Apr. 2007, doi: 10.1523/JNEUROSCI.5124-06.2007.

[167] Y. Fukazawa, Y. Saitoh, F. Ozawa, Y. Ohta, K. Mizuno, and K. Inokuchi, “Hippocampal LTP Is Accompanied by Enhanced F-Actin Content within the Dendritic Spine that Is Essential for Late LTP Maintenance In Vivo,” *Neuron*, vol. 38, no. 3, pp. 447–460, May 2003, doi: 10.1016/S0896-6273(03)00206-X.

[168] C. Sala, V. Piëch, N. R. Wilson, M. Passafaro, G. Liu, and M. Sheng, “Regulation of Dendritic Spine Morphology and Synaptic Function by Shank and Homer,” *Neuron*, vol. 31, no. 1, pp. 115–130, Jul. 2001, doi: 10.1016/S0896-6273(01)00339-7.

[169] M. Passafaro, T. Nakagawa, C. Sala, and M. Sheng, “Induction of dendritic spines by an extracellular domain of AMPA receptor subunit GluR2,” *Nature*, vol. 424, no. 6949, pp. 677–681, Aug. 2003, doi: 10.1038/nature01781.

[170] V. Anggono and R. L. Huganir, “Regulation of AMPA receptor trafficking and synaptic plasticity,” *Curr Opin Neurobiol*, vol. 22, no. 3, pp. 461–469, Jun. 2012, doi: 10.1016/j.conb.2011.12.006.

[171] N. C. Spitzer, “Electrical activity in early neuronal development,” Dec. 07, 2006, *Nature Publishing Group*. doi: 10.1038/nature05300.

[172] N. Yamamoto and G. López-Bendito, “Shaping brain connections through spontaneous neural activity,” *European Journal of Neuroscience*, vol. 35, no. 10, pp. 1595–1604, May 2012, doi: 10.1111/j.1460-9568.2012.08101.x.

[173] T. A. Weissman, P. A. Riquelme, L. Ivic, A. C. Flint, and A. R. Kriegstein, “Calcium Waves Propagate through Radial Glial Cells and Modulate Proliferation in the Developing Neocortex,” *Neuron*, vol. 43, no. 5, pp. 647–661, Sep. 2004, doi: 10.1016/j.neuron.2004.08.015.

[174] C. C. Gigli *et al.*, “Lack of methyl-CpG binding protein 2 (MeCP2) affects cell fate refinement during embryonic cortical development,” *Cerebral Cortex*, vol. 28, no. 5, pp. 1846–1856, May 2018, doi: 10.1093/cercor/bhx360.

[175] N. Mellios *et al.*, “Human cerebral organoids reveal deficits in neurogenesis and neuronal migration in MeCP2-deficient neural progenitors,” *Mol Psychiatry*, vol. 23, no. 4, pp. 791–791, Apr. 2018, doi: 10.1038/mp.2018.5.

[176] L. Scaramuzza *et al.*, “ The enhancement of activity rescues the establishment of Mecp2 null neuronal phenotypes ,” *EMBO Mol Med*, vol. 13, no. 4, Apr. 2021, doi: 10.15252/emmm.202012433.

[177] D. L. Egbenya, E. Aidoo, and G. Kyei, “Glutamate receptors in brain development,” *Child’s Nervous System*, vol. 37, no. 9, pp. 2753–2758, Sep. 2021, doi: 10.1007/s00381-021-05266-w.

[178] B. Birur, N. V. Kraguljac, R. C. Shelton, and A. C. Lahti, “Brain structure, function, and neurochemistry in schizophrenia and bipolar disorder—a systematic review of the magnetic resonance neuroimaging literature,” *NPJ Schizophr*, vol. 3, no. 1, p. 15, Apr. 2017, doi: 10.1038/s41537-017-0013-9.

[179] F. Fonnum, “Glutamate: A Neurotransmitter in Mammalian Brain,” *J Neurochem*, vol. 42, no. 1, pp. 1–11, Jan. 1984, doi: 10.1111/j.1471-4159.1984.tb09689.x.

[180] P. M. Headley and S. Grillner, “Excitatory amino acids and synaptic transmission: the evidence for a physiological function.,” *Trends Pharmacol Sci*, vol. 11, no. 5, pp. 205–11, May 1990, doi: 10.1016/0165-6147(90)90116-p.

[181] J. A. Stanley *et al.*, “Functional dynamics of hippocampal glutamate during associative learning assessed with in vivo 1 H functional magnetic resonance spectroscopy,” *Neuroimage*, vol. 153, pp. 189–197, Jun. 2017, doi: 10.1016/j.neuroimage.2017.03.051.

[182] C. Pittenger, M. H. Bloch, and K. Williams, “Glutamate abnormalities in obsessive compulsive disorder: Neurobiology, pathophysiology, and treatment,” *Pharmacol Ther*, vol. 132, no. 3, pp. 314–332, Dec. 2011, doi: 10.1016/j.pharmthera.2011.09.006.

[183] N. C. Danbolt, “Glutamate uptake,” *Prog Neurobiol*, vol. 65, no. 1, pp. 1–105, Sep. 2001, doi: 10.1016/S0301-0082(00)00067-8.

[184] E. Moretto, L. Murru, G. Martano, J. Sassone, and M. Passafaro, “Glutamatergic synapses in neurodevelopmental disorders,” *Prog Neuropsychopharmacol Biol Psychiatry*, vol. 84, pp. 328–342, Jun. 2018, doi: 10.1016/j.pnpbp.2017.09.014.

[185] M. Hollmann and S. Heinemann, “Cloned Glutamate Receptors,” *Annu Rev Neurosci*, vol. 17, no. 1, pp. 31–108, Mar. 1994, doi: 10.1146/annurev.ne.17.030194.000335.

[186] T. Miladinovic, M. Nashed, and G. Singh, “Overview of Glutamatergic Dysregulation in Central Pathologies,” *Biomolecules*, vol. 5, no. 4, pp. 3112–3141, Nov. 2015, doi: 10.3390/biom5043112.

[187] S. F. Traynelis *et al.*, “Glutamate Receptor Ion Channels: Structure, Regulation, and Function,” *Pharmacol Rev*, vol. 62, no. 3, pp. 405–496, Sep. 2010, doi: 10.1124/pr.109.002451.

[188] C. M. Niswender and P. J. Conn, “Metabotropic Glutamate Receptors: Physiology, Pharmacology, and Disease,” *Annu Rev Pharmacol Toxicol*, vol. 50, no. 1, pp. 295–322, Feb. 2010, doi: 10.1146/annurev.pharmtox.011008.145533.

[189] N. Scheefhals and H. D. MacGillavry, “Functional organization of postsynaptic glutamate receptors,” *Molecular and Cellular Neuroscience*, vol. 91, pp. 82–94, Sep. 2018, doi: 10.1016/j.mcn.2018.05.002.

[190] P. J. Flor, G. Battaglia, F. Nicoletti, F. Gasparini, and V. Bruno, “Neuroprotective Activity of Metabotropic Glutamate Receptor Ligands,” 2003, pp. 197–223. doi: 10.1007/978-1-4615-0123-7_7.

[191] J. N. C. Kew and J. A. Kemp, “Ionotropic and metabotropic glutamate receptor structure and pharmacology,” *Psychopharmacology (Berl)*, vol. 179, no. 1, pp. 4–29, Apr. 2005, doi: 10.1007/s00213-005-2200-z.

[192] G. Ayalon, E. Segev, S. Elgavish, and Y. Stern-Bach, “Two Regions in the N-terminal Domain of Ionotropic Glutamate Receptor 3 Form the Subunit Oligomerization Interfaces That Control Subtype-specific Receptor Assembly,” *Journal of Biological Chemistry*, vol. 280, no. 15, pp. 15053–15060, Apr. 2005, doi: 10.1074/jbc.M408413200.

[193] E. C. Twomey and A. I. Sobolevsky, “Structural Mechanisms of Gating in Ionotropic Glutamate Receptors,” *Biochemistry*, vol. 57, no. 3, pp. 267–276, Jan. 2018, doi: 10.1021/acs.biochem.7b00891.

[194] Y. Sun, R. Olson, M. Horning, N. Armstrong, M. Mayer, and E. Gouaux, “Mechanism of glutamate receptor desensitization,” *Nature*, vol. 417, no. 6886, pp. 245–253, May 2002, doi: 10.1038/417245a.

[195] R. Jin, S. Clark, A. M. Weeks, J. T. Dudman, E. Gouaux, and K. M. Partin, “Mechanism of Positive Allosteric Modulators Acting on AMPA Receptors,” *The Journal of Neuroscience*, vol. 25, no. 39, pp. 9027–9036, Sep. 2005, doi: 10.1523/JNEUROSCI.2567-05.2005.

[196] K. M. Partin, “Domain Interactions Regulating AMPA Receptor Desensitization,” *The Journal of Neuroscience*, vol. 21, no. 6, pp. 1939–1948, Mar. 2001, doi: 10.1523/JNEUROSCI.21-06-01939.2001.

[197] G. Lynch and C. M. Gall, “Ampakines and the threefold path to cognitive enhancement,” *Trends Neurosci*, vol. 29, no. 10, pp. 554–562, Oct. 2006, doi: 10.1016/j.tins.2006.07.007.

[198] P. Paoletti, C. Bellone, and Q. Zhou, “NMDA receptor subunit diversity: impact on receptor properties, synaptic plasticity and disease,” *Nat Rev Neurosci*, vol. 14, no. 6, pp. 383–400, Jun. 2013, doi: 10.1038/nrn3504.

[199] M. E. Flores-Soto, V. Chaparro-Huerta, M. Escoto-Delgadillo, E. Vazquez-Valls, R. E. González-Castañeda, and C. Beas-Zarate, “Estructura y función de las subunidades del receptor a glutamato tipo NMDA,” *Neurología*, vol. 27, no. 5, pp. 301–310, Jun. 2012, doi: 10.1016/j.nrl.2011.10.014.

[200] J. LoTurco, M. Blanton, and A. Kriegstein, “Initial expression and endogenous activation of NMDA channels in early neocortical development,” *The Journal of Neuroscience*, vol. 11, no. 3, pp. 792–799, Mar. 1991, doi: 10.1523/JNEUROSCI.11-03-00792.1991.

[201] K. B. Hansen *et al.*, “Structure, Function, and Pharmacology of Glutamate Receptor Ion Channels,” *Pharmacol Rev*, vol. 73, no. 4, pp. 1469–1658, Oct. 2021, doi: 10.1124/pharmrev.120.000131.

[202] R. L. Huganir and R. A. Nicoll, “AMPARs and Synaptic Plasticity: The Last 25 Years,” *Neuron*, vol. 80, no. 3, pp. 704–717, Oct. 2013, doi: 10.1016/j.neuron.2013.10.025.

[203] J. Schwenk *et al.*, “Regional Diversity and Developmental Dynamics of the AMPA-Receptor Proteome in the Mammalian Brain,” *Neuron*, vol. 84, no. 1, pp. 41–54, Oct. 2014, doi: 10.1016/j.neuron.2014.08.044.

[204] Y.-H. Chun, D. Frank, J.-S. Lee, Y. Zhang, Q.-S. Auh, and J. Y. Ro, “Peripheral AMPA receptors contribute to muscle nociception and c-fos activation,” *Neurosci Res*, vol. 62, no. 2, pp. 97–104, Oct. 2008, doi: 10.1016/j.neures.2008.06.007.

[205] N. B. Lawand, T. McNearney, and K. N. Westlund, “Amino acid release into the knee joint: key role in nociception and inflammation,” *Pain*, vol. 86, no. 1, pp. 69–74, May 2000, doi: 10.1016/S0304-3959(99)00311-5.

[206] N. V. Luchkina *et al.*, “Developmental switch in the kinase dependency of long-term potentiation depends on expression of GluA4 subunit-containing AMPA receptors,” *Proceedings of the National Academy of Sciences*, vol. 111, no. 11, pp. 4321–4326, Mar. 2014, doi: 10.1073/pnas.1315769111.

[207] G. H. Diering and R. L. Huganir, “The AMPA Receptor Code of Synaptic Plasticity,” *Neuron*, vol. 100, no. 2, pp. 314–329, Oct. 2018, doi: 10.1016/j.neuron.2018.10.018.

[208] V. Anggono and R. L. Huganir, “Regulation of AMPA receptor trafficking and synaptic plasticity,” *Curr Opin Neurobiol*, vol. 22, no. 3, pp. 461–469, Jun. 2012, doi: 10.1016/j.conb.2011.12.006.

[209] I. H. Greger, J. F. Watson, and S. G. Cull-Candy, “Structural and Functional Architecture of AMPA-Type Glutamate Receptors and Their Auxiliary Proteins,” *Neuron*, vol. 94, no. 4, pp. 713–730, May 2017, doi: 10.1016/j.neuron.2017.04.009.

[210] T. E. Chater and Y. Goda, “The Shaping of AMPA Receptor Surface Distribution by Neuronal Activity,” *Front Synaptic Neurosci*, vol. 14, Mar. 2022, doi: 10.3389/fnsyn.2022.833782.

[211] J. Díaz-Alonso and R. A. Nicoll, “AMPA receptor trafficking and LTP: Carboxy-termini, amino-termini and TARPs,” *Neuropharmacology*, vol. 197, p. 108710, Oct. 2021, doi: 10.1016/j.neuropharm.2021.108710.

[212] Y.-Y. Cao *et al.*, “Molecular Mechanisms of AMPA Receptor Trafficking in the Nervous System,” *Int J Mol Sci*, vol. 25, no. 1, p. 111, Dec. 2023, doi: 10.3390/ijms25010111.

[213] A. Arai and M. Kessler, “Pharmacology of Ampakine Modulators: From AMPA Receptors to Synapses and Behavior,” *Curr Drug Targets*, vol. 8, no. 5, pp. 583–602, May 2007, doi: 10.2174/138945007780618490.

[214] S. Brogi, G. Campiani, M. Brindisi, and S. Butini, “Allosteric Modulation of Ionotropic Glutamate Receptors: An Outlook on New Therapeutic Approaches To Treat Central Nervous System Disorders,” *ACS Med Chem Lett*, vol. 10, no. 3, pp. 228–236, Mar. 2019, doi: 10.1021/acsmedchemlett.8b00450.

[215] B. Kadriu *et al.*, “Positive AMPA receptor modulation in the treatment of neuropsychiatric disorders: A long and winding road,” *Drug Discov Today*, vol. 26, no. 12, pp. 2816–2838, Dec. 2021, doi: 10.1016/j.drudis.2021.07.027.

[216] G. T. Swanson, S. K. Kamboj, and S. G. Cull-Candy, “Single-Channel Properties of Recombinant AMPA Receptors Depend on RNA Editing, Splice Variation, and Subunit Composition,” *The Journal of Neuroscience*, vol. 17, no. 1, pp. 58–69, Jan. 1997, doi: 10.1523/JNEUROSCI.17-01-00058.1997.

[217] E. A. Golubeva, M. I. Lavrov, E. V. Radchenko, and V. A. Palyulin, “Diversity of AMPA Receptor Ligands: Chemotypes, Binding Modes, Mechanisms of Action, and Therapeutic Effects,” *Biomolecules*, vol. 13, no. 1, p. 56, Dec. 2022, doi: 10.3390/biom13010056.

[218] R. Dingledine, K. Borges, D. Bowie, and S. F. Traynelis, “The glutamate receptor ion channels.,” *Pharmacol Rev*, vol. 51, no. 1, pp. 7–61, Mar. 1999.

[219] D. P. Radin *et al.*, “Amplification of the therapeutic potential of AMPA receptor potentiators from the nootropic era to today,” *Pharmacol Biochem Behav*, vol. 248, p. 173967, Mar. 2025, doi: 10.1016/j.pbb.2025.173967.

[220] A. Copani *et al.*, “Nootropic Drugs Positively Modulate α-Amino-3-Hydroxy-5-Methyl-4-Isoxazolepropionic Acid-Sensitive Glutamate Receptors in Neuronal Cultures,” *J Neurochem*, vol. 58, no. 4, pp. 1199–1204, Apr. 1992, doi: 10.1111/j.1471-4159.1992.tb11329.x.

[221] W. Danysz, “CX-516 Cortex pharmaceuticals.,” *Curr Opin Investig Drugs*, vol. 3, no. 7, pp. 1081–8, Jul. 2002.

[222] E. Berry-Kravis *et al.*, "Effect of CX516, an AMPA-Modulating Compound, on Cognition and Behavior in Fragile X Syndrome: AControlled Trial," *J Child Adolesc Psychopharmacol*, vol. 16, no. 5, pp. 525–540, Oct. 2006, doi: 10.1089/cap.2006.16.525.

[223] E. Wezenberg, R. Jan Verkes, G. S. F. Ruigt, W. Hulstijn, and B. G. C. Sabbe, "Acute Effects of the Ampakine Farampator on Memory and Information Processing in Healthy Elderly Volunteers," *Neuropsychopharmacology*, vol. 32, no. 6, pp. 1272–1283, Jun. 2007, doi: 10.1038/sj.npp.1301257.

[224] R. J. Knapp *et al.*, "Antidepressant activity of memory-enhancing drugs in the reduction of submissive behavior model," *Eur J Pharmacol*, vol. 440, no. 1, pp. 27–35, Apr. 2002, doi: 10.1016/S0014-2999(02)01338-9.

[225] D. C. Goff *et al.*, "A Placebo-Controlled Pilot Study of the Ampakine CX516 Added to Clozapine in Schizophrenia," *J Clin Psychopharmacol*, vol. 21, no. 5, pp. 484–487, Oct. 2001, doi: 10.1097/00004714-200110000-00005.

[226] H. Wachtel and L. Turski, "Glutamate: a new target in schizophrenia?," *Trends Pharmacol Sci*, vol. 11, no. 6, pp. 219–220, Jun. 1990, doi: 10.1016/0165-6147(90)90243-2.

[227] J. C. Lauterborn, G. Lynch, P. Vanderklish, A. Arai, and C. M. Gall, "Positive Modulation of AMPA Receptors Increases Neurotrophin Expression by Hippocampal and Cortical Neurons," *The Journal of Neuroscience*, vol. 20, no. 1, pp. 8–21, Jan. 2000, doi: 10.1523/JNEUROSCI.20-01-00008.2000.

[228] G. Lynch, "Memory enhancement: the search for mechanism-based drugs," *Nat Neurosci*, vol. 5, no. S11, pp. 1035–1038, Nov. 2002, doi: 10.1038/nn935.

[229] A. Arai and G. Lynch, "AMPA receptor desensitization modulates synaptic responses induced by repetitive afferent stimulation in hippocampal slices," *Brain Res*, vol. 799, no. 2, pp. 235–242, Jul. 1998, doi: 10.1016/S0006-8993(98)00447-8.

[230] C. Krintel *et al.*, "Structural analysis of the positive AMPA receptor modulators CX516 and Me-CX516 in complex with the GluA2 ligand-binding domain," *Acta Crystallogr D Biol Crystallogr*, vol. 69, no. 9, pp. 1645–1652, Sep. 2013, doi: 10.1107/S0907444913011839.

[231] A. C. Arai, Y.-F. Xia, G. Rogers, G. Lynch, and M. Kessler, "Benzamide-Type AMPA Receptor Modulators Form Two Subfamilies with Distinct Modes of Action," *J Pharmacol Exp Ther*, vol. 303, no. 3, pp. 1075–1085, Jan. 2002, doi: 10.1124/jpet.102.040360.

[232] N. Nagarajan, C. Quast, A. R. Boxall, M. Shahid, and C. Rosenmund, "Mechanism and impact of allosteric AMPA receptor modulation by the AmpakineTM CX546," *Neuropharmacology*, vol. 41, no. 6, pp. 650–663, Nov. 2001, doi: 10.1016/S0028-3908(01)00133-2.

[233] K. Bernard *et al.*, "A 24-week double-blind placebo-controlled study of the efficacy and safety of the AMPA modulator S47445 in patients with mild to moderate Alzheimer's disease and depressive symptoms," *Alzheimer's & Dementia: Translational Research & Clinical Interventions*, vol. 5, no. 1, pp. 231–240, Jan. 2019, doi: 10.1016/j.trci.2019.04.002.

[234] M.-W. Chen *et al.*, “PKC and Ras are Involved in M1 Muscarinic Receptor-Mediated Modulation of AMPA Receptor GluA1 Subunit,” *Cell Mol Neurobiol*, vol. 40, no. 4, pp. 547–554, May 2020, doi: 10.1007/s10571-019-00752-x.

[235] G. Thiel, “Synapsin I, Synapsin II, and Synaptophysin: Marker Proteins of Synaptic Vesicles,” *Brain Pathology*, vol. 3, no. 1, pp. 87–95, Jan. 1993, doi: 10.1111/j.1750-3639.1993.tb00729.x.

[236] C. Grienberger and A. Konnerth, “Imaging Calcium in Neurons,” *Neuron*, vol. 73, no. 5, pp. 862–885, Mar. 2012, doi: 10.1016/j.neuron.2012.02.011.

[237] C. J. Howell *et al.*, “Activation of the Medial Prefrontal Cortex Reverses Cognitive and Respiratory Symptoms in a Mouse Model of Rett Syndrome,” *eNeuro*, vol. 4, no. 6, p. ENEURO.0277-17.2017, Nov. 2017, doi: 10.1523/ENEURO.0277-17.2017.

[238] J. M. Leyrer-Jackson, M. F. Olive, and C. D. Gipson, “Whole-Cell Patch-Clamp Electrophysiology to Study Ionotropic Glutamatergic Receptors and Their Roles in Addiction,” 2019, pp. 107–135. doi: 10.1007/978-1-4939-9077-1_9.

[239] Y. Li *et al.*, “Early transcriptional signatures of MeCP2 positive and negative cells in Rett syndrome,” Jun. 26, 2025. doi: 10.1101/2025.06.26.661761.

[240] D. Pozzer *et al.*, “Clinical-grade intranasal NGF fuels neurological and metabolic functions of *Mecp2* -deficient mice,” *Brain*, vol. 148, no. 3, pp. 845–860, Mar. 2025, doi: 10.1093/brain/awae291.

[241] S. S. Bajikar *et al.*, “MeCP2 regulates Gdf11, a dosage-sensitive gene critical for neurological function,” *Elife*, vol. 12, Feb. 2023, doi: 10.7554/eLife.83806.

[242] Z. U. N. Mughal *et al.*, “Trofinetide receives FDA approval as first drug for Rett syndrome,” *Annals of Medicine & Surgery*, vol. 86, no. 5, pp. 2382–2385, May 2024, doi: 10.1097/MS9.0000000000001896.

[243] N. Panayotis, Y. Ehinger, M. S. Felix, and J. Roux, “State-of-the-art therapies for Rett syndrome,” *Dev Med Child Neurol*, vol. 65, no. 2, pp. 162–170, Feb. 2023, doi: 10.1111/dmcn.15383.

[244] A. L. Carvalho, C. B. Duarte, and A. P. Carvalho, “Regulation of AMPA Receptors by Phosphorylation,” *Neurochem Res*, vol. 25, no. 9–10, pp. 1245–1255, Oct. 2000, doi: 10.1023/A:1007644128886.

[245] V. Derkach, A. Barria, and T. R. Soderling, “Ca^{2+} /calmodulin-kinase II enhances channel conductance of α-amino-3-hydroxy-5-methyl-4-isoxazolepropionate type glutamate receptors,” *Proceedings of the National Academy of Sciences*, vol. 96, no. 6, pp. 3269–3274, Mar. 1999, doi: 10.1073/pnas.96.6.3269.

[246] L. Wang *et al.*, “Brain Development and Akt Signaling: the Crossroads of Signaling Pathway and Neurodevelopmental Diseases,” *Journal of Molecular Neuroscience*, vol. 61, no. 3, pp. 379–384, Mar. 2017, doi: 10.1007/s12031-016-0872-y.

[247] J. M. , V. P. , T. M. E. , & de V.-S. E. Cisneros-Franco, “Critical periods of brain development,” 2020, pp. 75–88. doi: 10.1016/B978-0-444-64150-2.00009-5.

[248] T. Chari, S. Griswold, N. A. Andrews, and M. Fagiolini, “The Stage of the Estrus Cycle Is Critical for Interpretation of Female Mouse Social Interaction Behavior,” *Front Behav Neurosci*, vol. 14, Jun. 2020, doi: 10.3389/fnbeh.2020.00113.

[249] N. C. Donner and C. A. Lowry, “Sex differences in anxiety and emotional behavior,” *Pflugers Arch*, vol. 465, no. 5, pp. 601–626, May 2013, doi: 10.1007/s00424-013-1271-7.

[250] N. S. Mehta, L. Wang, and E. E. Redei, “Sex differences in depressive, anxious behaviors and hippocampal transcript levels in a genetic rat model,” *Genes Brain Behav*, vol. 12, no. 7, pp. 695–704, Oct. 2013, doi: 10.1111/gbb.12063.

[251] N. Kokras, K. Antoniou, H. G. Mikail, V. Kafetzopoulos, Z. Papadopoulou-Daifoti, and C. Dalla, “Forced swim test: What about females?,” *Neuropharmacology*, vol. 99, pp. 408–421, Dec. 2015, doi: 10.1016/j.neuropharm.2015.03.016.

[252] N. Picard, A. E. Takesian, M. Fagiolini, and T. K. Hensch, “NMDA 2A receptors in parvalbumin cells mediate sex-specific rapid ketamine response on cortical activity,” *Mol Psychiatry*, vol. 24, no. 6, pp. 828–838, Jun. 2019, doi: 10.1038/s41380-018-0341-9.

[253] C. Galvin and I. Ninan, “Regulation of the Mouse Medial Prefrontal Cortical Synapses by Endogenous Estradiol,” *Neuropsychopharmacology*, vol. 39, no. 9, pp. 2086–2094, Aug. 2014, doi: 10.1038/npp.2014.56.

[254] M. L. Phillips, H. A. Robinson, and L. Pozzo-Miller, “Ventral hippocampal projections to the medial prefrontal cortex regulate social memory,” *Elife*, vol. 8, May 2019, doi: 10.7554/eLife.44182.

[255] P. R. Huttenlocher and A. S. Dabholkar, “Regional differences in synaptogenesis in human cerebral cortex,” *J Comp Neurol*, vol. 387, no. 2, pp. 167–178, Oct. 1997, doi: 10.1002/(SICI)1096-9861(19971020)387:2<167::AID-CNE1>3.0.CO;2-Z.

[256] N. C. Cottam *et al.*, “From circuits to lifespan: translating mouse and human timelines with neuroimaging based tractography,” Jul. 29, 2024. doi: 10.1101/2024.07.28.605528.

[257] D. Pozzer *et al.*, “Clinical-grade intranasal NGF fuels neurological and metabolic functions of *Mecp2* -deficient mice,” *Brain*, vol. 148, no. 3, pp. 845–860, Mar. 2025, doi: 10.1093/brain/awae291.